



**NTNU – Trondheim**  
Norwegian University of  
Science and Technology

# Experimental Studies of the Two Phase Flow and Monodispersed Pickering Emulsions Stabilized by LaponiteRD in a Microfluidic T- Junction

**Humaira Idris**

Condensed Matter Physics

Submission date: June 2014

Supervisor: Jon Otto Fossum, IFY

Norwegian University of Science and Technology  
Department of Physics





**NTNU – Trondheim**  
Norwegian University of  
Science and Technology

# **Experimental Studies of the Two Phase Flow and Monodispersed Pickering Emulsions Stabilized by LaponiteRD in a Microfluidic T- Junction**

**Humaira Idris**

**Master of Science in Condense Matter Physics**

**Submission date: 16.06.2014**

**Supervisor: Jon Otto Fossum,**

**Norwegian University of Science and Technology**  
**Department of Physics**

## Abstract

In this thesis, the experiments were divided into two parts. The first part of the experiments are experimental studies of two phase microfluidic oil-water flow (with or without clay) in a T-junction whereas in the second part monodispersed Pickering emulsion was stabilized by Laponite clay. The aim of the experiment was to understand better than before, the underlying droplet formation mechanism in a T- junction and how the different parameters such as flow rates, viscosity or capillary numbers affect the droplets in the microchannel. In addition we wish to understand better the physics behind, how clay particles coat water droplets embedded in oil, and protect them from coalescing.

Monodispersed droplets were produced in a microfluidic T-junction by controlling flow rates of dispersed and continuous phases. The space between each droplet was controlled and it was similar between different droplets. The main observation of the experiments is that the droplet size is directly proportional to the flow rate of dispersed phase and inversely proportional to the flow rate of the continuous phase. The effect of viscosity on drop size is not straightforward but the influence of viscosities on droplet formation can be deduced from the capillary number. In the squeezing regime droplets are sheared off right at T-junction and the breakup is dominated by the interfacial tension force. As the velocity of the driving flow increases so called the dripping and jetting regimes happen, and the interfacial velocity is not high enough for clean snap-off, and fluids proceed in laminar flow for some distance before the snap-off occurs. Adding clay in dispersed phase slightly increases the droplet size and capillary value. Even in the same regime for different viscosities in continuous phase, capillary number varied a lot but not as much for the clay. We expect either higher concentration of clay or sufficient time needs to affect the clay on droplet size effectively.

The most stable water-in-oil emulsions was formed in the experiment by using Laponite RD as emulsifier under conditions where the particles are flocculated via salt at higher concentrations of clay and high viscous polar oil (castor oil) used as continuous phase. Emulsions have been generated in a T-junction in two situations. First, emulsions at constant salt concentration for different clay concentrations. Second, emulsions at constant concentration of Laponite RD with decreasing concentration of salt. The changes in the drop size distributions with time are rationalized in terms of either coalescence or Ostwald ripening which is prompt initially but eventually stable. Emulsions were made with both non-polar oil (silicone oil) and polar oil (castor oil). It was found that the stability of emulsions dependent on the type of oil. Nonpolar oils like silicon oil was not suitable for preparing stable W/O emulsions, whereas polar oil like castor oil made stable W/O emulsions possible.

# Acknowledgements

I would like to express my thanks and gratitude to my supervisor Professor Jon Otto Fossum<sup>1</sup> for his help and guidance throughout the thesis work and for giving me opportunity to work in his research group with this interesting project. I wish to thank everyone that contributed to both the work described in this thesis and to the pleasure I experienced while working with them. My foremost thanks go to Zbigniew Rozynek<sup>2</sup> and Azarmidokht Gholamipour-Shirazi<sup>3</sup>. Their encouragement and active guidance have helped me overcome the challenges that I met during my thesis work. I am also thankful for the assistance of all members of the Laboratory of Soft and Complex Matter studies at NTNU, especially PhD student Alexander Mikkelsen and technician Ole Tore Buset.

---

<sup>1</sup> Norwegian University of science and Technology.

<sup>2</sup> Institute of Physical Chemistry at Polish Academy of Sciences.

<sup>3</sup> Pontificia Universidade Catolica do Rio de Janeiro.

# Table of Contents

<b>1</b>	<b>INTRODUCTION.....</b>	<b>9</b>
<b>2</b>	<b>THEORY .....</b>	<b>12</b>
2.1	CLAY MINERALS.....	12
2.1.1	General structure of smectite clay minerals .....	12
2.1.2	Laponite .....	14
2.1.3	Colloidal dispersion of Laponite.....	15
2.2	EMULSION .....	16
2.2.1	Emulsion formation and droplets aggregation .....	16
2.2.2	Processes of breakdown in emulsion .....	17
2.2.3	Emulsion stability .....	18
2.3	SURFACTANT STABILIZED EMULSION .....	19
2.4	PICKERING EMULSION .....	22
2.4.1	Stabilization mechanisms of Pickering emulsion .....	23
2.4.2	Parameter influencing the stability of Pickering emulsions.....	24
2.5	VISCOSITY AND FLOW RATE OF FLUIDS .....	25
2.6	SURFACE TENSION.....	26
2.6.1	Parameters influencing interfacial tension .....	27
2.7	WETTABILITY AND CONTACT ANGLE.....	28
2.8	TWO PHASE MICROFLUIDIC FLOW .....	29
2.8.1	Fundamentals of two phase flow in microchannel.....	29
2.8.2	The geometry of the T-junction .....	30
2.8.3	Droplet formation regimes in T-junction .....	31
2.8.4	Droplet formation mechanism in T-junction.....	32
2.8.5	Parameters effect on two phase flow .....	34
2.9	MATERIALS OF THE MICROFLUIDIC T-JUNCTION .....	35
<b>3</b>	<b>EXPERIMENT .....</b>	<b>37</b>
3.1	EXPERIMENTAL SET UP .....	37
3.1.1	Injection system .....	37
3.1.2	Fluids, clay and flocculated agent.....	38
3.1.3	Microfluidic chip.....	39
3.1.4	Acquisition system.....	40
3.2	EXPERIMENTAL METHOD .....	41
3.2.1	Two phase microfluidic flow in T-junction .....	41
3.2.2	Experimental study of Pickering emulsion stabilized by Laponite RD in a microfluidic T-junction .....	43
<b>4</b>	<b>RESULTS AND DISCUSSION .....</b>	<b>47</b>
4.1	EFFECT OF FLOW RATE AND VISCOSITY ON DROPLET SIZE .....	47
4.2	EFFECT OF CLAY AND VISCOSITY ON DROPLET SIZE IN DIFFERENT REGIMES .....	51
4.3	PICKERING EMULSION STABILIZED BY LAPONITE RD IN A MICROFLUIDIC T-JUNCTION .....	55
4.3.1	Generation of emulsions with non-polar oil and Laponite RD in water .....	55
4.3.2	Generation of emulsions with polar oil and Laponite RD in water .....	57
<b>5</b>	<b>CONCLUSION AND FUTURE STUDIES .....</b>	<b>67</b>
5.1	CONCLUSION .....	67
5.1.1	Two phase microfluidic flow experiments.....	67
5.1.2	Stability of monodispersed Pickering emulsion by Laponite RD .....	68
5.2	FUTURE STUDIES .....	69
<b>6</b>	<b>APPENDIX.....</b>	<b>71</b>
<b>7</b>	<b>BIBLIOGRAPHY .....</b>	<b>72</b>

# List of Figures

Figure 2.1: (a) Tetrahedron (b) Octahedron structure.....	12
Figure 2.2: Two dimensional schematic diagram of the smectite clay structure. The figure is taken from (Odom, 1984). .....	13
Figure 2.3: Smectite clay from (a) macro scale grain to (d) nano scale atom structure. The fig is taken from the master thesis of Mikkelsen, 2012. ....	14
Figure 2.4: (a) Chemical formula, (b) Crystallographic structure, (c) characteristic shape and dimensions of a laponite particle. Figure adapted from Ruzicka et al., 2010.....	15
Figure 2.5: Schematic representation of the various breakdown processes in emulsions. Figure adapted from F. Tadros, 2013.....	18
Figure 2.6: Illustration of A) an amphiphilic molecule with a hydrophilic and a hydrophobic part. ....	20
Figure 2.7: Schematic representation of (a) structure of surfactant, (b) surfactant molecules at the interface, and (c) spherical surfactant micelles (Pichot, 2010). ....	21
Figure 2.8: A typical graph displaying surface tension ( $\gamma$ ) verses log of surfactant concentration ( $C_s$ ) added and the graph shows three phases 1) at very low $C_s$ , only a slight change in $\gamma$ is detected. 2) Adding more surfactants decreases $\gamma$ up to the CMC. 3) Saturated surface tension. Graph adapted from Attension. ....	22
Figure 2.9: (Upper) Various contact angles of a small particle at a planar oil-water interface; (Lower) Position of solid particles at a curved interface – for $\theta < 90^\circ$ (left) O/W emulsion can be formed, for $\theta > 90^\circ$ (right) W/O emulsion can be formed. Figure adapted from Binks, 2002.....	23
Figure 2.10: The intermolecular forces in a liquid, molecule at the surface form stronger bonds. ....	26
Figure 2.11: Interfacial forces acting on a liquid drop (L) placed on a solid (S) surrounded by vapour (V). $\gamma_{SV}$ is the interfacial tension between the solid and the vapour; $\gamma_{SL}$ is the interfacial tension between the solid and the liquid; $\gamma_{LV}$ is the interfacial tension between the liquid and the vapour. ....	28
Figure 2.12: Wetting described by various values of the contact angle; (a) Perfect Wetting, (b) Partial Wetting, (c) Non wetting, and (d) Perfect non-wetting. ....	29
Figure 2.13: The geometry of a T- junction. The figure got from the manufacturer, Institute of Physical Chemistry at Polish Academy of Sciences.....	31
Figure 2.14: Droplet formation mechanism in a T- junction. ....	32
Figure 3.1: Experimental setup of Microfluidic flow system: Two syringe pumps (NE-300) are used to control the flow rate. Liquids from the syringe are carried to the microfluidic chip via polyethylene tubes. Live view shoot of droplet formation in T-junction on computer using Axio vision software.....	37
Figure 3.2: Image of a) Microfluidic chip, b) Niddle (0.8*40mm), c) Syringe connected with Polyethylene tubing, d) 2-D image of T-junction.....	38
Figure 3.3: Configuration of the chips used in the experiment done by using paint. The measured widths were almost similar to the information got from the manufacturer. ....	40
Figure 3.4: Image of droplet formation in microfluidic T-junction. The continuous flows in the horizontal channel with flow rate $Q_C$ , while the disperse phase flows in the vertical channel with flow rate $Q_d$ . $L$ is measured droplet length and $W$ represents the microchannel diameter. ....	41

Figure 3.5: a) Anti-Bancroft system, b) Bancroft system. Figure adapted from Golemanov et al., 2006. ....	44
Figure 3.6: Droplets are in different parts of the reservoir. (a) At the beginning of the reservoir. (b) At middle part of reservoir and (c) At the end of the reservoir.....	46
Figure 4.1: Regular sized monodispersed with equal spacing droplets in a T-junction. The average diameter of the droplets in the figure is 0.56mm ~ 1/2mm. The distance between each droplet was around 1mm. ....	47
Figure 4.2: L verses $Q_{water}$ for constant value of $Q_{oil}$ (0.5 $\mu$ L/min) with corresponding droplets lengths images, $Q_{water}$ =2.0-0.2 $\mu$ L/min.....	48
Figure 4.3: L verses $Q_{oil}$ for constant value of $Q_{water}$ (1.0 $\mu$ L/min) with corresponding droplets lengths images, $Q_{water}$ = 3.0-0.3 $\mu$ L/min.....	48
Figure 4.4: Effect of continuous flow rate ( $Q_c$ ) on droplet size in different constant value of dispersed phase ( $Q_d$ ). Smallest droplet size was found around 400 $\mu$ m or 0.4mm.....	49
Figure 4.5: There are five different series of data plotted on this graph, each corresponding to a different combination of viscosity ( $\mu$ ) of the continuous phase and its rate of flow ( $Q_{oil}$ ). The legend is given in the figure.....	51
Figure 4.6: (a) Microphotograph of formation of plugs at low value of Ca ( $4.7 \times 10^{-3}$ ). The sharp breakup of droplet plugs due to the domination of the interfacial tension at low flow rates u (21mm) (b) microphotograp of flow that is in transition to laminar flow. By increasing the flow rates (41mm) and the Ca number ( $8.9 \times 10^{-3}$ ), the disperse phase flow a bit into the horizontal channel and forms a neck before the plugs are sheared off. (c) Microphotography of flow where long neck is formed and plugs sizes become smaller when the flow rates (58mm) and Ca ( $1.2 \times 10^{-2}$ ), increases further. This is due to the relative viscous force becomes more dominant and the interfacial tension force is not sufficient for sharp plugs breakups. For all picture, $Q_c$ is silicon oil (10cS) and $Q_d$ , De-ionized water with 1m%clay. length of the laminar segment is 2mm. ....	52
Figure 4.7: Effect of clay and viscosity in continuous phase on droplet size.....	53
Figure 4.8: Very unstable droplets in the reservoir when the viscosity of the continuous phase (silicone oil) is 100cSt. Dispersed phase, 2% Laponite RD with 0.1 M aqueous NaCl. ....	55
Figure 4.9: Few stable droplets found in the system, viscosity of the continuous phase (silicone oil) is 500cSt and dispersed phase 2% Laponite RD with 0.1 M aqueous NaCl). Droplets are (a) at the beginning of the reservoir (b) & (c) at the middle part of the reservoir (d) at the end of the reservoir and (e) droplets after 30 minutes in the middle part of the reservoir. ....	56
Figure 4.10: Sampled collected in the small glass ampules. Left, stable water in oil emulsions by using castor oil as continuous phase. Right, unstable water in oil emulsions by using silicon oil as continuous phase. In both cases Laponite concentration is 2% and salt concentration is $10^{-1}$ M. In unstable water in oil emulsions by using silicon oil as continuous phase, we found two clear, separate water (down) and oil (up) phase which are marked by arrow (red) signs. The appearances of the emulsions are after one week of preparation. ....	57
Figure 4.11: Unstable emulsion formed in $10^{-1}$ M salt at low 0.5% Laponite RD. ....	58
Figure 4.12: Stable W/O emulsion with 1.5% Laponite at 0.1 M salt. Water droplets at different time (a) droplets at zero minutes (b) droplets at 15 minutes (c) at 20 minutes and (d) at 30 minutes (e) at 45 minutes and (f) at one hour.	



Images (b) to (f), were taken from the same part of the reservoir (near exit of reservoir) and image (a) taken from at the beginning of the reservoir. ....	59
Figure 4.13: Stable W/O emulsion with 2% Laponite concentration at 0.1 M salt. Water droplets at different time: (a) droplets at zero minutes, (b) droplets at 15 minutes, (c) at 30 minutes, (d) at 45 minutes, (e) 60 minutes and (f) after one day. Image (b) to (f), taken from the same part of the reservoir (near the exit) and image (a), taken from at the beginning of the reservoir.....	60
Figure 4.14: Stable W/O emulsion with different Laponite RD concentration at constant salt 0.1% concentration. (a) Laponite RD 1% (b) Laponite RD 1.5% and (c) Laponite RD 2%. It was found that coalescence of the droplets increases slightly with higher clay content. In each of the image droplets are 30 minutes aged. ....	61
Figure 4.15: Sampled collected in the small glass ampules. From left to right, emulsion with 2%, 1.5% and 0.5% Laponite RD concentration at constant 0.1 M salt. The stable emulsions found with higher clay concentrations. The appearances of the emulsions are after one week of preparation.....	61
Figure 4.16: Water in oil emulsions with 2% Laponite RD at different salt concentrations at zero minute. (a) Emulsion without any salt. (b) Emulsion with $10^{-3}$ M salt. (c) Emulsion with $10^{-2}$ M salt and (d) Emulsion with $10^1$ M salt. ....	62
Figure 4.17: Water in oil emulsions with 2% Laponite RD at different salt concentrations at 30 minutes. (a) Emulsion without any salt. (b) Emulsion with $10^{-3}$ M salt. (c) Emulsion with $10^{-2}$ M salt and (d) Emulsion with $10^1$ M salt.....	63
Figure 4.18: Sampled collected in the small glass ampules. From left to right, emulsion with $10^{-1}$ M, $10^{-2}$ M, $10^{-3}$ M and 0 M salt concentration at a constant 2 % Laponite RD. The stable emulsions found with $10^{-1}$ M concentrations. Emulsion found without adding any salt was better than lower salt ( $10^{-2}$ M & $10^{-3}$ M) concentrations where two clear phases, water (down) and oil (up) are visible. A small amount of emulsion stabilized between these two phases (see red arrows in last glass ampules from the left to right). The appearances of the emulsions are one week after preparation. ....	64
Figure 4.19: Droplet diameter size distributions for water-in-castor oil emulsions stabilized by 2% Laponite RD in 0.1M NaCl. Times since emulsion formation are 60 minutes (upper green) and 24hours (lower blue). The blending of two curves designates that they are coincides and droplets are stable. ....	65

## List of Tables

Table 2.1: Physical properties of Laponite. CEC is the cation exchange capacity, BET is the particle surface area calculated with BET theory, $\rho$ is the particle charge density and $\rho_L$ is the bulk density. Table adapted from (Kaviratna et al., 1996).....	15
Table 3.1: Density ( $\rho$ ), dynamic viscosity ( $\mu$ ) and Surface tension ( $\sigma$ ) at 25°C for castor oil, silicon oils and water.....	39
Table 4.1: Different regimes (squeezing and transition to dripping) in terms of capillary number (Ca).....	53
Table 4.2: The experimental results at constant salt concentration with varying clay concentrations.....	62
Table 4.3: The experimental results at constant LP with varying salt concentrations.....	64

# Chapter 1

## 1 Introduction

Microfluidics is the area of science and technology, focused on simple or complex, mono or multiphase flows that are circulating in natural or artificial micro systems (Tabeling, 2005). In microfluidics systems, we study the behaviour of fluids in microchannels as well as discussed the manufacturing of microfluidic devices for application such as Lab-on-chip (Tabeling, 2005). Fluid flow in natural microchannels as blood vessels or plants capillaries are examples of natural microfluidic systems. The man made microfluidic systems deals with devices on the micrometer length scale. The small size of microfluidics devices has many advantages over that of the normal sized system. Small sample volume can quickly be analyzed at low cost with high resolution and sensitivity. Short molecular diffusion distances, the capability for precise control and manipulation of flows are other important microfluidics device characteristics (EIT village, NTNU, 2013).

The first commercialized product produced on a large scale using microfluidics technology was the ink jet printer head (Tabeling, 2005). In recent years, this area has received considerable attention and experienced great development. For example, digital microfluidics, the object of this field is to transport and transform fluid samples in a controlled manner, not in the canals but in drops (Tabeling, 2005). Potential applications of droplets in microsystems include pumping of flows, chemical reactions, emulsion formation and rapid mixing of liquids at low Reynolds numbers (Stone et al., 2004). In 2001, microfluidics was declared to be one of ten technologies capable of “changing the world” (Weigl and Hedine, 2002).

Two phase microfluidic flows are formed when two immiscible (or partially miscible) fluids are brought into contact in microfluidic devices. The most popular microfluidic device used for the generation of monodispersed droplets is a T-junction which was first incorporated into a microfluidic chip by Thorsen et al., 2001. T-junction geometry by using the cross flow shear method generates droplets that are highly monodispersed with an equal spacing between drops. Other frequently used structures are flow focusing, co-flowing. In addition, there are some other methods such as straight-through microchannel (MC), membrane, etc. (Zhao et al, 2011). In a typical T-junction, using the cross flow shear method, one phase flows in the main channel (the continuous phase), and exerts a shearing force on the liquid entering from the perpendicular channel (the dispersed phase). The shear force tends to deform and stretch the entering liquid, while the interfacial tension at the interface between the phases counteracts this deformation (Zhao et al, 2011). The flow situation is not the only one encountered in microscale two-phase flows. Depending on the relative velocities of the two phases, their viscosities, and the interfacial tension between the liquids, a variety of flow in the main channel downstream the T-junction may occur. (Dreyfus et al., 2003; Tica et al., 2004; Garstecki et al., 2006).

The term clay refers to a natural occurring material composed of primarily of fine- grained minerals, which is generally plastic at appropriate water contents and become hardened if dried or fired (Guggenheim and Martin, 1995). Industrial application of clays ranges from petroleum relevant areas such as rheology modification, oil well drilling and stability to food and cosmetic industry (Velde, 1992). Among others, research and studies of smectite clays have increased significantly the recent years because of their unique physiochemical properties. However, understanding the complex physical phenomena in smectite clay

systems and their applications is far from complete (Odom, 1984). The smectite clay particles are expected to be surface active and thus alter the capillary force and droplet properties in the two phase flow. This is why we have chosen to perform the two phase flow experiment by using the cross flow shear method in a microfluidic T-junction with Laponite (one of the smectite clays). The use of clay particle is also expected to influence the stability of emulsions.

Emulsions are resulting from the mixing of two immiscible liquids. One of the liquids, the dispersed phase, is distributed as droplets in the other liquid, the continuous phase. Emulsions are generally stabilized by amphiphilic molecules, such as surfactants that lower the interfacial tension of the liquid/liquid interface. In 1907, Pickering observed that colloidal particles situated at the oil-water interface can also stabilize emulsions of oil and water. These are referred to as either Pickering emulsions or solid-stabilized emulsions. The solid particles adsorb at the interface of two liquids and create a physical barrier that hinders coalescence. Clay minerals are known to produce very stable Pickering emulsion (Melle et al., 2004; Binks, 2002; Ashby and Binks, 2000).

Emulsions are important in several every day and industrial contexts, including foods, cosmetics, and pharmaceuticals as well as in the petroleum industry for certain drilling muds, and for enhanced oil recovery. Many crude oils contain water droplets (for example, the North Sea oil) and these must be removed by coalescence followed by separation. Pumping water down to the porous media produces a two phase flow involving complex dynamics of coalescence and breaking up of droplets, resulting in a wide distribution of droplets sizes. The oil-water interfaces are difficult to stabilize and separate, and the difficulties result in residual oil in pores and increased extracting expenses (Kokal, 2005). Pumping water with clay particles in the porous media through oil, resembles the stirring of oil- water mixtures, could produce a kind of Pickering emulsion that would stabilize the oil-water interfaces. Depending on the solubility of the particles, an oil-in- water emulsion can be transformed into a water-in-oil emulsion depending on whether the solid particles are hydrophobic or hydrophilic (Yan et al., 2001). According to the literature data, the percentage of oil recovery in porous media, considering the residual oil saturation, is essentially zero when the capillary number (which represents the relative effect of viscous forces of interfacial tension forces) is less than  $10^{-6}$  and essentially 100% when higher than  $10^{-3}$  (Baviere,1991). Thus, by tailoring the water-oil emulsion and increasing the number of capillary action by 3 or 4 orders of magnitude, it is possible to achieve a recovery of almost 100% of oil in the swept area (EIT village, NTNU, 2013).

In this thesis, the experiments were divided into two parts. To improve the understanding of the fundamental of droplet formation mechanisms in the T-junction and how the different parameters such as flow rates, viscosity or capillary number affect the droplets in the microchannel, experiments with or without smectite clay minerals have been performed in a microfluidic chip. The droplets were formed in the T-junction by using the cross-flow shear method. Experimental studies also performed for the monodispersed Pickering emulsion stabilized by smectite clay with the T-junction geometry. The goal of the experiment was to improve the understanding of the background physics of stabilization of water-in-oil emulsion by Laponite RD in micro system.

This thesis report is composed of five chapters: an introduction, a literature review, an experiment chapter, results and discussion chapters and a conclusion. Chapter 1 is an introduction underlining the interest and the aims of this work; Chapter 2 is a literature review that defines the main notions used throughout this study and summarizes the scientific

knowledge related to the subjects mentioned in this report. Chapter 3 gives the details, necessary to understand the experiments performed during work. Chapter 4 presents the result and its discussion and Chapter 5 summarizes the conclusions made throughout this study and suggests the fulfilment of future works.

# Chapter 2

## 2 Theory

### 2.1 Clay minerals

The fascinating material clays are present almost everywhere on the Earth. They are abundant, inexpensive and environment friendly. Most of the natural clay minerals are very heterogeneous mixtures of minerals. However, pure clay minerals can be made synthetically. Clay minerals are composed of extremely fine, usually plate-shaped crystal layers typically with diameters less than 2  $\mu\text{m}$  and less than a few nm thick (Da Silva et al., 2002).

Among others, there are a vast range of uses and scientific interest in the smectite clay minerals group due to their unique and varied physicochemical properties such as extremely small crystal size, variations of internal chemical composition, structural characteristics caused by chemical factors, large cation exchange capacity, large chemically active surface area, variations in types of exchangeable ions and surface charge, as well as interaction with inorganic and organic liquids. Smectite clays are formed and most stable in surface and shallow subsurface environments. They have been important in the industrial revolution and in petroleum energy resource development. It has been proposed that the beginnings of life originated when organic molecules were photo chemically synthesized on the surface of iron-rich smectite clays (Odom, 1984).

#### 2.1.1 General structure of smectite clay minerals

Smectite clays are composed of layers with negatively charged oxygen atoms together with different types of positive charged cations placed in fixed and specific positions. A two dimensional schematic diagram of the structure is presented in fig 2.2. Oxygen and silicon atoms (and sometimes  $\text{Al}^{3+}$  and  $\text{Fe}^{3+}$ ) together form tetrahedral sheets (Layer 1 and 3 in fig 2.2) with the tetrahedral apexes pointing towards each other. Between the two tetrahedral layers there is an octahedral sheet that may contain cations like  $\text{Al}^{3+}$ ,  $\text{Fe}^{3+}$ ,  $\text{Fe}^{2+}$ ,  $\text{Mg}^{2+}$  or  $\text{Li}^+$ . Smectite structures are classified as 2:1 phyllosilicates based on the presence of the two tetrahedral sheets and the one octahedral sheet (Odom, 1984). The basic structure of tetrahedral and octahedral represented in Figure 2.1.

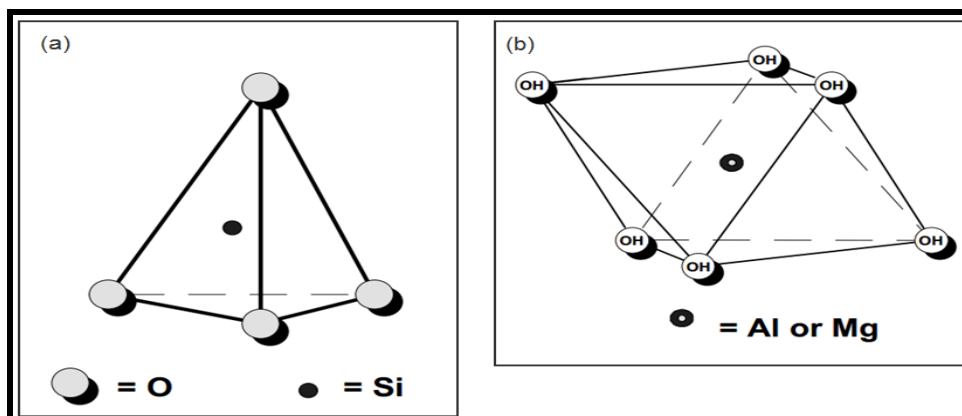


**Figure 2.1: (a) Tetrahedron (b) Octahedron structure.**

An interlayer consisting of loosely held hydrated cations separates the smectite structural units (layer1-3). The presence of these cations is necessary to balance the negative charged

structure caused by internal substitution of ions in the tetrahedral and octahedral sheet. Interlayer surface and cation hydration between smectite structural units is a unique property of smectite clays (Odom, 1984). Type and location of cations in the tetrahedral and octahedral framework distinguish different clays in the smectite group. The charge on the smectite layers is intermediate and varies from 0.4 to 1.2  $e^{-1}$  per unit cell ( $Si_8O_{20}$ ) (Beson et al., 1974). Laponite, Kalonite, Na-Fiuorohectorite, Montmorillonite (bentonite) etc. are some examples of smectite group. The smectite has been used in our experiment is Laponite RD.

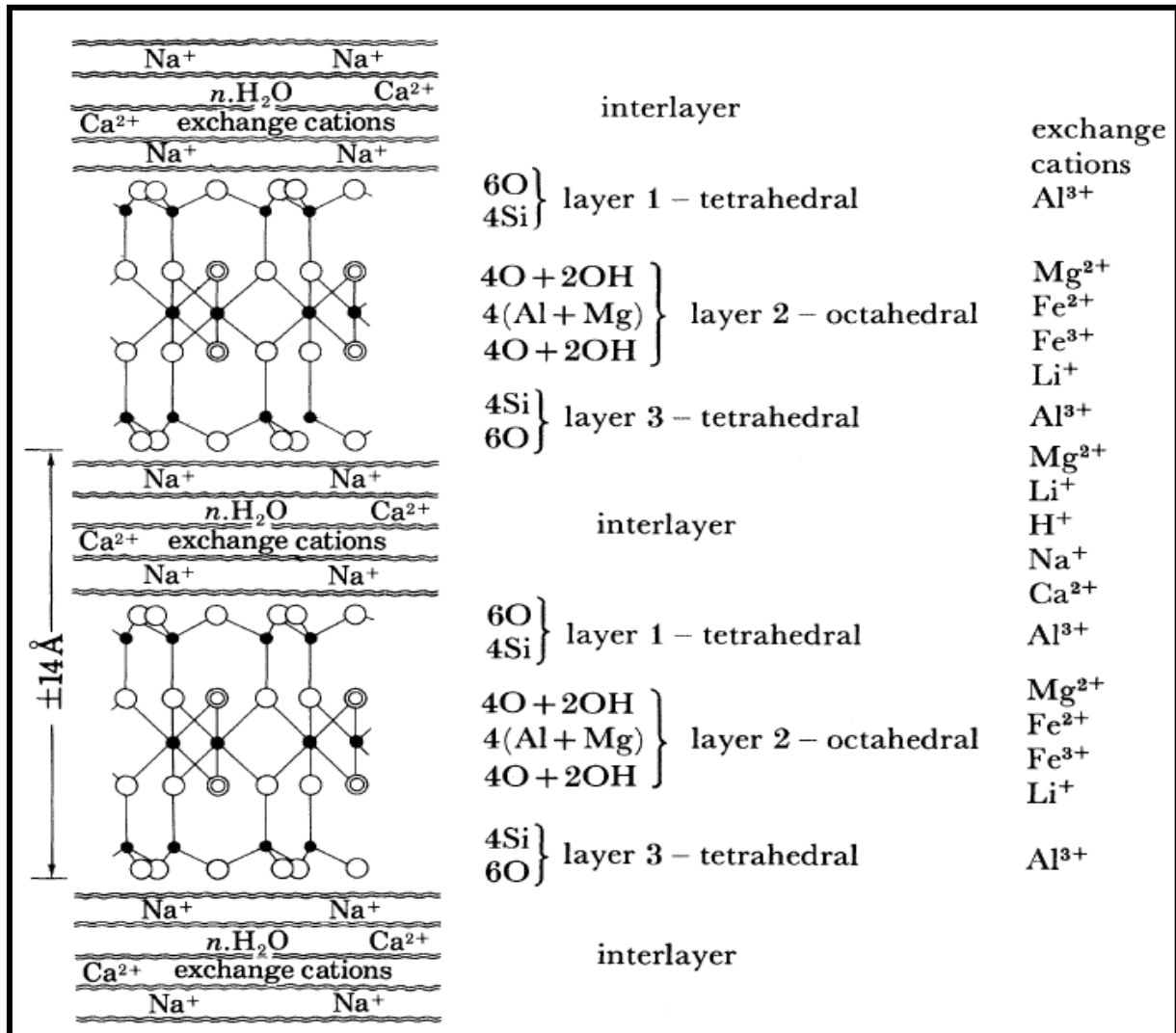


**Figure 2.2: Two dimensional schematic diagram of the smectite clay structure (Odom, 1984).**

In dry form, clay can be seen as small grains (Figure 2.3 a) made of crystalline platelets (Figure 2.3 b). Each platelet is made of unit cells (Figure 2.3 d) repeated in two directions, resulting in a disc shape structure (Figure 2.3 c). The height of each unit cell is approximately 1nm.

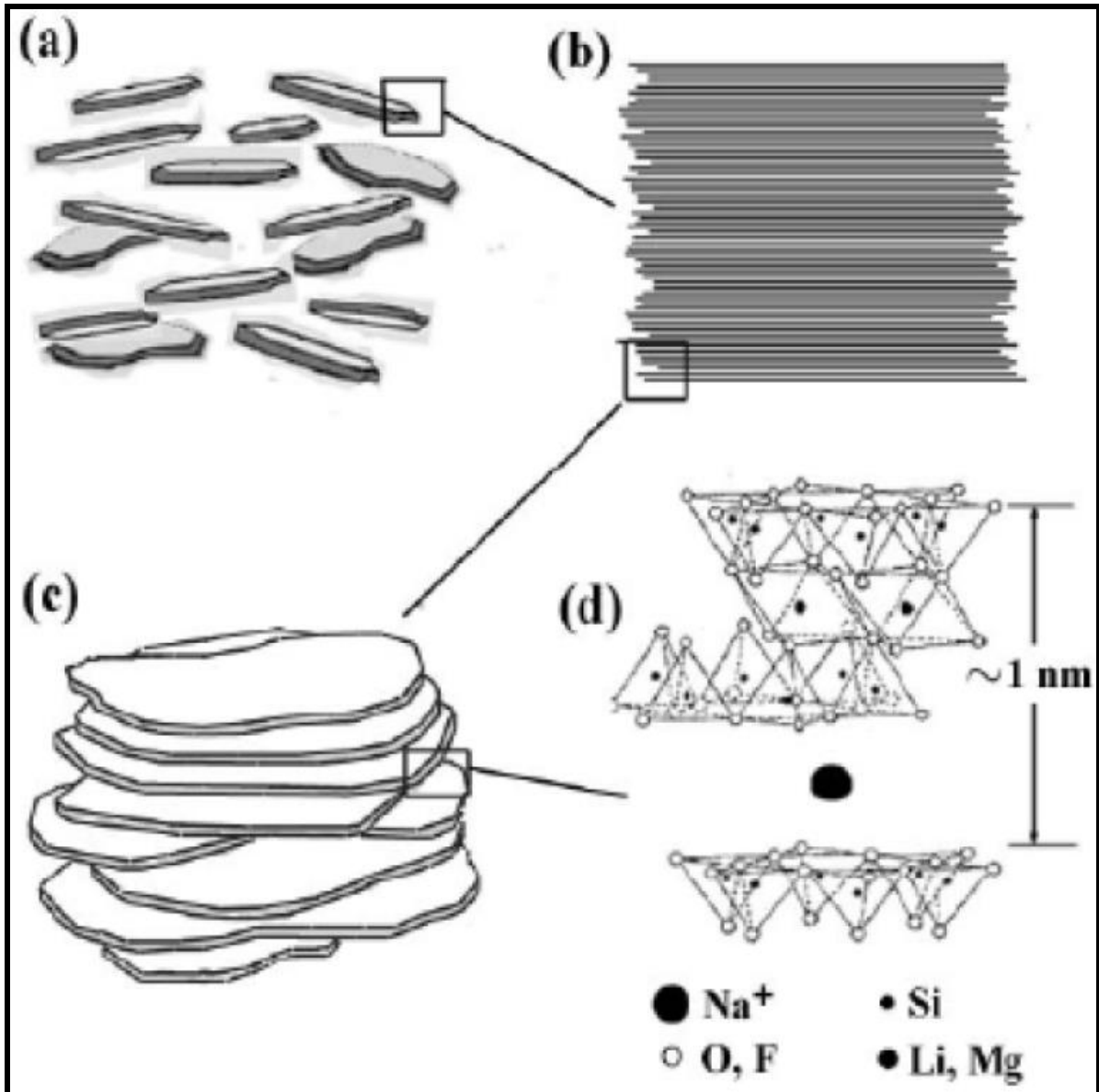


**Figure 2.3: Smectite clay from (a) macro scale grain to (d) nano scale atom structure. The fig is taken from the master thesis of Mikkelsen, 2012.**

### 2.1.2 Laponite

Laponite is a synthetic hectorite type smectite with chemical formula  $\text{Na}^{+0.7}[\text{Si}_8\text{Mg}_{5.5}\text{Li}_{0.3}\text{H}_4\text{O}_{24}]^{-0.7}$ , diameter around 25 nm and a thickness of 1 nm. (Paula et al., 2009). Each Laponite particle is a three layer silicate composed of a central octahedral coordinated magnesium-oxygen-hydroxide sandwiched between two tetrahedral coordinated silica-oxygen sheets (Farouji et al., 2008). A laponite particle and its crystallographic structure are shown in Figure 2.1. It has been estimated that a typical laponite crystal contains up to 2000 unit cells (Rockwood, 2010).



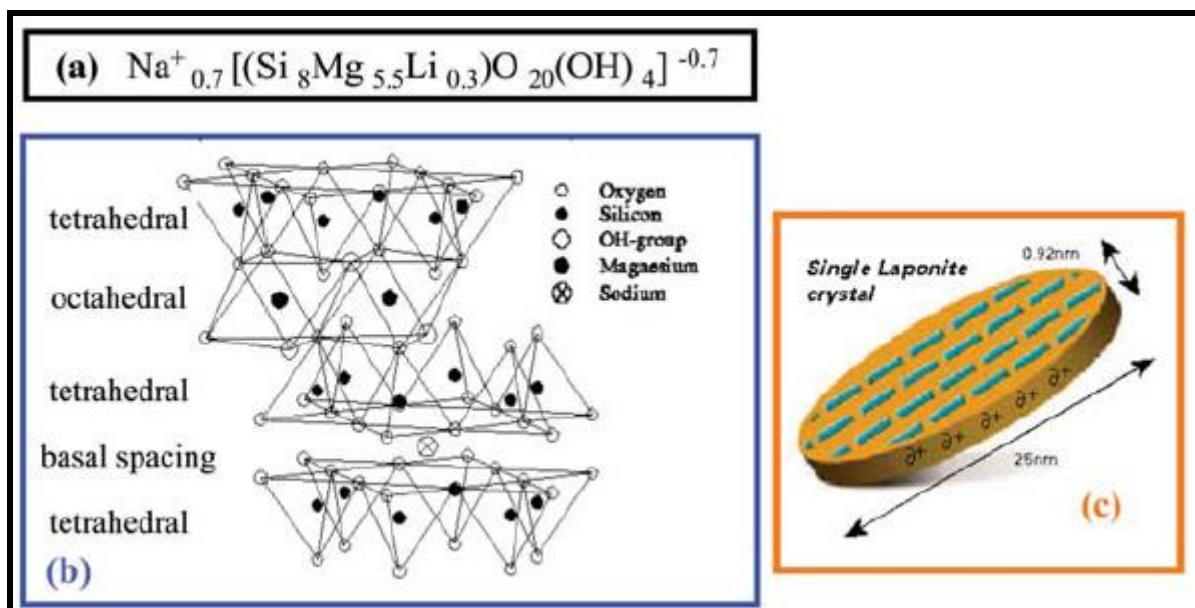


Figure 2.4: (a) Chemical formula, (b) Crystallographic structure, (c) characteristic shape and dimensions of a laponite particle. Figure adapted from Ruzicka et al., 2010.

Table 2.1: Physical properties of Laponite. CEC is the cation exchange capacity, BET is the particle surface area calculated with BET theory,  $\rho$  is the particle charge density and  $\rho_L$  is the bulk density. Table adapted from (Kaviratna et al., 1996).

Clay	Part. Size ( $\text{\AA}$ )	CEC(meg/100mg)	BET ( $\text{m}^2\text{g}^{-1}$ )	$\rho$ ( $\text{e}^{-1}/\text{u. cell}$ )	$\rho_L$ ( $\text{g}/\text{cm}^3$ )
Laponite	200	48	300	0.4	2.65

Laponide RD is used in the experiments in this report. Laponide RD with the chemical formula ( $\text{Si}_8\text{Mg}_{5.45}\text{Li}_{0.4}\text{H}_4\text{O}_{24}\text{Na}_{0.7}$ ), is dispersed in water as individual plate-like sheets having a thickness of  $10 \text{ \AA}$  and an average diameter close to  $300 \text{ \AA}$ . Laponite dispersions are very sensitive to pH. For  $\text{pH} < 9$ , Laponite RD particles dissolve slowly over time. Prior studies on Laponite RD showed that the Laponite RD dispersions are stable at  $\text{pH} = 10$  (A. Mourchid, 1998 and L. Jyotsana, 2000).

### 2.1.3 Colloidal dispersion of Laponite

The exceptional water absorption characteristic makes the smectites attractive and important in nanotechnologies. Smectites are able to absorb up to half of their mass in water. When Laponite powder is dispersed in water, it is first white and non-transparent and becomes transparent after being stirred for a while. Laponite platelets do not remain in the stacks when dispersed in water. The sodium ions in the interlayer hydrate, the structure swells and the plates separate, resulting in nanometer thick platelets, which is impossible to see bare eye but can be seen by for example TEM or X-ray techniques (F. Bergaya, 2006). This distinct “nano-size” allows laponite to form clear gels and films. Addition of polar compounds like salt and surfactants to the laponite dispersion will reduce the osmotic pressure holding the sodium ions away from the particle surface. This allows the weaker positive charge on the edge of the crystals to interact with the negative surfaces of adjacent crystals (Rockwood, 2010).

## 2.2 Emulsion

An emulsion is a mixture of two immiscible liquids where one liquid is dispersed in the form of small drops in another liquid that forms a continuous phase (Rhutesh et al, 2008). A mixture of water droplets in oil is known as water-in-oil emulsion such as butter whereas the mixture of oil in water is oil-in-water emulsion, for example milk. In our experiments (studies of two phase flow in T-junction and preparation of stable Pickering emulsions of laponite clay) water drops dispersed in the oil phase. Emulsification is the process of mixing two liquids together in order to prepare emulsions. Mixtures of oil and water are not stable as oil or water droplets tend to merge with each other. This phenomenon is known as coalescence and the introduction of a third agent, called emulsifier is necessary to stabilize the emulsions. In our experiment laponite clay was used as emulsifier. According to the size of droplets, emulsion can be distinguished such as macroemulsion (droplets  $> 400$  nm), miniemulsions (droplets between 100 and 400 nm) and micellar emulsions or microemulsions (droplets  $< 100$  nm). In a micro emulsion system, emulsion is made from sub micrometric micelles. The macro – emulsion is a meta-stable state since phase separation (e.g. milk to cream) is energetically favorable. But micro-emulsion is stable because micelles do not gain energy by coalescing (Tabeling, 2005).

### 2.2.1 Emulsion formation and droplets aggregation

When oil and water are placed together, a layer of oil is formed over a layer of water (density of oil is lower than the water) because this represents their thermodynamically most stable state. Such a layer's position minimizes the contact area between the two phases, minimizing their free energy. In order to form an emulsion, it is required to change this layer position by bringing energy into the system. When droplets (oil or water) are formed under agitation they are constantly moving due to the Brownian motion thus collide with each other. There are two main types of aggregation of droplets, coalescence and flocculation. Another kind droplet aggregation is Ostwald ripening. Flocculation is the aggregation of droplets that keep their physical properties. Coalescence is the aggregation of droplets that merge together. Flocculation may be reversible (weak flocculation) or irreversible (strong flocculation) while coalescence is irreversible (Dickinson, 2009).

Emulsion droplets are surrounded by the continuous phase in which the droplets are formed and dispersed. As droplets move close to each other, a thin film layer of the continuous phase is formed between the droplets. As long as this film exists, there is no droplet contact due to hydrodynamic resistance induced by the presence of the thin film (Ivanov et al., 1999; Sanfeld et al., 2008.). Droplet aggregation can only occur when the liquid is squeezed out of the thin layer.

The thickness of the thin film depends on the nature of the colloid and hydrodynamic interaction in the system. The thicker the film is, the weaker the collisions are. The thin film forms a barrier between the droplets. The rupture of the film requires a certain level of energy, which determines the nature of the collisions. At the high energy barrier there is no aggregation and the droplets will move apart. At slightly lower energy barrier droplets are weakly flocculated and at low energy barrier droplets are strongly flocculated with a very thin film existing between the droplets. In the last instance the energy barrier is so low that the film is broken which results in droplet coalescence (Petsev, 2000; Ivanov et al., 1999; Sanfeld et al., 2008; Dickinson, 2009).

By coalescence large droplets are formed and due to gravity these droplets merge together to re-form the oil and water layers (Lobo et al., 2002). The use of emulsifiers is thus necessary to avoid the droplets to merge. By adsorbing at the oil – water interface emulsifier molecules form a layer around the droplets that prevents coalescence. However the concentration of emulsifier must be high enough to cover the droplet surface. In case of concentration is too low droplets are likely to coalesce with their neighbors. Another factor that affects the droplet size is the time required by the emulsifier to adsorb at the interface ( $\tau_{ADS}$ ) compared to the time between droplet collisions ( $\tau_{col}$ ). In order to minimize the coalescence during the emulsification process it is necessary to insure that  $\tau_{ADS} / \tau_{col} \ll 1$ .

## **2.2.2 Processes of breakdown in emulsion**

### **2.2.2.1 Coalescence, Flocculation and Ostwald ripening**

As we discussed in the previous section (2.2.1) coalescence is the merging of two or more droplets to form a larger single droplet and results in the formation of a layer of oil at the top of the emulsion (in the case of O/W emulsions) or a layer of water at the bottom of the emulsion in the case of W/O emulsions (Marrucci, 1969). This can only occur when the thin film separating two droplets is ruptured. Emulsion droplets are moving constantly and so collision time may be very short. However, if this time is long compared to the time required for the film to break coalescence is likely to occur (Tempel, 1961). The film rupture mechanisms are largely dependent on the continuous phase properties and on the properties of emulsifiers adsorbed at the droplets. Indeed, emulsifier molecules form a layer, usually called interfacial membrane, around the droplets that protects them from rupture. These mechanisms are very complicated and almost unique for each emulsion as they strongly depend on the system properties. Preventing droplet coalescence is a major issue in emulsion stabilization. A few methods have been developed to control or even prevent coalescence. As coalescence depends both on the colloidal and hydrodynamic interactions between the droplets, and the physic-chemical properties of the components used in the emulsion (particularly the continuous phase and the emulsifier), reducing or preventing droplets contact and interface membrane rupture are the two points on which efforts have to be made to prevent coalescence (Kabalnov1998). Droplet coalescence is mostly prevented by the presence of emulsifiers adsorbed at the oil-water interface. Surface active agents (Surfactants) are the most common emulsifiers. They are very efficient to reduce interfacial tension and prevent droplet contact. Fine divided solid particles also provide very good stability against coalescence. Solid particles adsorb at the interface and form a solid layer that prevents coalescence. Due to the nature of this emulsifier, the stabilization mechanisms are quite different from those of emulsions containing surfactant (Pickering1907; Binks and Lumsdon, 1999; Aveyard et al. 2003).

Droplet flocculation process refers to the aggregation of the droplets (without any change in primary droplet size) into larger units. It is the result of the van der Waals attraction that is universal with all disperse systems. Flocculation occurs when there is not sufficient repulsion to keep the droplets apart to distances where the van der Waals attraction is weak. Flocculation may be “strong” or “weak,” depending on the magnitude of the attractive energy involved (F. Tadros, 2013).

Ostwald ripening in emulsions is a process of gradual growth of the larger droplets at the expense of smaller ones due to mass transport of soluble dispersed phase through the continuous phase (Taylor, 1995). Even though droplet flocculation and coalescence are the

most common factors of emulsion instability, Ostwald ripening is an important cause of instability in some emulsion application (F. Tadros, 2013).

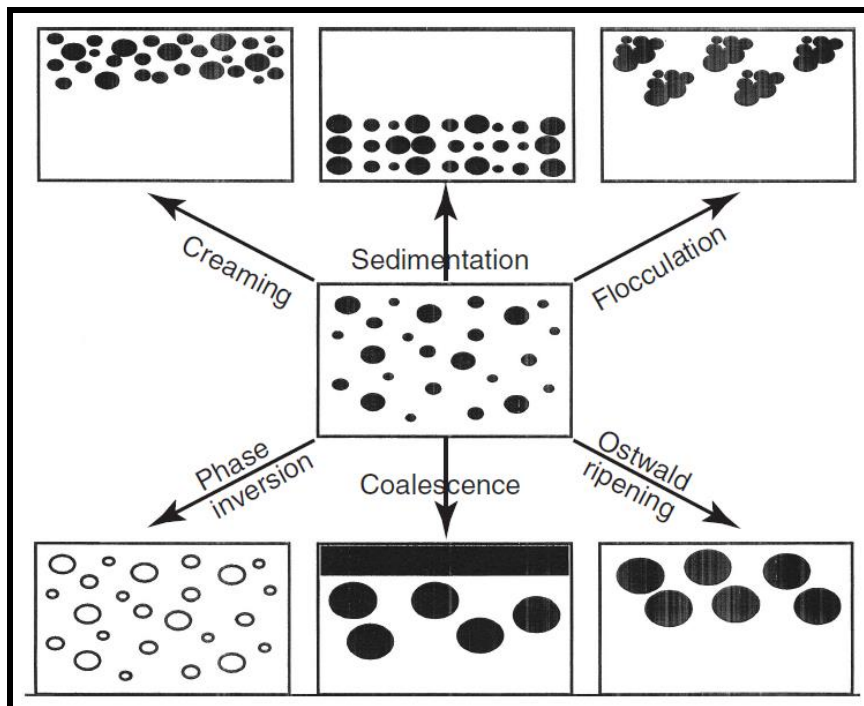


**Figure 2.5: Schematic representation of the various breakdown processes in emulsions.**  
Figure adapted from F. Tadros, 2013.

### 2.2.2.2 Phase separation

The term phase separation refers the density difference between the two phases that is usually present. Due to gravity, droplets tend to move up or down through the continuous phase. If the droplets have a lower density, they tend to move up to form a layer of emulsion droplets at the top of the emulsion. This phenomenon is known as creaming. On the contrary, if the droplets have a higher density, they tend to move down to form a layer at the bottom of the emulsion. This phenomenon is known as sedimentation. Generally, the density of oil is lower than the density of water, thus droplets of O/W emulsions tend to cream, while those of W/O emulsions tend to sediment. To prevent instability, increasing the viscosity of the liquid surrounding a droplet decreases the velocity at which the droplet moves up. Moreover, increasing the droplet concentration can prevent instability. At very high concentrations, droplets will be closely packed, which tends to prevent their movement (Robins, 2000; Dickinson, 2009).

### 2.2.3 Emulsion stability

The ability of an emulsion to keep its properties unchanged over a certain period of time is known as emulsion stability. There are two kinds of instability: Thermodynamic and kinetic. Thermodynamics give information about the processes taking place during emulsification and kinetics gives information about the rate at which these processes occur. Mixing oil and water results in the formation of opaque emulsions. After a certain time, distinct layers of oil and water are visible. Phenomena (coalescence of oil or water droplets) taking place in this example are due to thermodynamic instability. The time taken by the droplets to merge is related to kinetics. Emulsions are thermodynamically unstable systems because their free energy of formation  $\Delta G_f$  is greater than zero and such will show a tendency to break. This

instability is a result of the energy associated with the large interfacial area of the droplets within the emulsion, given by  $A \gamma$  where  $A$  is the total surface area of the drops and  $\lambda$  the interfacial tension existing between two phases. This energy term outweighs the entropy of formation  $\Delta S_f$  associated with the formation of the droplets from the bulk constituents. The free energy of formation of the emulsion in simple terms is given by from the second law of thermodynamics

$$\Delta G_f = \Delta A \gamma - T \Delta S \quad (2.1)$$

In most cases,  $\Delta A \gamma \gg -T\Delta S$ , which means that  $\Delta G_f$  is positive, that is, the formation of emulsions is nonspontaneous and the system is thermodynamically unstable. In the absence of any stabilization mechanism, the emulsion will break by flocculation, coalescence, Ostwald ripening, or a combination of all this process. In the presence of a stabilizer, an energy barrier created between the droplets, and the system becomes kinetically stable (F. Tadros, 2013).

Microemulsions are thermodynamically stable since the interface energy term is very small owing to the very low interfacial tensions (typically  $10^{-4}$  to  $10^{-5}$  N m<sup>-1</sup>) obtained by the use of emulsifier systems at high concentrations. Moreover, as a result of their very small size and hence greater number, the positive entropy of formation of microemulsion droplets may be orders of magnitude larger than that in emulsions. This term dominates the free energy of formation of microemulsions and the systems become thermodynamically stable. The sizes of microemulsion droplets are in the range of a few hundreds of nanometers, so the solutions are transparent.

There are many phenomena (discussed in section 2.2.2) that can alter emulsion stability such as droplets coalescence, phase separation etc. To prevent droplets coalescence a third agent (emulsifier) a surfactant or solid particle is necessary to introduce. The main two functions of an emulsifier during homogenization are, to decrease the oil-water interfacial tension to facilitate droplet disruption, and secondly to form a protective layer around the oil droplets to prevent coalescence. A surfactant is an amphiphilic molecule consisting of a hydrophilic and hydrophobic part. The surfactant molecules migrate to the liquid-liquid interface and inhibit droplet coalescence by reducing the interfacial tension. When particles, instead of surfactant molecules, are used to stabilize an emulsion it is termed as Pickering emulsion. The solid particles (nano or micron sized) are often trapped at the fluid interfaces due to capillary or electrostatic forces and thereby create a physical barrier that hinders coalescence. For example, clay minerals are known to produce very stable Pickering emulsions (Binks, 2002; Ashby and Binks, 2000). The droplets have to be covered by at least one mono layer of clay, otherwise they coalesce (Yan and Masliyah, 1994).

### 2.3 Surfactant stabilized emulsion

For most surfactants, there are two segments; the hydrophilic part is an ion forming “polar head” which tries to stay in contact with water while the hydrophobic tail formed by one or several aliphatic chains  $[\text{CH}_3 (\text{CH}_2)_n]$  avoids water. The surfactant structure is called amphiphilic.

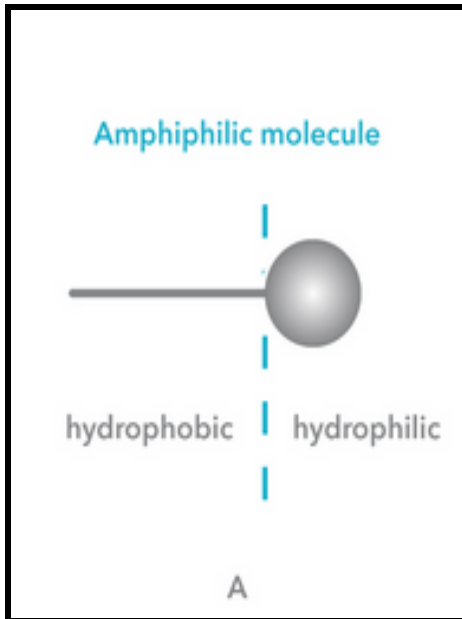


**Figure 2.6: Illustration of A) an amphiphilic molecule with a hydrophilic and a hydrophobic part.**

The surfactant's solubility in aqueous media is determined by the affinity of the surfactant hydrophilic part by the media. Due to its amphiphilic character, the surfactant has its hydrophilic moiety in water and its hydrophobic moiety in oil. The molecules of surfactant adsorbed at the interface replaces the water and oil molecules of the original interface, and thus, the interaction across the interface is now between the hydrophilic group of the surfactant and water on one side and between the hydrophobic group and the oil on the other side of the interface. The presence of surfactant at the interface increases the interactions between oil and water molecules, which tend to reduce the tension across the interface. It seems obvious that by increasing the concentration of surfactant, the interfacial tension decreases. This trend continues until the surface is saturated when  $C_S$  (surfactant concentration) =  $C_{sat}$  (Figure 2.8). The interfacial tension continues to decrease after this, but much more slowly. When the concentration reaches CMC (critical micellar concentration), the interfacial tension saturates at its lowest level. After that an increase of surfactant concentration will only increase the number of micelles and will not alter the energy of the system. Different surfactants also lower the interfacial tension to a different degree which affects the final droplet size.

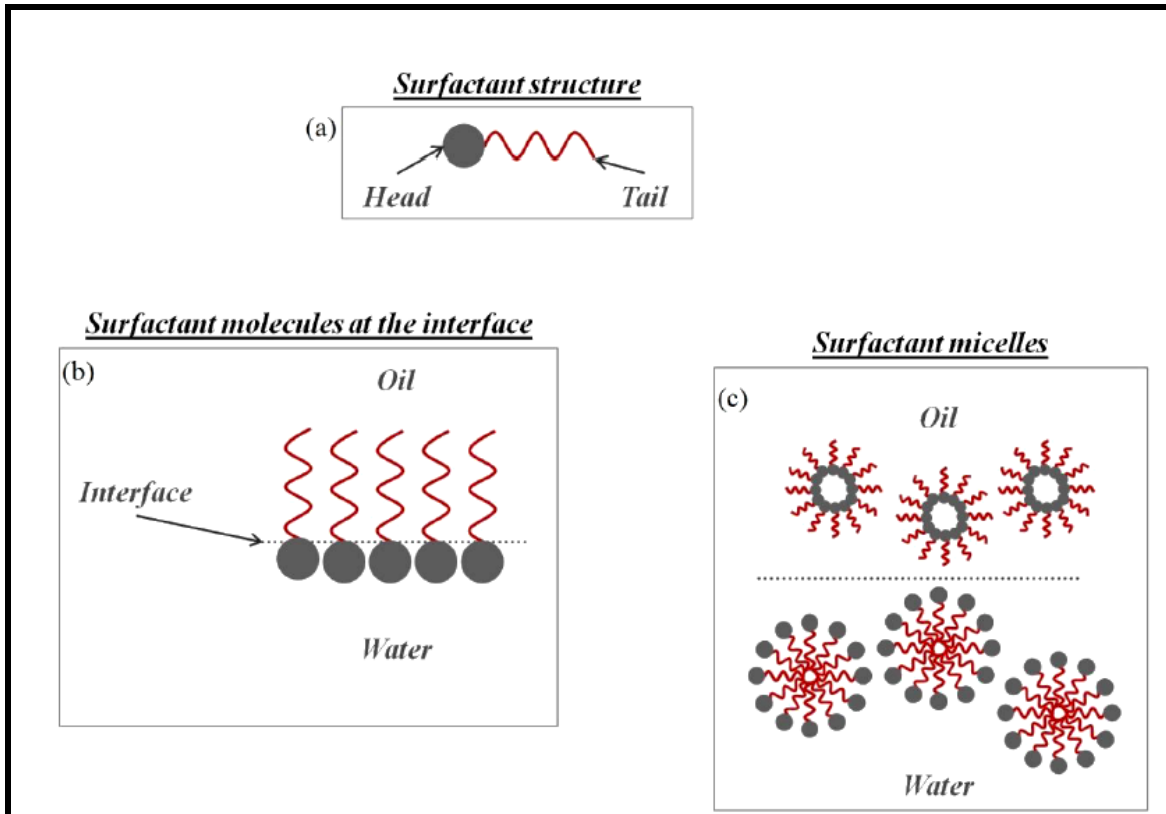


**Figure 2.7: Schematic representation of (a) structure of surfactant, (b) surfactant molecules at the interface, and (c) spherical surfactant micelles (Pichot, 2010).**

Re-coalescence also depends on the surfactant concentration in the system. If the surfactant concentration is too low to form a protective layer around the droplets, droplets tend to coalesce as they collide. Prevention of coalescence of forming droplets is due to the Gibbs-Marangoni effect. Consider two droplets insufficiently covered by surfactant, moving towards each other. During their approach, more surfactants get adsorbed at the interface of the two droplets. However, the amount of surfactant available for adsorption is the lowest where the film between the droplets is the thinnest. The coverage of the droplets is then not uniform; less surfactant molecules are present in the region of the interface where the droplets are the closest. This leads to an interfacial tension gradient, which is the highest where the film is the thinnest. The gradient causes surfactant to move at the interface towards the site of the lowest surfactant coverage. This causes oil to move in the direction of the highest interfacial tension, which thus drives the droplets away from each other. Moreover, due to the specific properties of the surfactant (anionic, cationic, etc.), repulsive interactions exist at the droplet surface which also enhance the prevention of coalescence, during emulsification (Schramm, 2000).

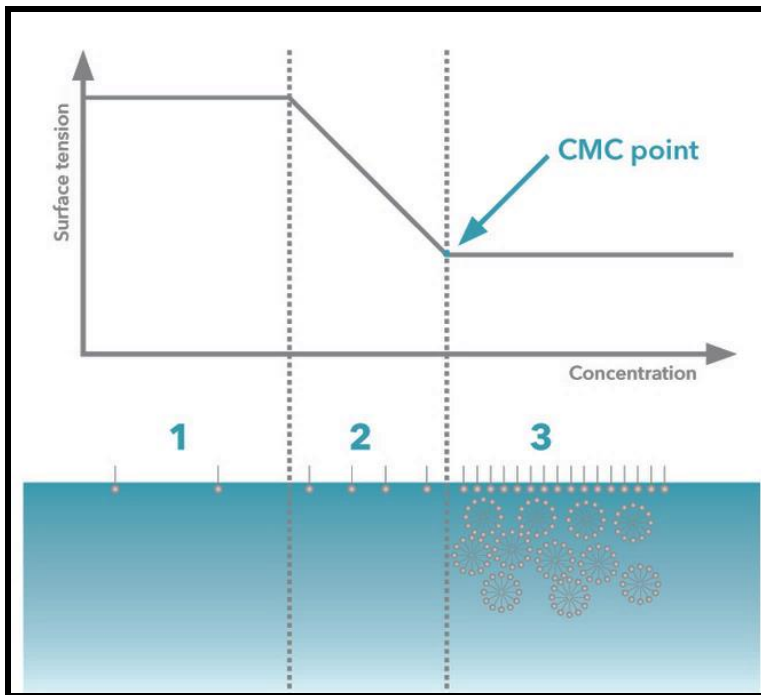


**Figure 2.8: A typical graph displaying surface tension ( $\gamma$ ) versus log of surfactant concentration ( $C_s$ ) added and the graph shows three phases 1) at very low  $C_s$ , only a slight change in  $\gamma$  is detected. 2) Adding more surfactants decreases  $\gamma$  up to the CMC. 3) Saturated surface tension. Graph adapted from Attension.**

Surfactants can be dissolved in oil or water, depending on the size of the head group and tail group. Bancroft linked the surfactant ability to stabilize W/O or O/W emulsions to its solubility in oil or water. This is known as Bancroft rule. Oil soluble surfactant tends to stabilize W/O emulsion, while the water soluble surfactant tends to stabilize O/W emulsions (W. D. Bancroft, 1915). There are different methods to select surfactant as emulsifying agents in a given system. The most frequently used method is the Hydrophilic-Lipophilic-Balance (HLB), which first described by W. C. Griffin, 1949. Adding surfactants also affect the contact angle. By adding the right type and sufficient amount of surfactant, a system might go from a partial wetting regime to a total wetting regime. Thus increasing surfactant concentration decreases the contact angle (Wasen, 1988).

## 2.4 Pickering emulsion

Over a century ago, Ramsden first mentioned that solid matter has the power of forming persistent emulsion (Ramsden, 1903). Later Pickering (hence the term “Pickering emulsion”), published the first extensive experimental study on particle stabilized emulsions for plant spray applications. Pickering recognized that the buildup of particles on liquid drops, could hinder drop coalescence, and therefore be used as emulsion stabilizers (Pickering, 1907). After that a significant amount of work has been published due to the growing interest in emulsions stabilized by fine solid particles during the last decade. Experimenting with clay particles and Pickering emulsion in microfluidic geometries constitutes a departure point for the development of a system that may, in the future, allow for the creation of “tailor-made” emulsion (Tabeling, 2005).



### 2.4.1 Stabilization mechanisms of Pickering emulsion

Emulsion stabilization by colloidal particles occurs as a result of their strong adsorption at the water –oil interface, which was first quantified by Levine et al., 1989. The parameter of choice to describe the Pickering emulsion is contact angle of the adsorbed particles. The contact angle is the angle between the tangent to the drop's profile and the surface at the intersection of the solid, liquid or vapor. This angle is used to define and compare the liquid wettability's on different surfaces. It has been shown that for contact angle in the range 30° - 90° stable oil-in-water emulsion are formed, whereas larger values of the contact angle lead to stabilize the water-in-oil emulsion. Assume, such a colloidal particle is small enough that the effect of gravity on it can be neglected, thus the energy required to remove a spherical particle from the oil-water interface is given by,

$$E = \pi R^2 \gamma_{ow} (1 \pm \cos \theta)^2 \quad (2.2)$$

Where R is the radius of the particle,  $\gamma_{ow}$  the interfacial tension between oil and water and  $\theta$  is the contact angle that the particle has at the interface (fig 2.9). The sign inside the bracket is negative if the particle is removed into the water phase and positive if removed into the oil phase. This equation (2.2) shows that the maximum energy required to remove the particle from the interface is reached for  $\theta = 90^\circ$ . Thus a pure hydrophilic particle (very small contact angle) or a too hydrophobic (very high contact angle) particle is more likely to stay dispersed in water or the oil phase respectively, giving rise to very unstable emulsion (Binks, 2002). Particles at intermediate hydrophobicity ( $\theta$  around  $90^\circ$ ) can be dispersed in both water and oil (Binks and Lumsdon, 2000) and they can produce very stable emulsions such as water-in oil. (Yan et al., 2001).

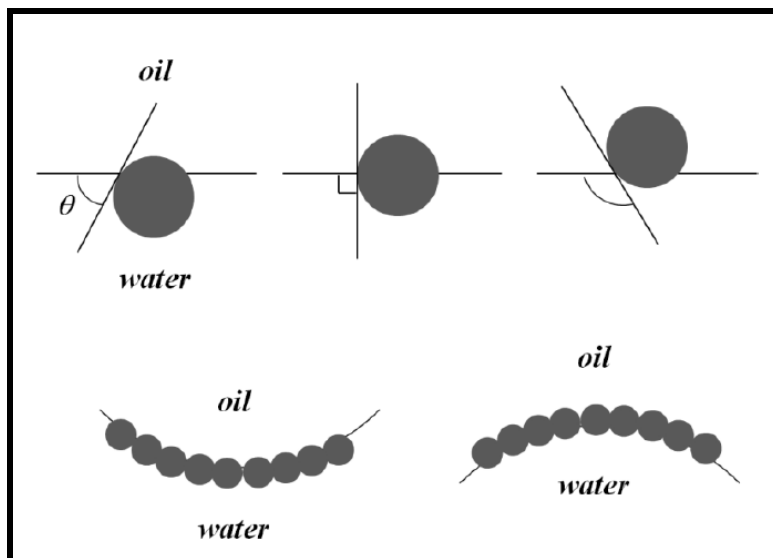


**Figure 2.9: (Upper) Various contact angles of a small particle at a planar oil-water interface; (Lower) Position of solid particles at a curved interface – for  $\theta < 90^\circ$  (left) O/W emulsion can be formed, for  $\theta > 90^\circ$  (right) W/O emulsion can be formed. Figure adapted from Binks, 2002.**

In other words, the ability of particles to stabilize an emulsion depends on its wettability by the oil and water phase of the emulsion. A liquid is wetting if the contact angle is below  $90^\circ$  and non-wetting if it is above  $90^\circ$  (Lien and Løvholden, 2001). The particle must be wetted more by one liquid than the other, which determines the type of emulsion. Water wetted

particles should stabilize o/w emulsions while oil-wetted particles should stabilize w/o emulsions (Pickering, 1907, 91, 2001-2021; Finkle et al., 1923; Binks and Clint, 2002). Yan and Masliyah, 2001 show that pH changes the wettability of clay particles and alters the droplet size. The value of pH also alters the surface charge of particles.

In section 2.3, we have discussed that surfactants stabilize an emulsion by lowering the interfacial tension, but in the case of Pickering emulsion stability cannot be directly linked to the lowering of the interfacial tension. So, it is worth wondering how solid particles stabilize emulsions. Pickering, 1907 was the first to mention that emulsion stabilization should not depend on a decrease of the interfacial tension but on the size of the colloidal particles. Tambe and Sharma, 1993, investigated the mechanism of coalescence of droplets covered with solid particles. When they are adsorbed at the interface, solid particles form a solid layer around the droplets which prevents the droplets to coalesce. The ability of particles to stabilize the emulsion depends on the magnitude of the steric hindrance to droplet coalescence. The effectiveness of solid particles in stabilizing emulsions seems to be due to the formation of a closely packed layer of particles at the oil-water interface (Tambe and Sharma, 1993). However, some recent studies have shown that emulsions could be stabilized by solid particles despite of low droplet surface coverage ( Vignati et al., 2003 ;Midmore, 1999).

#### **2.4.2 Parameter influencing the stability of Pickering emulsions**

##### **Hydrophobicity**

The strength at which a particle is adsorbed at the oil-water interface depends on its hydrophobicity, which is directly related to the contact angle of that particle assumes at the oil-water interfaces. Particles must be wetted by both liquids to be adsorbed at the interface. Too hydrophilic or hydrophobic particles remain in the liquid in which they are dispersed. Binks and co-workers have shown that predictions based on considerations of the energy of attachment of a spherical particle at the oil-water interface (Equation 2.2) were directly related to emulsion stability. It is generally accepted nowadays that particles with a contact angle between 60° and 80° stabilize O/W emulsions while those with a contact angle between 100° and 130° stabilize W/O emulsions.

##### **Oil type and volume fraction**

The type of emulsions stabilized by particles with a contact angle around 90° depends on the volume fraction of water. For emulsions prepared with toluene and water, it was shown that for the lowest volume fractions of water a W/O emulsion was formed while an O/W emulsion was formed for higher volume fractions of water. The ability to make O/W or W/O emulsions with the same particles, for a given oil-water system, represents a significant advantage compared to surfactant systems (Binks and Lumsdon, 2000). Particles at intermediate hydrophobicity (contact angle around 90°) can be dispersed in both water and oil. For the same toluene-water system Binks and Lumsdon showed that, in the presence of particles at intermediate hydrophobicity, the type of emulsion was dictated by the phase in which the particles were initially dispersed; W/O emulsions were preferentially formed if particles were dispersed in oil, while O/W emulsions were preferentially formed if particles were dispersed in water (Binks and Lumsdon, 2000). The effect of oil type was also investigated in the same study. The authors showed that O/W emulsions were preferentially formed when non-polar oils (hydrocarbons) were used, whereas W/O emulsions were preferentially formed when polar oils (esters, alcohols) were used. This was confirmed by Frelichowska et al., 2009.

## Solid particle concentration

Tambe and Sharma, 1993 showed that droplets must be covered with a closely packed layer of particles in order to prevent coalescence. This was confirmed by Frelichowska et al., who investigated the effect of hydrophobic silica particles on the stability of O/W emulsions (Frelichowska et al., 2010). They proved that at low silica concentrations, emulsions were not stable, while by increasing the silica content, emulsion stability was enhanced. Moreover, they showed that droplet size could be controlled by adjusting particle concentration, and that beyond a certain silica concentration, there was no change in the droplet size. They also showed that the oil-to-silica ratio was the relevant parameter to control the droplet size. During emulsification high particle content limit re-coalescence, which provides small size droplets in the emulsion. By increasing particle concentration, more colloids are available in the system to adsorb at the newly formed droplet surfaces, thus more coalescence is stopped at higher particle content (Aveyard et al., 2003; Guillot et al., 2009).

## Flocculated particles

If the finely divided solid forms a stable suspension in one of the liquids, it may be necessary to add a weak flocculating agent before a satisfactory emulsion can be produced. But a powerful flocculation agent will usually prevent emulsification (Briggs, 1921). The two main methods to achieve a particle flocculation are the addition of electrolytes in the system and the adjustment of the pH of the aqueous phase (Yan et al., 2006; 2007; Binks and Whitby, 2005). Ashby and Binks (2000), showed that Stable O/W emulsion with Laponite RD clay particles are better formed under conditions where the particles are flocculated via salt (NaCl) and at intermediate concentrations of clay. NaCl is a weak flocculator which has been used in our experiment also with Laponite RD to produce a better stable W/O emulsion. The relative flocculating power of Na<sup>+</sup> is 1.0 which is much lower than K<sup>+</sup> (1.7), Mg<sup>2+</sup> (27) or Ca<sup>2+</sup> (43) etc.. The cation (Na<sup>+</sup>) helps to flocculate negatively charged clay plates.

## 2.5 Viscosity and flow rate of fluids

The dynamic viscosity of a fluid is its resistance to flow to an applied stress. It is a quantitative property of a fluid, be it liquid or gas, and can be used as an index in quality control applications of oils, paints or other fluids where flow is a critical property. Viscosity arises from the directed motion of molecules past each other and the transfer of momentum. Poiseuille (1844) did much work concerning the interpretation of liquid flow through tubes. One important result of his mass transport analysis is the following equation:

$$\mu = \frac{\pi r^4 P t}{8 V L} \quad (2.3)$$

where  $\mu$  is the viscosity,  $t$  is the elapsed time,  $V$  is the volume of liquid passing through the tube,  $P$  is the hydrostatic pressure of the liquid and  $L$  is the distance travelled by the liquid in time  $t$ . The unit of viscosity ( $\mu$ ), is named in his honor and is called the poise (P). It has units of 1 g/cm.s (or dyne-seconds/cm<sup>2</sup>).

The kinematic viscosity is the ratio of the dynamic viscosity  $\mu$  to the density of the fluid  $\rho$ . This represents as,

$$v = \mu / \rho \quad (2.4)$$

The flow rate of a liquid is how much liquid passes through an area in a given time. The flow rate can be expressed in either terms of cross sectional area and velocity or volume and time.

$$Q = v \times a \quad (2.5)$$

where  $Q$  is the flow rate,  $v$  is the velocity of the fluid, and  $a$  is the area of the cross section of the space the fluid is moving through. Or,

$$Q = V/t \quad (2.6)$$

where  $Q$  is the flow rate,  $V$  is the Volume of fluid, and  $t$  is elapsed time

In our experiment we measured dynamic viscosity of silicone oil for given kinematic viscosities (10 and 100cSt) by using equation 2.4 and, flow rates in the experiment were in term of volume and time such as  $\mu\text{l}/\text{min}$  or  $\text{ml}/\text{hr}$ .

## 2.6 Surface tension

Liquids consist of molecules, each of which is surrounded by other molecules with a distance close the molecule diameter and there is strong, short-range and attractive cohesive forces (Van Der Waals forces) that act between the liquid molecules which are responsible for the phenomenon known as surface tension. If the surface is between two liquids such as water and oil, it is called interfacial tension. An interface is a surface forming a common boundary between two phases. The work required to change the shape of a given interface is known as interfacial tension. To remove the molecule from the other molecules, force act against the intermolecular force. The bulk of the liquid, the force of cohesion between the molecules is the same in all directions (Figure 2.10). But the molecules on the surface get a net force of attraction that pulls them back into the body of the liquid since there are more molecules below than above and outside the surface. Each of the molecules inside the liquid is bound by the other molecules and they possess a negative potential energy. This potential energy increases when it tries to move the molecules outside the liquid. Therefore, molecules on the surface have higher potential energy than the molecules in the bulk of the liquid. Every system tries to keep the lowest potential energy. To achieve this, the liquid tries to take the shape that has the biggest possible surface area/volume ratio, namely the shape of a sphere.

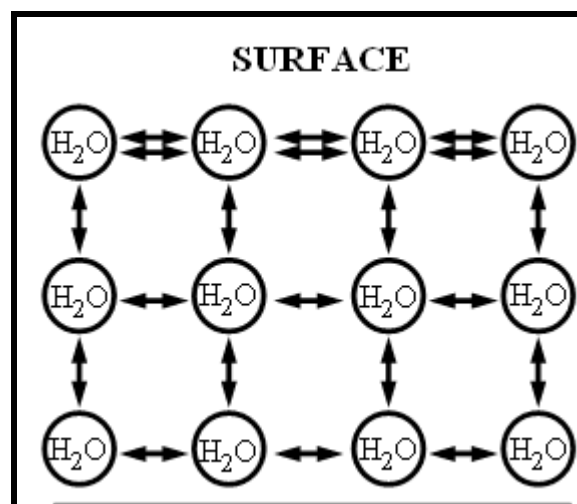


**Figure 2.10: The intermolecular forces in a liquid, molecule at the surface form stronger bonds.**

The surface area of a fluid volume reaches its minimum value in equilibrium. To increase the surface area, the work against the molecular forces has to be performed. The surface tension  $\gamma$  is defined as the work per unit required increasing the surface in constant temperature:

$$\gamma = dW/dA \quad (2.7)$$

$\gamma$  is also defined as the surface energy of the liquid and typically measured in  $J/m^2$  or  $N/m$ . Interfacial and surface tension effects will generally lead to a curvature of the interface. Upon mechanical equilibrium, the contraction forces acting at the interface must be balanced by a pressure difference across it. This pressure difference is related to the radius of curvature of the interface by the Young-Laplace equation:

$$\Delta P = \gamma (1/R_1 + 1/R_2) \quad (2.8)$$

where  $R_1$  and  $R_2$  are the radii of curvature of the surface in any two orthogonal tangents and is  $\Delta P$  the pressure difference. For a spherical droplet,  $R_1 = R_2 = R$ , and the pressure difference become:

$$\Delta P = 2\gamma/R \quad (2.9)$$

The pressure difference  $\Delta p$  is always such that the pressure is higher on the concave side of the interface. Because of the small dimensions typically encountered in microfluidic devices, the radii of curvature are also small, leading to large pressure differences across an interface. This effect may be exploited to drive liquid plugs at high velocities through microchannels - a technique referred to as capillary pumping (Yang et al., 2002; Stone et al., 2004).

### 2.6.1 Parameters influencing interfacial tension

The two main parameters affecting the interfacial tension are the temperature and the presence of a solute (sugar, salt, surfactant, etc.) in the bulk phases. Interfacial tension is strongly dependent on the temperature. Lutton et al. (1969) showed that triglyceride oil-water interfacial tension increased by increasing the temperature. On the contrary, Jennings (1967) showed that the interfacial tension of pure oil/pure water (benzene and n-decane/water) systems decreased with increasing the temperature. Cabrerizo-Vilchez et al. (1995) showed the same kind of behavior; interfacial tension decreasing with temperature. There is no theoretical model to describe the evolution of interfacial tension as a function of temperature, only empirical equations were developed, such as Eötvös' or Guggenheim-Katayama's law (1931).

The presence of solute is the other main factor that influences the interfacial tension. Solute types can be very different, such as sugar, salt, surfactant, etc. Sugar is considered for having no or extremely little effect on interfacial tension. Salt is known to usually to slightly increase the interfacial tension (Gaonkar, (1991). The effect of surfactant on the interfacial tension has been long investigated (Miller and Neogi, 2008; Rosen, 1989). Surfactants replace molecules of water and oil at the interface. The interaction across the interface is then between the hydrophilic moiety of the surfactant and water molecules on one side of the interface and between the hydrophobic moiety of the surfactant and the oil molecules on the other side of the interface. These interactions are much stronger than the original oil-water interactions, which reduces significantly the interfacial tension.

## 2.7 Wettability and Contact Angle

Wetting is a phenomenon easily observable in everyday life. For example, a drop of water on a horizontal glass surface tends to spread to form a thin film layer, while the same drop on a waxed surface tends to remain as a drop, eventually slightly deformed. The ability of a liquid drop to spread on a solid or to keep its original shape depends on the liquid's affinity for the solid. Strong affinity will lead the drop to spread, while weak affinity will lead the drop to remain as a drop or to form smaller beads when a shear force is applied on the drop. This affinity is referred to as wettability. In other words, wettability is the ease with which an air/solid interface can be converted to a liquid/solid interface when a liquid is dropped onto the solid (Rosen, 1989; Yasuda, 2005; Miller and Neogi, 2008). The most relevant parameter to characterize the wettability of a solid surface by a liquid is the contact angle ( $\theta$ ) that a liquid drop makes with the surface (Figure 2.11). As wettability is the ability of a liquid to spread on a solid, the interfacial energies must also be taken into consideration.

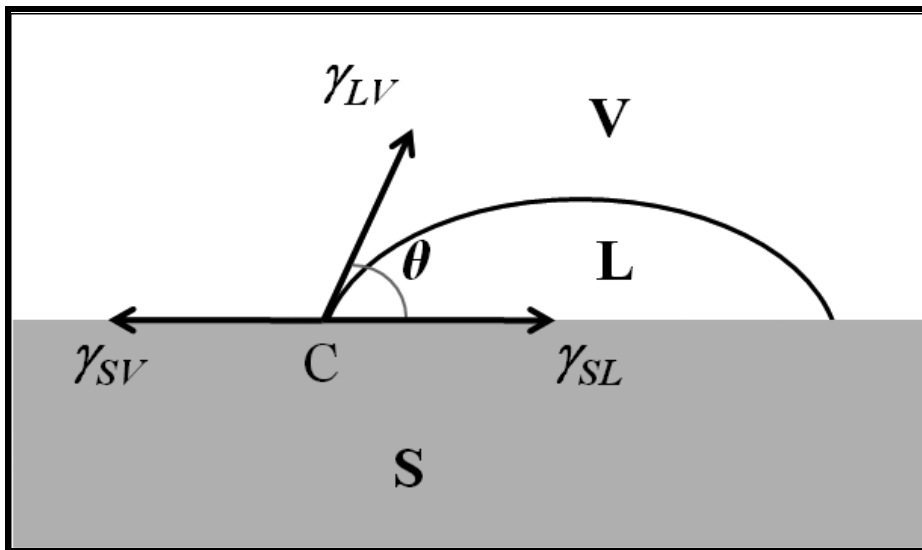


**Figure 2.11: Interfacial forces acting on a liquid drop (L) placed on a solid (S) surrounded by vapour (V).  $\gamma_{SV}$  is the interfacial tension between the solid and the vapour;  $\gamma_{SL}$  is the interfacial tension between the solid and the liquid;  $\gamma_{LV}$  is the interfacial tension between the liquid and the vapour.**

In Figure 2.11, the two fluid phases are liquid and vapor but the scheme would be the same if the vapour was replaced by a liquid, under the conditions that this liquid is immiscible with the liquid that forms the drop on the solid. In this figure, there are three interfaces: solid-liquid ( $\gamma_{SL}$ ) solid-vapour ( $\gamma_{SV}$ ) and liquid-vapour ( $\gamma_{LV}$ ). The line common to the three phases is called the contact line. The contact angle is very convenient to discuss the wettability of a solid by a liquid, as it can be seen in Figure 2.12.

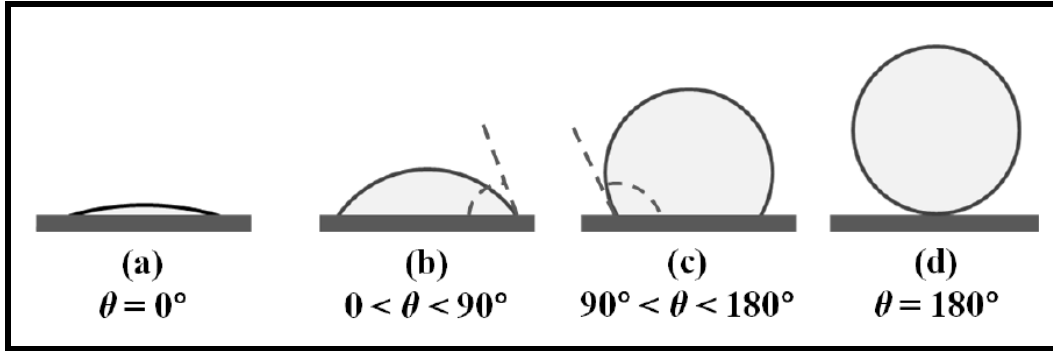


**Figure 2.12: Wetting described by various values of the contact angle; (a) Perfect Wetting, (b) Partial Wetting, (c) Non wetting, and (d) Perfect non-wetting.**

When the contact angle is zero (or very close to zero), the solid is perfectly wetted by the liquid. When the contact angle is between  $0^\circ$  and  $90^\circ$ , the solid is partially wetted. Between  $90^\circ$  and  $180^\circ$ , the solid is considered as non-wetted, and at  $180^\circ$  the liquid does not wet at all the solid. It is also common to characterize the wettability of a solid by its surface energy. For example, the wettability of a solid of high surface energy (e.g. Magnesium oxide or mercury) by water is excellent, while the wettability of solid of low surface energy (e.g. Polyethylene) of water is very poor (Yasuda, 2005).

## 2.8 Two phase microfluidic flow

### 2.8.1 Fundamentals of two phase flow in microchannel

The channel geometry, flow conditions and the properties of the two fluids control the two phase flow in microchannel. Some important dimensionless numbers are used to describe these factors such as the Reynolds number, Bond number, capillary pressure etc.

Flow of fluids in microfluidic system is usually characterized by low value of the Reynolds number. The Reynolds number ( $Re$ ) describes the relative importance of inertial forces of viscous forces

$$Re = \rho u d / \mu \quad (2.10)$$

where  $\rho$  is fluid density ( $kg/m^3$ ),  $u$  is the characteristic velocity (m/s),  $d$  specifies a characteristic length scale (m) and  $\mu$  dynamic viscosity (Pa.s) of the fluid. The Bond number ( $Bo$ ) compares the importance of gravitational forces relative to interfacial tension forces.

$$Bo = \Delta \rho g d^2 / \sigma \quad (2.11)$$

Where  $\Delta \rho$  is the fluid density difference ( $kg/m^3$ ),  $\sigma$  is the surface or interfacial tension of the two fluids in contact (N/m) and  $g$  is the gravitational acceleration ( $m/s^2$ ). On the micro scale Bond and Reynolds numbers are far smaller than 1. Therefore, two forces (interfacial and viscous) dominate inertial and gravitational forces. Thus the capillary number ( $Ca$ ) becomes the most important dimensionless parameter which represents the relative effect of viscous forces to interfacial tension forces

$$Ca = \mu u / \sigma \quad (2.12)$$

Where  $\mu$  is the dynamic viscosity (Pa.s),  $u$  is the characteristic velocity of the flow (m/s) and  $\sigma$  is the interfacial tension between the two fluids (N/m).

Each of the parameters in the equation (2.12) can be controlled. For example, the interfacial tension between two fluids (oil and water) can be lowered by adding a surfactant to the water similarly by changing flow rate, velocity of the fluids can be changed.

Two other important parameters based on Ca and Re are Ohnesorge number (Oh) and the Weber number (We). Oh number relates the importance of viscous force to inertial and interfacial tension forces, while the We number compares inertial effects to surface tension.

$$\text{Oh} = (\text{Ca} / \text{Re})^{1/2} = \mu / (\rho d \sigma)^{1/2} \quad (2.13)$$

$$\text{We} = \text{Re} \text{Ca} = \rho u^2 d / \sigma \quad (2.14)$$

Another group of dimensional parameters is related to the fluid properties and the operating conditions, including the density ratio ( $\alpha$ ), viscosity ratio ( $\beta$ ) and flow rate ration ( $\varphi$ ):

$$\alpha = \rho_c / \rho_d \quad (2.15)$$

$$\beta = \mu_c / \mu_d \quad (2.16)$$

$$\varphi = Q_c / Q_d \quad (2.17)$$

Where  $Q$  is the fluid flow rate ( $\mu\text{L}/\text{min}$ ) and the subscripts  $c$  and  $d$  represent the continuous and disperse phase respectively (Zhao and Middleberg, 2011).

## 2.8.2 The geometry of the T-junction

Microfluidic structures play an important role in controlling liquid-liquid flows. The most popular and most frequently used microfluidic device for the generation of droplets is a T-junction. In a T-junction, two channels of the junction merge at a right angle. It operates one of two modes, cross flowing and a perpendicular flowing. In cross flowing the continuous phase is introduced from the horizontal channel and the disperse phase flows through the perpendicular channel so that the droplets are sheared off by the cross-flowing shear force (Thorsen et al., 2001). Perpendicular flowing contrary to cross flowing in which continuous phase flow introduced from the perpendicular channel and the disperse phase flow from the horizontal channel (Xu et al., 2006). Compare with the perpendicular flowing technique, the cross flowing rupture technique produces droplets with a narrower range of droplet size (Zhao and Middleberg, 2011). Garstecki et al., 2006 experimentally proved the geometry of the device plays a significant role in the break-up process. According to their experiment the geometry that promotes the squeezing mechanism can be described by two conditions. The first condition is that the width of the main channel should be greater than its height and the width of the inlet channel should be at least equal to half the width of the main channel.

In our system, it has been used cross flowing shear method in T-junction. In the experiment, the carrier fluids were castor oil and silicone oil of different viscosities that introduced from



the horizontal channel of the junction while the disperse phase (de-ionized water with clay or without clay) flows through the vertical channel. The channels have an oval cross section. The geometry of one of the T-junction used in this thesis report is given below in Figure 2.13

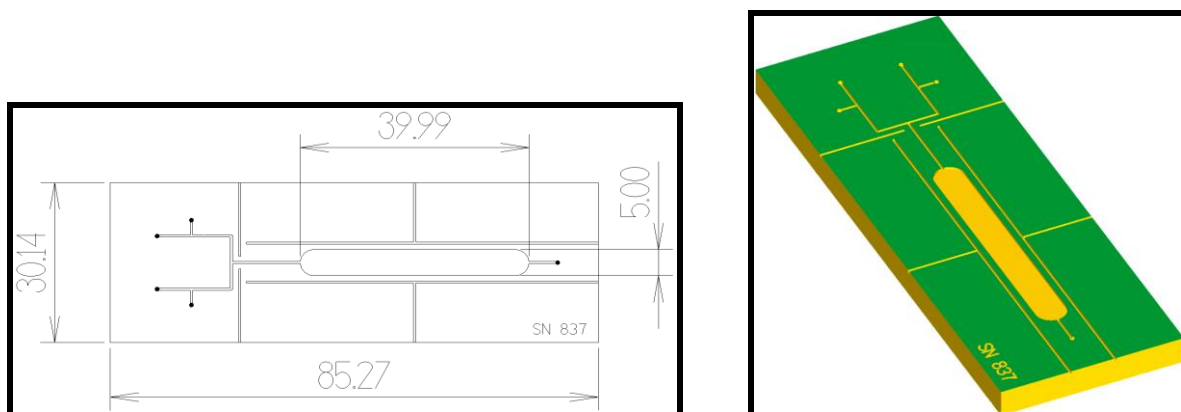


**Figure 2.13: The geometry of a T- junction. The figure got from the manufacturer, Institute of Physical Chemistry at Polish Academy of Sciences<sup>4</sup>.**

### 2.8.3 Droplet formation regimes in T-junction

There are two kinds of droplet patterns produced at the T- junction, short spherical droplets and longer ‘plug’ droplets by varying the flow rates of the continuous and disperse phases. The plug length decreases with the flow rate ratio of the continuous phase to the disperse phase ( $Q_c/Q_d$ ) and the total flow rate in cross flowing mode (Nisisako et al.,2002; Xu et al,2005). Tica et al (2004) observed three droplet formation regimes when changing the flow rate. These are squeezing, dripping and jetting regimes. In the squeezing regimes both flow rates and capillary number are low ( $Ca$  typically less than 0.01) and droplet plugs are sheared off right at the T-junction. The sharp break up is due to the domination of the interfacial tension force pronounced at low flow rates. By increasing the flow rates and  $Ca$  number, the disperse phase flows a bit into the horizontal channel and forms a long neck before the plugs are sheared off. This is dripping regimes. Even longer necks are formed in the jetting regimes, but the plug size becomes smaller when the flow rates and  $Ca$  increases further. The relative viscous force becomes more dominant when the flow rate increases and the interfacial tension force are no longer sufficient for sharp plug breakups. This allows a laminar flow of the disperse phase in the horizontal channel before the shear off takes place. According to Tica et al. the range of squeezing, dripping and jetting regime are  $7.0 \times 10^{-2} \leq Ca \leq 7.6 \times 10^{-2}$ ;  $1.9 \times 10^{-3} \leq Ca \leq 8.2 \times 10^{-2}$  and  $2.2 \times 10^{-2} \leq Ca \leq 1.1 \times 10^{-1}$  respectively. These three regimes have been confirmed numerically by Demench et al., 2008.

In our system we observed how the droplets length varies with the flow velocity of continuous and disperse phases. We found the transition of droplets from squeezing to the dripping regime in flow experiment which will be discussed in more details later in result and discussion section (chapter 4).

<sup>4</sup> Institute of Physical Chemistry at Polish Academy of Sciences, by courtesy of Zbigniew Rozynek.

## 2.8.4 Droplet formation mechanism in T-junction

It is very much important to understand the droplet formation mechanism in a T-junction to control and adjust the behavior of the flow pattern. One approach was taken by Thorsen et al., 2001 and Tan et al., 2004, analyzed the forces involved in the droplet formation process. Variables that affect the dynamics of droplet formation in T-junction are channel geometry, structure and properties (channel type, hydrophobicity), fluid properties (density, viscosity, interfacial tension and contact angle) and operating parameters (pressure, flow rate ratio, temperature, electric field etc.). There are several dimensionless parameters used to express these variables and some variables depending on parameters are more dominant than the others. As mention before, the micrometer scale, the effect of gravity and inertia can typically be ignored and therefore the capillary number becomes the most important dimensionless parameter which distinguishes the three droplet formation regimes that have been defined as squeezing, dripping and jetting regimes.

Corresponding to these three flow regimes there are two more dynamical models for a droplet break-up in a microfluidic T-junction. When the capillary number is below 0.01 (squeezing regime), the shear stress is much smaller than the inertial force. So, the droplet break-up is governed by the hydrostatic pressure drop across the emerging droplets. In a T-junction two immiscible fluids form an interface at the junction of the inlet and main channel. The discontinuous phase penetrates into the main channel and droplet begins to grow (Figure 2.14, 1).

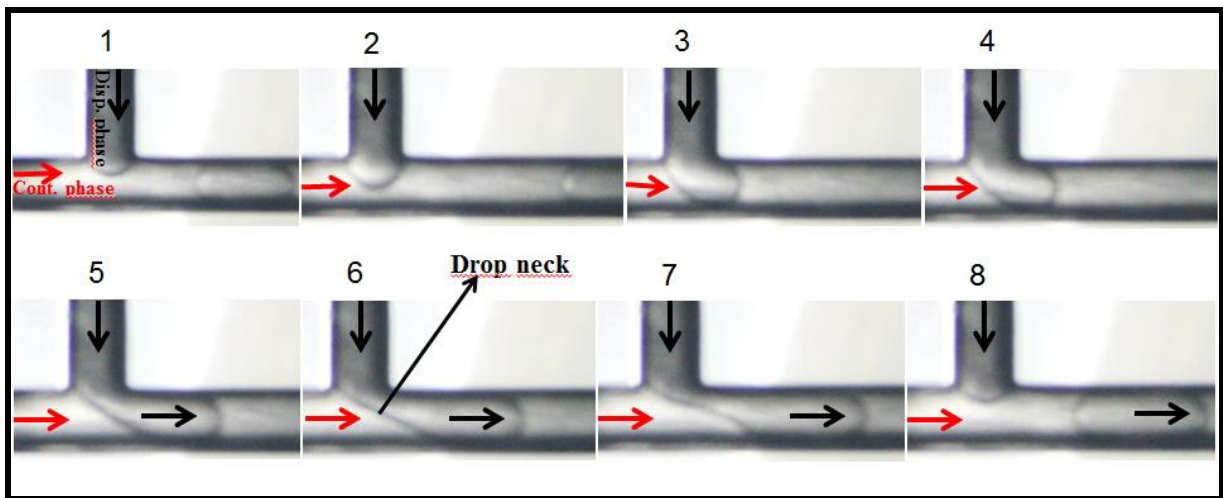


**Figure 2.14: Droplet formation mechanism in a T- junction.**

This growing droplet expels the continuous fluids around itself and induce extra pressure which is called Laplace pressure. There is a local velocity and pressure fluctuation during the droplet formation period and the fluctuation decreases in amplitude when the continuous phase velocity increases (Li et al., 2012). Li and his team found that inner droplet circulation motion caused by shearing on the interface and Laplace pressure. This motion indicates that the pressure inside the droplet is dynamic. The local pressure near the T-junction inlet increases as the droplet formed and it reaches to its peak right the before the drop reaches the wall (Figure 2.14, 2). Then the pressure in the continuous flow is higher than the Laplace pressure (resistance pressure). The Laplace pressure in disperse phase decreases with increasing the curvature of the drop. The droplet travels downstream direction and droplet neck decrease until it breakup (Figure 2.14, 3 to 8). The disconnected liquid plug flows

downstream in the main channel while the tip of the stream of the discontinuous phase retracts to the end of the inlet and the process repeats (Li et al., 2012 and Garstecki et al., 2006). This droplet formation mechanism in squeezing regime is known as “rate –of- flow controlled” breakup or confined breakup (Garstecki et al., 2005, 2006a).

Over a wide range of rates of flow of both phases, this process generates uniformly sized droplets. The volume of these droplets can be adjusted by changing the rates of flow of dispersed phase ( $Q_{water}$ ) and the carrier fluid ( $Q_{oil}$ ). Garstecki et al (2006) proposed a simple scaling law for the size of a droplet in the squeezing regime

$$L/w = 1 + \alpha Q_{in}/Q_{out} \quad (2.18)$$

Where  $L$  is the droplet length,  $w$  is the width of the channel,  $Q_{in}$  and  $Q_{out}$  are the rates of flow of the dispersed and carrier fluids respectively, and  $\alpha$  is a constant of order one, whose particular value depends on the geometry of the T- junction. This scaling relation is almost independent of the fluid properties, but the effect is specific for microsystem at low flow rate and low value of capillary number. This scaling law was later modified by Xu et al. (2008) and verified numerically by De Menech et al., 2008. The modified scaling law is

$$L/w = \varepsilon + \delta Q_d / Q_c \quad (2.19)$$

Where,  $\varepsilon$  and  $\delta$  are fitting parameters depending on the geometry of the T-junction.  $Q_d$  and  $Q_c$  are the flow rate of the dispersed and continuous phase respectively. Tica et al., 2003 and Xu & Luo et al., 2008, also reported scaling law as

$$L/w = 1.9 + 1.46 Q_d / Q_c \quad (2.20)$$

$$L/w = 1.38 + 2.52 Q_d / Q_c \quad (2.21)$$

When the capillary number is above a certain critical value such as  $Ca > 0.01$ , shear stresses start to play an important role in the processes of droplet formation mechanism in T-junction. This dynamical model is called shear-driven breakup (Thorsen et al., 2001) or unconfined breakup (Husny & Cooper-White, 2006; Christopher & Anna, 2007). At this stage, the system in the T-junction starts to operate in a mode similar to the dripping regime in which the size of the droplet is controlled by the capillary number. Thus the droplet diameter decreases with increasing continuous phase flow rate, total flow rate and continuous phase viscosity ( $Ca \propto 1/D_d$ ). Xu et al., 2008 observed when the two phase flow is within the transitional regime between the squeezing and dripping regime, the dynamics of the droplet breakup are controlled by both of the mechanism. They proposed following the scaling law to describe the droplet size

$$L/w = \varepsilon + k (Q_d / Q_c)^\alpha (1/Ca)^\beta \quad (2.22)$$

where  $\varepsilon$  &  $k$  are fitting parameters and their values depend on channel geometries and  $\alpha$  &  $\beta$  are the ratio of two mechanisms (Xu et al., 2006 a, b c, 2008).

### 2.8.5 Parameters effect on two phase flow

There are different factors that affect the flow pattern and droplet formation in microfluidic channels. For example, phase parameters such as viscosity, interfacial tension, viscoelasticity; channel geometry, surfactant etc.

#### Effect of viscosity

Tica et al., 2009 studied the effect of viscosity on droplet formation in microfluidic channels and observed that it is possible to form a regular plug with both lower viscous (2.0 m PaS) and higher viscous (18 m PaS) dispersed and continuous phases and three regimes were found for all four combinations of low and high viscosity disperse and continuous phases. Actually the effect of viscosity on drop size is not straight forward, but the influence depends on the channel geometries and channel properties among other factors. Sometimes even in the same microchannel behavior can be complicated. Kobayashi found that in straight-through microchannel, the dispersed phase viscosity  $\eta_d$  greatly influenced the droplet size and not the type of oil. The droplet size decreases with increasing viscosity of disperse phase ( $Q_d$ ) below the threshold value, but above the threshold value its size slightly increases with  $Q_d$ . It is generally easier to compare the interaction between different properties with a dimensionless number then look at each property alone. The influence of viscosity on droplet formation can thus be read from the capillary number.

In our experiment we observed the effect of viscosity in continuous phase on droplet size formed in microchannel and how the influence of viscosity related with capillary number. It will discuss more elaborately in the result and discussion section (Chapter 4).

#### Interfacial effects on flow patterns

Interfacial effects become dominant and crucial when the length scale is reduced to the micrometer scale. There are two interfaces in microfluidic two phase flows, fluid-fluid and fluid-wall. The wetting properties of the fluid-wall interface are very important to determine whether ordered or disordered flow patterns occur (Dreyfus et al., 2003). The hydrophobicity or hydrophilicity property of a solid surface is also found to be important. The wall properties can be expressed quantitatively by contact angles. It is found that ordered flow patterns can only be observed for fluids, making contact angles larger than  $90^\circ$  (Xu et al., 2006c) with the channel wall. For contact angle beneath this, only disordered flow patterns can be observed. However, the contact angle can be changed by adding surfactants at different concentrations (Xu et al., 2006a).

#### Surfactant effect

At the micrometer scale, the large surface area to volume ratio makes surface effects more salient. However, at the same time, the actions of the surfactants are reduced due to the scale effect (Tabeling, 2005). Adding surfactants to the dispersed and continuous phase is often needed to stabilize the droplet formation (with regards to droplet size and spacing). Study shows that use of surfactants in the dispersed phase in T-junction droplet formation experiments decreases the interfacial tension between the liquids and droplet diameter compared to systems without surfactants (van der Graaf et al., 2005; Campos, 2011). When the interfacial tension between the dispersed and continuous phase is decreased, the flow resistant pressure in the droplet is smaller and its ability to withstand the pressure for the

continuous phase is impaired. The droplet neck will thus break faster and less disperse phase will flow into the main channel before the droplet form and flow downstream.

It is also found that increasing the surfactant concentration in the continuous phase results in smaller droplet sizes. The influence of surfactants in droplet formation is complex. Surfactants can reduce the interfacial equilibrium interfacial tension, but they may also exert dynamic effects by altering interfacial rheology and introduce dynamic interfacial tension effects (Schroder et al., 1998, van der Graaf et al., 2004). The mentioned effects affect droplet formation in a complex way that is not fully understood. It is observed that dynamic interfacial tension between two liquid phases is neither constant nor uniform and becomes more significant at low surfactant concentrations (Sugiura et al., 2004).

### **Effect of microfluidic geometry**

As we have already discussed in section 2.8.2, the geometry of microfluidic has an important role in controlling liquid- liquid flows. In our system, we used cross flowing shear method in T-junction. The advantage of this method comparable with the perpendicular flowing technique in a T - junction is, the cross flowing rupture technique produces droplets with a narrower range of droplet size. (Zhao and Middleberg, 2011). The T- junction having microchannels with rectangular cross sections have four open gutters and a thin film above the droplet where continuous fluid flows around the moving droplet.  $\mu$ -PIV experiments show that for a quadratic cross section microchannel, at least 25% of the continuous fluid volume leaks through the four gutters before droplets detachment (van Steijn et al., 2007). In the squeezing regime, such leakage leads to a flow reversal that dominates the droplets detachment process. For oval cross section microchannels, as used in our experiments, this leakage is minimal because there is practically no available space around the formed droplets. This results in an increase in the pressure exerted by the continuous phase on the drop and less time for the disperse phase to fill the microchannel. Thus a T- junction having microchannels with circular geometry is expected to produce shorter droplets than a T-junction with rectangular microchannels. Laizoa et al, 2013, showed that the cross-sectional area of the main channel can influence the volume of droplets detached significantly in both squeezing regimes as well as in dripping regime.

To produce the stable O/W or W/O emulsion, droplet size is an important fact which depends on microchannel width. In the experiment studied here in this thesis report, mono dispersed,  $\leq 0.4$  mm size droplets were produced in T-junction. Microchannel thickness was  $\sim 400\mu\text{m}$  and reservoir was 7mm wide. The depth of the reservoir is  $\sim 2000\mu\text{m}$ .

## **2.9 Materials of the microfluidic T-junction**

The historical progress of microfluidics has depended on the development of their suitable microfabrication schemes. There is a wide range of available techniques for fabrication of microfluidic chips in glass, quartz, silicon, and metals after two decades of research. Several polymers have been evaluated for fabrication of microchips. The most common are polydimethylsiloxane (PDMS) and poly-methyl methacrylate (PMMA). In laboratory practice the most common architectures of microfluidic chips comprise layers of PDMS or PDMS glass, PMMA and PC (polycarbonate)[Whitesides, 2006; Fletcher et al., 2002; Tiggelaar et al., 2006.; Capretto et al., 2008; Workman et al., 2007; Huangetal., 2007]. The chip has been used in our experiment was made of polycarbonate (PC).

Polycarbonate is an attractive material for the construction of microfluidic devices because of its high impact resistance, low moisture absorption, good machining, high glass transition temperature, transparency in the visible, biocompatibility, and relatively low cost. The mechanical strength of PC makes it possible to fabricate integrated, multilayer microfluidic devices that could contain a large number of droplet generators in parallel and to flow liquids at rates higher than those possible in soft polymers (e.g. PDMS). Importantly, PC is a material that can be processed easily at scale (e.g. using injection moulding), making it feasible to mass produce chips. The one remaining problem is the control of wetting of the surface of PC by aqueous and organic phases. It is thus necessary to increase the hydrophobicity of PC, because partial wetting of the walls of the channels by the dispersed phase prevents the production of stable droplets (Jankowski et al., 2010). The known and often used a modification of PC, particularly useful for modification of the surfaces of microchannels is caused by amine. The amine reacts with the carbonate groups to create urethane bonds. Bonding of an amine terminated with an alkyl chain renders a hydrophobic surface (Li and Wilkes, 1998; Oyama et al., 2001).

## Chapter 3

### 3 Experiment

The experiment was divided into two parts. In the first part, two phase microfluidic flow was observed while in the second part monodispersed Pickering emulsion was stabilized by Laponite clay. The experiment was performed at the Laboratory for Soft and Complex Matter Studies at NTNU. The experimental setup and method of the experiment described below.

#### 3.1 Experimental set up

The experimental setup is displayed in Figure 3.1. It consists of an injection system, microfluidic chip and acquisition devices.

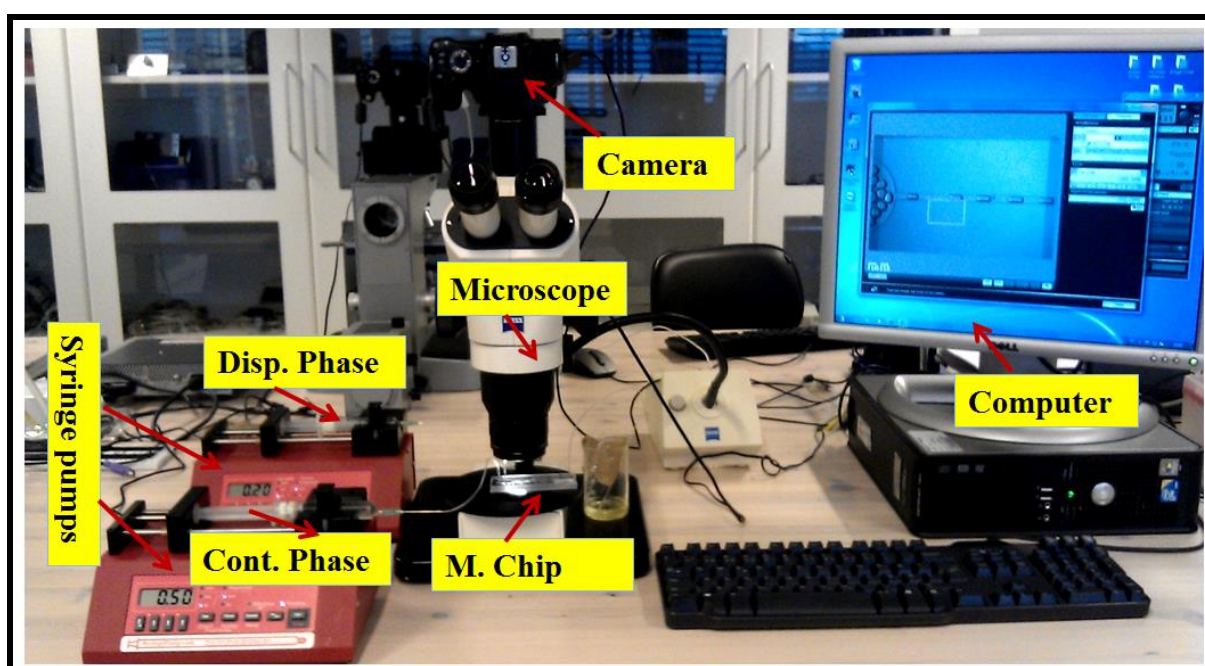


**Figure 3.1: Experimental setup of Microfluidic flow system: Two syringe pumps (NE-300) are used to control the flow rate. Liquids from the syringe are carried to the microfluidic chip via polyethylene tubes. Live view shoot of droplet formation in T-junction on computer using Axio vision software.**

##### 3.1.1 Injection system

The injection system consists of two syringes holding by two syringe pumps (NE-300) and a microfluidics chip which is connected to pumps and syringes with needles and thin narrow tubes.



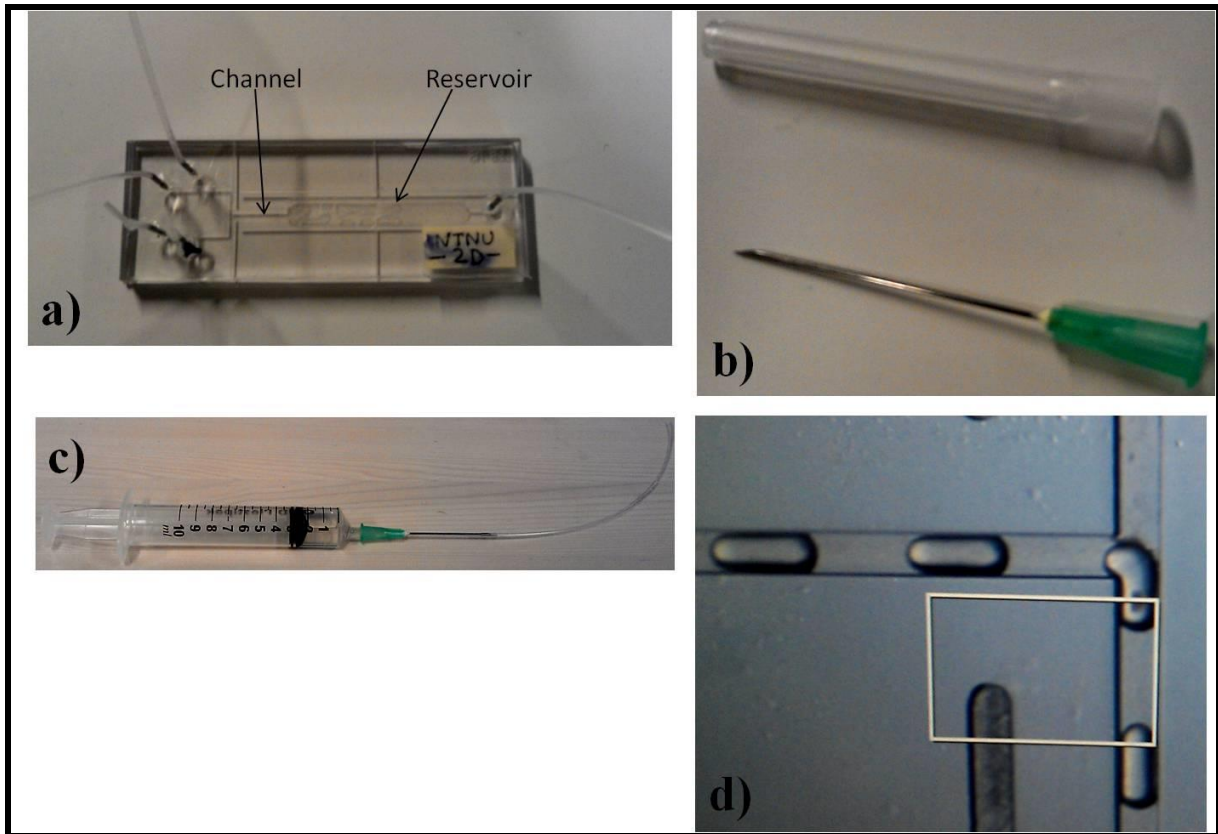


**Figure 3.2: Image of a) Microfluidic chip, b) Needle (0.8\*40mm), c) Syringe connected with Polyethylene tubing, d) 2-D image of T-junction.**

Syringes are made of BD plastic with a diameter of 14.50 mm, can contain 10 ml liquid. They are used to inject the fluids in the microfluidics chip. Two thin and narrow white non-toxic, non-radiopaque polyethylene tubes were connected with syringes by using two needles (0.8\*40mm). The other two ends of the tubes were connected with the main channel and inlet channel of the microfluidic chip respectively.

The syringe pump acts as pressure controller and pressure reducer. According to the information sheet from manufacturer NE-300 is a general purpose single syringe pump, capable of infusing at digitally set pumping rates. Infusion pumps of syringes up to 140cc. Pumping rates from 0.73 $\mu$ l/hr with a 1 cc to 1500 ml/hr with a 60 cc.

### 3.1.2 Fluids, clay and flocculated agent

In the two phase flow experiment, the effect of flow rate and viscosity on droplet size has been observed. For these reasons, silicone oil (delivered by Dow Corning 200, U.S.A) with different viscosities has been used as continuous phase while water with or without clay used as dispersed phase in the experiment. Silicone oil is similar to traditional hydrocarbon oil except for its molecular chain replaces carbon units with siloxane units. This oil is a nonflammable, nontoxic, tasteless, and odorless material. The silicone oils used in this experiment have kinematic viscosity 10 and 100cSt and dynamic viscosity 0.00 935 Pa.s and 0.096 Pa.s respectively at 25°C. The viscosity of the water is  $8.90 \times 10^{-4}$  Pa.s at about 25°C. The water used in the experiments was purified de-ionized water. Silicone oil has been chosen for the experiment due to the availability with different viscosities of it (10, 100, 200, 500, 1000 cSt etc) in the lab.



To find the stable W/O Pickering emulsion, experiments performed with both castor oil (LO4224) and silicone oil with different viscosities (100 cSt, 500cSt, 1000cSt). Castor oil is a colorless to very pale yellow vegetable oil, which has been delivered by Alfa Aesar, Germany. It has high viscosity. At a 25°C temperature its dynamic viscosity is 0.65Pa.s, density is 961kg/l.

**Table 3.1: Density ( $\rho$ ), dynamic viscosity ( $\mu$ ) and Surface tension ( $\sigma$ ) at 25°C for castor oil, silicon oils and water.**

Fluids	Density(kg/l)	Dynamic viscosity (Pa.s)	Surface tension(mN/m)
Castor oil	0.961	0.65	39
Silicone oil (10cSt)	0.935	0.00935	20.1
Siliconeoil (100cSt)	0.965	0.0965	20.9
Water	998.5664	$8.90 \times 10^{-4}$	63.7

One of the main differences between castor oil and silicone oil is their polarity. Silicone oil is non-polar oil; they lack an electronegative element like oxygen, which results in their typical hydrocarbon feel whereas castor oil is polar oil. Polar Oils contain heteroatoms that differ in electronegativity. This results in a dipole moment. These oils have unique characteristics due to their polar nature. They require higher HLB emulsifiers to make stable emulsions; they dissolve materials that are insoluble in nonpolar oils (Tony, 2008). Water is also a polar molecule as the H side of the molecule is partially positive and the O side of the molecule is partially negative.

The clay sample, a synthetic Laponite RD powder used in this experiment is pursued from Rockwood, England. The information about Laponite RD is described in more detail in section 2.1.2. To find, the better stability of W/O emulsion, a flocculated agent salt (NaCl), used in our experiment. This is a weak flocculator. The relative flocculating power of Na<sup>+</sup> is 1.0, which is much lower than K<sup>+</sup> (1.7), Mg<sup>2+</sup> (27) or Ca<sup>2+</sup> (43) etc. The cation (Na<sup>+</sup>) helps to flocculate negatively charged clay plates.

### 3.1.3 Microfluidic chip

The chips used in this experiment are microfluidic T-junctions which are made of two polycarbonate (PC) pieces manufactured in Poland<sup>5</sup>. It has been used high pressure (0.7 Mpa) with a temperature of 130° C for an hour to connect these two pieces by thermal sintering. For simplicity, we call the chips as 2D and 3D chips. The width of the channels in both chips is around 400µm. The only difference between the two chips is their reservoir. In 3D chip the reservoir thicknesses and width are > 2mm and 7mm respectively, whereas reservoir depth and width in 2D chip are ~ 0.4mm and 5mm respectively. Due to the very less thickness of the reservoir, second chip is called as 2D, where big droplets are getting squeezed. These polycarbonate(PC) chips have hydrophobic surface so that they were capable to produce W/O emulsion only. The surfaces of the chips are very smooth and they have high visibility. They are applicable for fluid mixing, micro-droplet formation and reactions etc.. The geometry of the channels presents an oval cross-section with same size throughout the whole length of the channel. The configurations of the chips used in the experiment are given below in Figure 3.3.

<sup>5</sup> Institute of Physical Chemistry at Polish Academy of Sciences, by courtesy of Zbigniew Rozynek

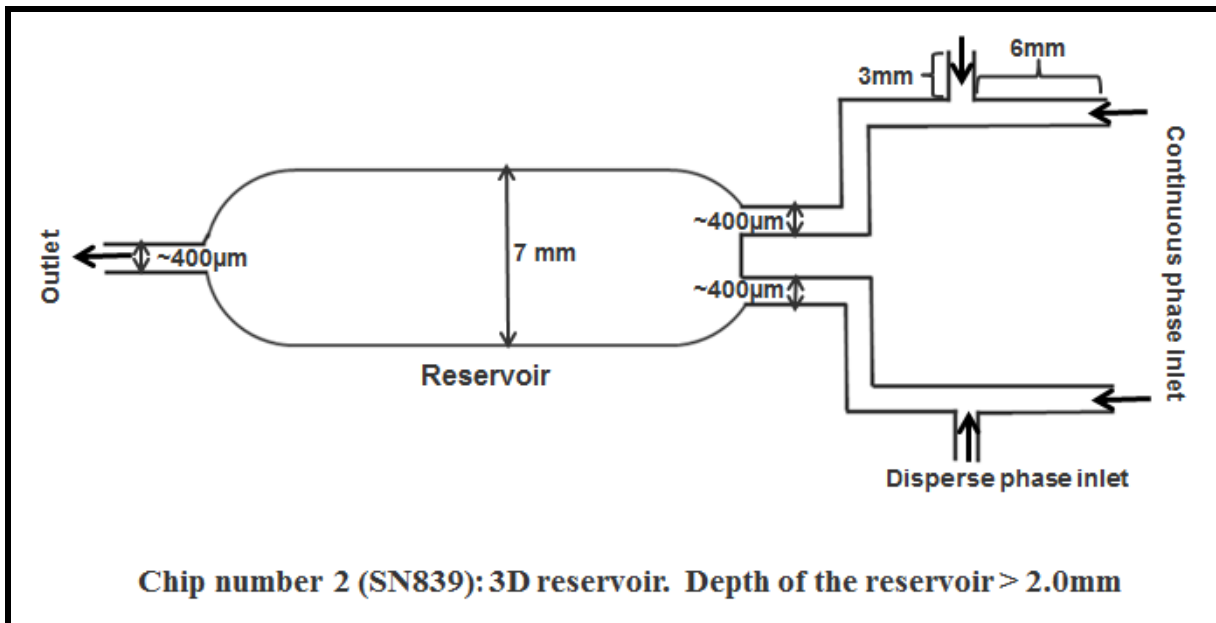
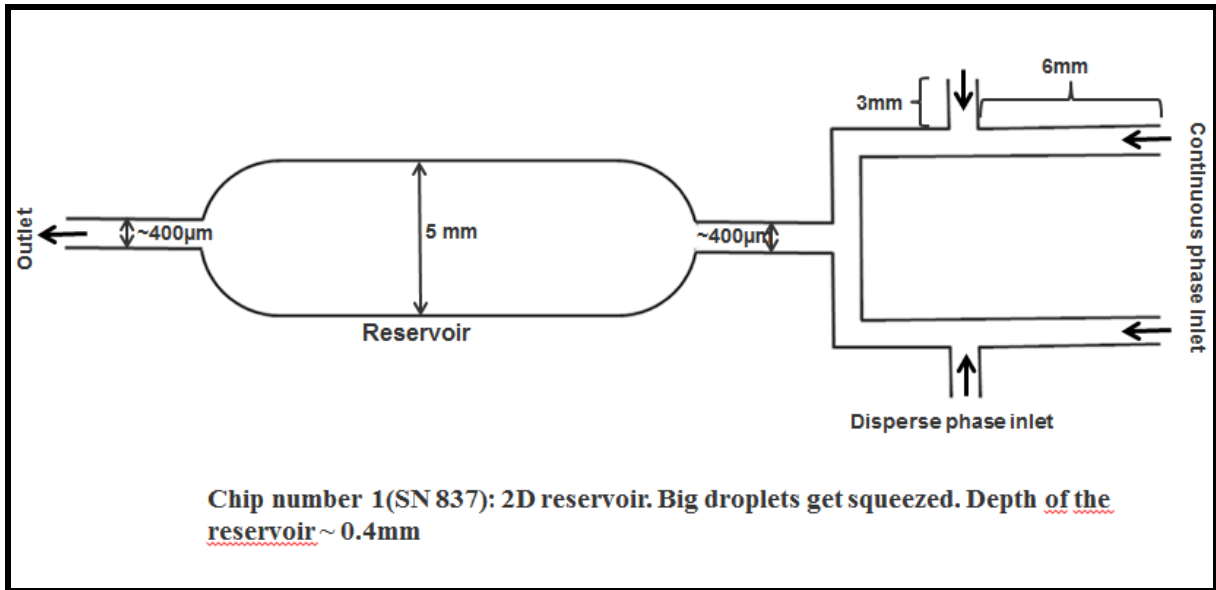


**Figure 3.3: Configuration of the chips used in the experiment done by using paint. The measured widths were almost similar to the information got from the manufacturer.**

### 3.1.4 Acquisition system

The acquisition system consists of an Axiovert 40MAT (Carl Zeiss) optical microscope with adjustable light. This microscope has different lenses that can be used. In our experiment used lens was 2.0x 45 50 28. A camera (Canon, EOS 550D) is connected to the microscope as well as with the computer. This set-up allows a live view on the computer so that it is possible to observe exactly the same thing on the computer screen as through the microscope. The Axio Vision software developed by Carl Zeiss has been used for this analysis. This software is well suited for capturing and processing picture and videos. It also has tools for manual and automatic measurements of parameters like distances, diameters and areas.

## 3.2 Experimental method

### 3.2.1 Two phase microfluidic flow in T-junction

Two phase (liquid-liquid) microfluidic flow experiments have been performed by using the cross flow shear method in T-junction. Monodispersed droplet produced in the microchannel and effect of clay and different parameters such as flow rates, viscosity or capillary numbers on droplets size has been observed.

#### 3.2.1.1 Experimental observation of formation of droplet and effect of flow rate and viscosity on it in microfluidic T-junction

All microfluidic channels, tubing and needles have been flushed with Isopropanol before the experiment for proper cleaning. Later on, the syringes were filled with sample fluids. Syringes with tubes were held vertically and around 1/2 ml of fluids was pushed out from syringes to avoid air bubbles in the syringes and pipes. Confirming no air bubbles left in the syringes and pipes, the syringes were fastened to the syringe pumps and other ends of the pipes were connected to the microfluidic chip. Avoiding air bubbles are very important because they can alter the result. Similarly, another important thing is to prevent leakage which hampers to provide accurate flow rate. For this reason connection should be tight. Microfluidic T-junction was placed in the microscope picture center.

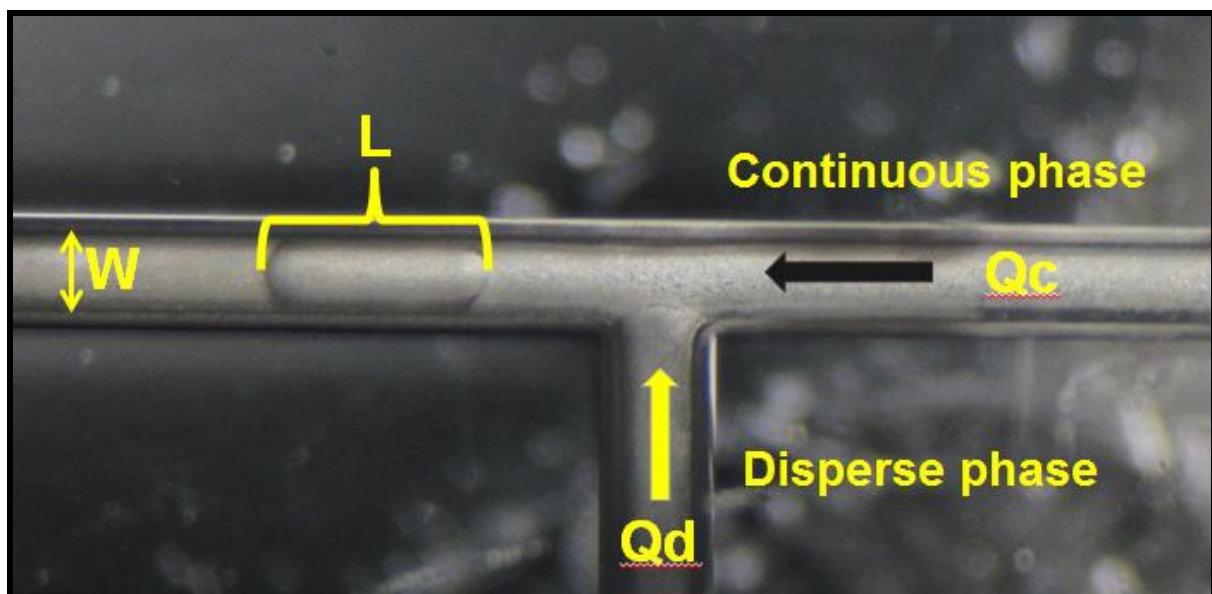


**Figure 3.4:** Image of droplet formation in microfluidic T-junction. The continuous flows in the horizontal channel with flow rate  $Q_c$ , while the disperse phase flows in the vertical channel with flow rate  $Q_d$ .  $L$  is measured droplet length and  $W$  represents the microchannel diameter.

At first, the pump with silicon oil was turned on where silicone oil has been used as continuous phase. The reason for choosing oil as continuous phase of the experiment is the hydrophobic surface of the chip which can produce W/O emulsion only. We know continuous phase is carrier fluid. So it should fill the microchannel first and wet all surfaces. Later on, the dispersed phase (water) was pumped in. The cross flowing mode has been initiated here by introducing the continuous phase from horizontal channel and discontinuous phase flowed through the perpendicular channel. The initial flow rates on both pumps were  $0.50 \mu\text{L}/\text{min}$  and  $1 \mu\text{L}/\text{min}$  respectively. Camera and Axio vision software were turned on.

After 15 to 30 minutes both fluids were flowing continuously and the system became stable with these flow rates, since the droplets formed in the T- junction had more or less the same length and interval. After a few more minutes images were captured with either 10 or 30 second interval between each shot.

To see how the droplet size varies with flow rate, one phase was kept constant and other phase was changing. First, the continuous phase flow rate was constant and dispersed phase changed. Then dispersed phase flow rate kept constant for different values of the continuous phase. Every time the flow rate was changed and I waited 20 to 30 minutes for the system to stabilize before taking pictures. Droplet lengths were measured manually from captured picture in Axio vision by using S size scale whose resolution was 4  $\mu\text{m}$  per pixel for 0.65 magnifications.

To characterize the shear stress exerted by the continuous phase on the interface in the break-up process, we measured the length (L) of the droplets produced in the reference T-junction ( $w=400\mu\text{m}$ ) as a function of  $Q_{\text{water}}$ , at different values of flow rate ( $Q_{\text{oil}}$ ) and viscosities ( $\mu$ ) of oil. In the experiment, silicon oil was used as a continuous fluid with two different viscosities (10cS and 100 cSt) and the values of  $Q_{\text{oil}}$  were 2.5, 5, and 10  $\mu\text{L}/\text{min}$ . Same as the previous experiment, water without clay was in dispersed phase. Each time to change the viscosity of silicon oil as continuous phase; we pumped it at least 30 minutes through the micro-channel. Thus, it can fill the channel thoroughly before starting the experiment.

### **3.2.1.2 Experimental study of different droplet formation regime in T-junction and effect of clay and viscosity on droplet size**

In this experiment water with or without laponite RD was dispersed phase and silicone oil with two different viscosities (10 & 100 cSt ) was continuous phase. Clay concentration was 1% in De- ionized water. Droplet sized measured as function of continuous phase flow rate  $Q_c$ , at a fixed value of  $Q_d$ . Before starting the experiment with clay, we prepared the 1% clay sample. After finishing the experiment chip were thoroughly cleaned. The cleaning is especially important when the sample contains clay particles that may block the microchannels. The cleaning procedure for clay is as follows: empty the syringes, microfluidic chips and tubes. Pumps water with 0.1 % HCl through the chip around 3hrs with a flow rate 2 ml/ hr. At the end, the microchannels were dried by blowing compressed air through them.

#### **Sample preparation**

The weight of the water and clay were measured separately by the balance machine (Ohaus Analytical plus) before they were stirred together by a stirring machine (Heidolph Vibramax 100). For 43.5 g water, it has been added 0.435g Laponide RD for preparing 1% clay sample. The clay solution is prepared under room temperature  $\sim 25^\circ\text{C}$ , and stirred for around 2 hours to make sure all the Laponite is uniformly dissolved in water and make the solution transparent. To prevent aggregation of clay particle and remove all air bubbles from solution the samples were ultrasonicated for at least 5 minutes.

#### **Dynamic viscosity measurement**

The dynamic viscosity ( $\mu$ ) of the silicone oil was calculated by multiplying the kinematic viscosity ( $\nu$ ) with the density ( $\rho$ ) of the sample by using following equation (2.23).

$$\mu = \nu \times \rho \quad (2.23)$$

For kinematic viscosity 10 and 100 cSt of silicon oil measured dynamic viscosity were 0.00935 Pa.s and 0.0965 Pa.s respectively.

### **3.2.2 Experimental study of Pickering emulsion stabilized by Laponite RD in a microfluidic T-junction**

In this experiment Laponite RD used as an emulsifier to produce stable W/O Pickering emulsion in a microfluidic T-junction. According to the Bancroft rules, the emulsifier must be soluble in the continuous phase to get a stable emulsion. But anti Bancroft emulsion (emulsifier in dispersed phase) could also be stable because in the case of Pickering emulsion the stability is ensured by steric effect of dense particle adsorption layers while the surface elasticity plays a secondary role. In other words, the stability of considered Pickering emulsions of anti- Bancroft type requires the formation of closely packed particle monolayers which provides steric stabilization. To produce stable W/O emulsion in our system, Laponite RD was in dispersed phase (water) and continuous phase was Castor oil and silicone oil. Therefore the system used in this experiment was based on the Anti- Bancroft rule (Figure 3.5. a).

Different concentrations of Laponite RD (0.5%; 1%, 1.5% and 2%) have been used in the experiment. It has been mentioned earlier that higher concentration of LP in water produce gel, but in our experiment, we want to use only liquid form of Laponite solution. Therefore, the highest concentration of laponite in our experiment was 2%. In the absence of added salt, Laponite RD was successfully dispersed in water and produced clear and non-viscous solution. . According to Briggs (1921), it is necessary to add a weak flocculating agent with emulsifier to get a satisfactory emulsion. But a powerful flocculation agent will usually prevent emulsification. Due to this fact, salt (NaCl) used as a weak flocculated agent in this experiment. Satisfactory stabilization was found with higher concentration of Laponite RD (1.5% Or 2% LP) + 0.1 %M salts (NaCl) in water when continuous phase was castor oil.

For high salt concentrations ( $>0.1M$ ) flocculation occurs at all clay concentrations in which a gray, turbid phase separates from clear, supernatant liquid (Ashby and Binks, 2000). So the optimum concentration of salt has been taken in our experiment 0.1M. At a fixed concentration of clay, increasing salt concentration leads to chaotic dispersions of increased viscosity (Ashby and Binks, 2000). In our experiment, at 2% Laponite RD a little clearer, but free flowing dispersion form at  $10^{-3}$  M salt, which became a slightly turbid gels at  $10^{-2}$  M and more turbid, flocculated system found at  $10^{-1}$  M salt.

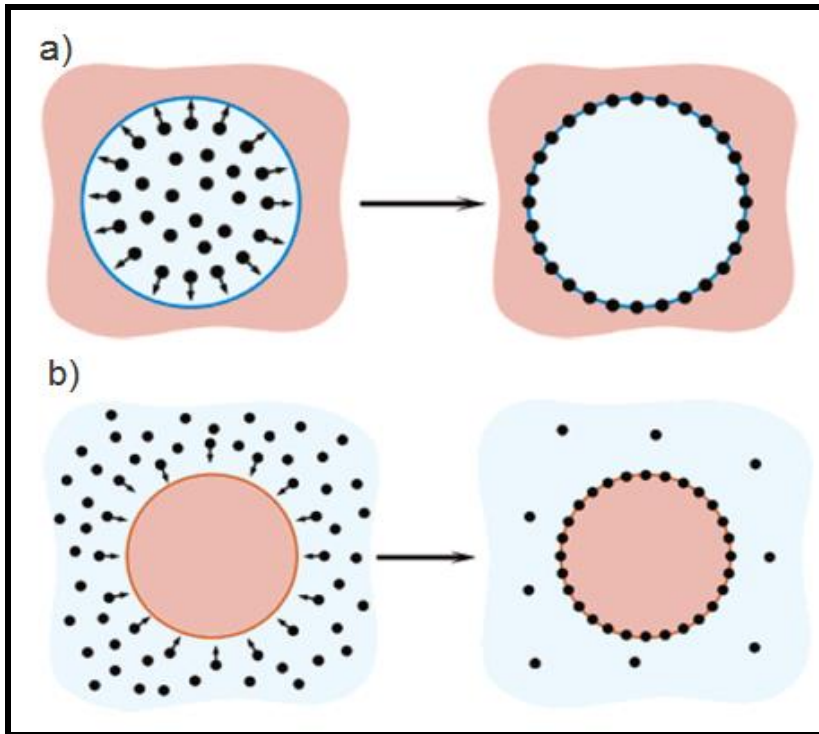


**Figure 3.5: a) Anti-Bancroft system, b) Bancroft system. Figure adapted from Golemanov et al., 2006.**

The experiment was started with a lower concentration (0.5%) of clay in the water without adding salt and carrier fluid was silicon oil (100cSt). Monodispersed droplets produced, but they were coalesced rapidly in the reservoir. Even with higher concentration of clay (2%) by adding higher concentration of salt (0.1%), droplets stability couldn't be established. Increasing the viscosity of the liquid surrounding a droplet decreases the velocity at which the droplet moves up and hence prevents coalescence (Dickinson, 2009). Therefore, we decided to increase the concentration of the continuous phase. Silicon oil with 500cSt and later 1000cSt also has been used to get stability, but inappropriately they didn't work at all.

In the next attempt, high viscous polar oil (castor oil) has been taken into account in our experiment for the stability of droplets it has been found successfully stable water droplets in the oil phase in this system. Even without adding any salt and with a lower concentration (0.5%), droplets stability was observed, but they were very few in numbers and duration of stability was very short. Better stability and maximum numbers of droplets are found with higher concentration of Laponite RD (2%) by adding NaCl (0.1%) in water.

All the samples (different concentration of aqueous dispersions of Laponite RD without salt or with lower to higher concentration of salt) prepared in the same conditions (at room temperature, 25°C; same duration of stirring etc.). It is important to keep the same conditions for preparing samples, otherwise it might affect the result (duration of stability of droplets, number of stable droplets etc.). First the weight of the water & clay or water, clay & salt (when salt added) were measured by the balance machine (Ohaus Analytical plus) separately before they were stirred together by a stirring machine (Heidolph Vibramax 100). All samples were stirred at 1200 rpm for 2 hours. For each experiment we used fresh samples, it means that we prepared each sample just before the experiment not by preparing all the samples at a time.

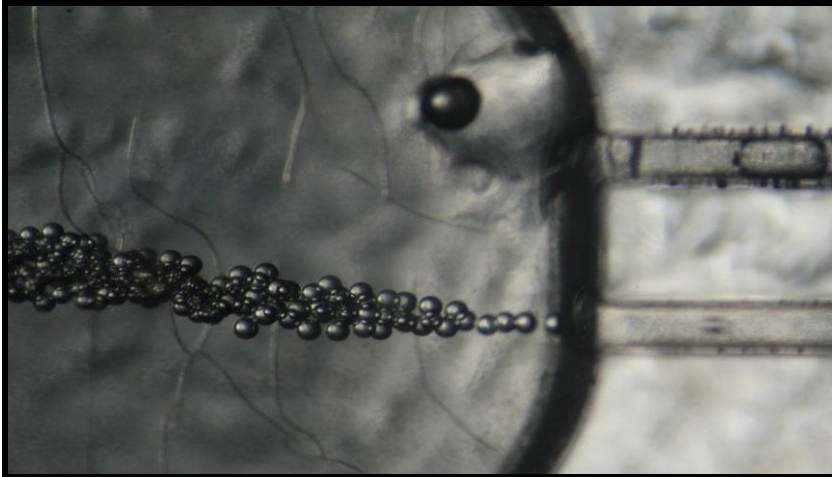
Same flow rates were maintained for each sample in the experiment. The surface had been wetted thoroughly with the high rate of continuous phase before the dispersed phase was introduced. Finally, the continuous phase flow rate was fixed at 50 $\mu$ L/min and the dispersed phase at 1 $\mu$ L/min for each sample with different concentration of aqueous dispersions of Laponite RD without salt or with lower to higher concentration of salt. The image and video were taken after flowing the both pumps for an hour with those flow rates mentioned above. The reason of this is to make the system stable with these flow rates. The picture has been taken from different parts of the reservoir as well as in different time intervals to find the duration of stability of droplets in the reservoir. After more 30 minutes of continuous flowing (total 1 and half hour flowing), we stopped the dispersed phase flow thus no more droplets produced in the microchannels. Gradually over 5 minutes, we also stopped continuous phase flow. Even stopping both pumps, due to the capillary pressure some droplets will reach in the reservoir and their sizes are larger than the old droplets of the reservoir. But within five minutes, the droplets remaining in the reservoir (new and old) becomes very constant. Some of them remain the same size, some coalesces becomes larger, flocculated but don't flow and don't leave the reservoir. In this situation we fixed the camera in a position near the outlet of the reservoir (because old droplets are fixed here) and start taking pictures by giving 5 to 10 minute intervals to see how droplet sizes are changed with time.

According to the manufacturer the length of the reservoir is around 40mm (Figure 2.13 in section 2.8.2). It has been calculated that to pass this length (from beginning to end of the reservoir) for a cluster of droplets need around 10 minutes time. Therefore the picture taken from the beginning of the reservoir considered as a zero minute age of produced droplets and in the middle part their age was considered as 5mins and near outlet they were 10 minutes aged droplets (Figure 3.6). [video 1](#), [video 2](#) and [video 3](#) attached in the Appendix to show the movement of droplets in different part of the reservoir.

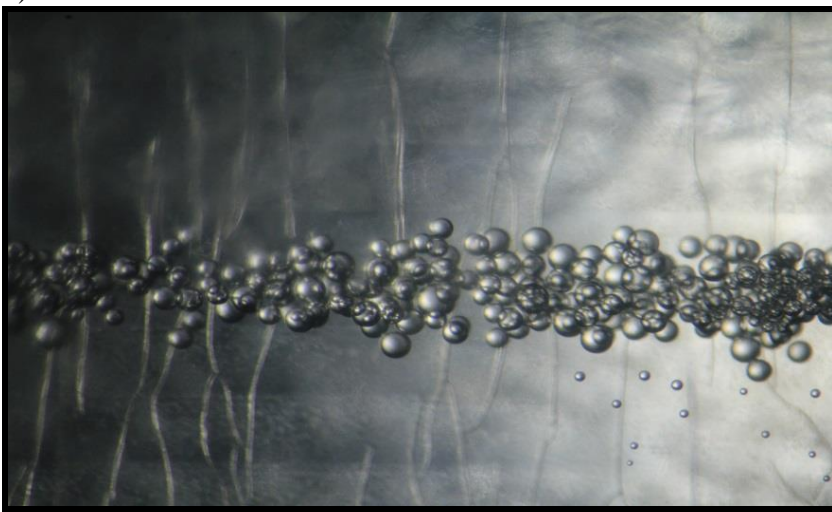
A small quantity of the water-in-oil emulsions was sampled and collected in the small glass ampoules from each sample for monitoring visually the evolution of the emulsion with time. Emulsion stability characterized from the size distribution of droplets with time. Droplet sizes were measured manually by using Paint software. In stable macroemulsion system volume fraction of oil and water is an important issue for getting stable emulsion which is not considerable in microemulsion but the most important thing is that, keeping the droplet size as small as possible by controlling the flow rates of both phases. Bigger droplets coalesce promptly and the emulsion becomes unstable. The smallest droplets in our experiment have been found at the ratio of continuous flow rate and dispersed phase flow rate,  $Q_d/Q_c = 1/50$ .



a)



b)



c)

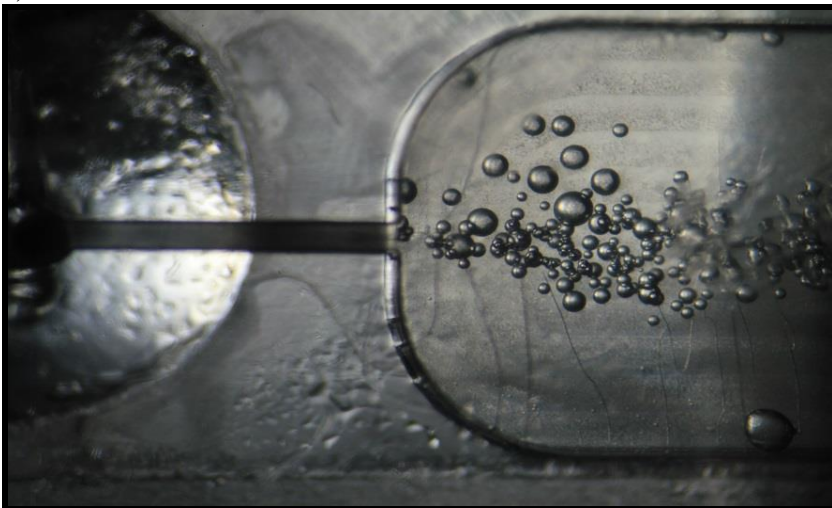


**Figure 3.6: Droplets are in different parts of the reservoir. (a) At the beginning of the reservoir. (b) At middle part of reservoir and (c) At the end of the reservoir.**



## Chapter 4

### 4 Results and Discussion

#### 4.1 Effect of flow rate and viscosity on droplet size

Regular sized monodispersed with equal spacing droplets of De-ionized water in silicon oil were generated at the T- junction in this experiment (Figure 4.1). The volume of the droplets was adjusted by changing the rate of flow of the dispersed phase (water) and the carrier fluid (silicone oil). We found controlled rate of flow in squeezing regime.

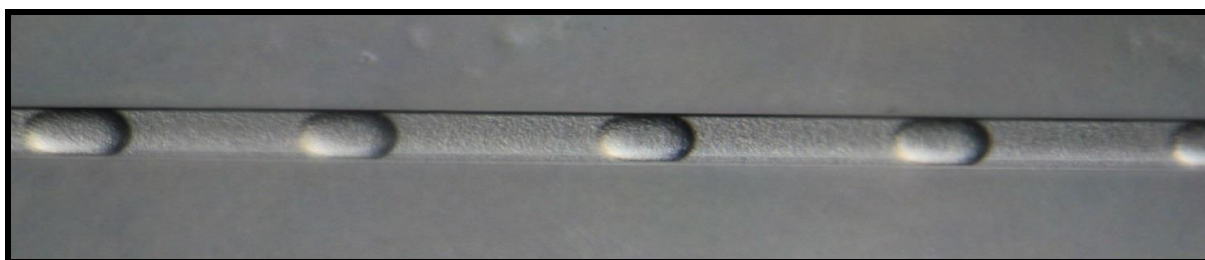


**Figure 4.1: Regular sized monodispersed with equal spacing droplets in a T-junction. The average diameter of the droplets in the figure is 0.56mm ~ 1/2mm. The distance between each droplet was around 1mm.**

At the constant value of the flow rate ( $0.50 \mu\text{L}/\text{min}$ ) of the continuous phase, the dispersed phase flow varies from  $0.2$  to  $2.00 \mu\text{L}/\text{min}$ . The measured lengths of droplets show the proportional relation with the disperse phase flow. When the dispersed phase flow is higher, the droplet size is also bigger. By decreasing the value of flow rate, droplet size decreases. Corresponding exponential curve (Figure 4.2) shows the same; droplet size is directly proportional to the flow rate of the dispersed phase.

Figure 4.3 shows, droplet size measurements for constant value of dispersed phase at  $1.00 \mu\text{L}/\text{min}$ ,  $Q_{\text{oil}}$  varied from  $0.3$  to  $3.00 \mu\text{L}/\text{min}$ . For a given flow rate ( $1.0 \mu\text{L}/\text{min}$ ) of dispersed phase (water), the droplet decreased as the continuous phase flow velocity increased, and the diameter of droplets reached approximately  $0.5\text{mm}$  or  $500\mu\text{m}$  at  $3.0\mu\text{L}/\text{min}$  indicates that droplet size is inversely proportional to the flow rate of the continuous phase. In the Figure 4.4 shows the effect of flow rate of continuous phase flow on droplet size at three different constant values of dispersed phase. With the increasing velocity of continuous phase flow, the droplet size starts to decrease linearly at  $10.0 \mu\text{L}/\text{min}$ . It is expected that much smaller droplets, for example  $50\text{-}100 \mu\text{m}$  in diameter might be possible at higher flow rate of continuous phase, but in our experiment we found an almost constant size of droplets for further increase of the continuous phase flow rate (Figure 4.4). So, the minimum size of droplets able to form in this experiment was  $L \sim w$  ( $400 \mu\text{m}$  or  $0.4 \text{mm}$ ). This lower limit of droplet size suggests that the geometry of the microfluidic device plays an important role in the break-up process. The narrower microchannel might be able to produce smaller droplets.

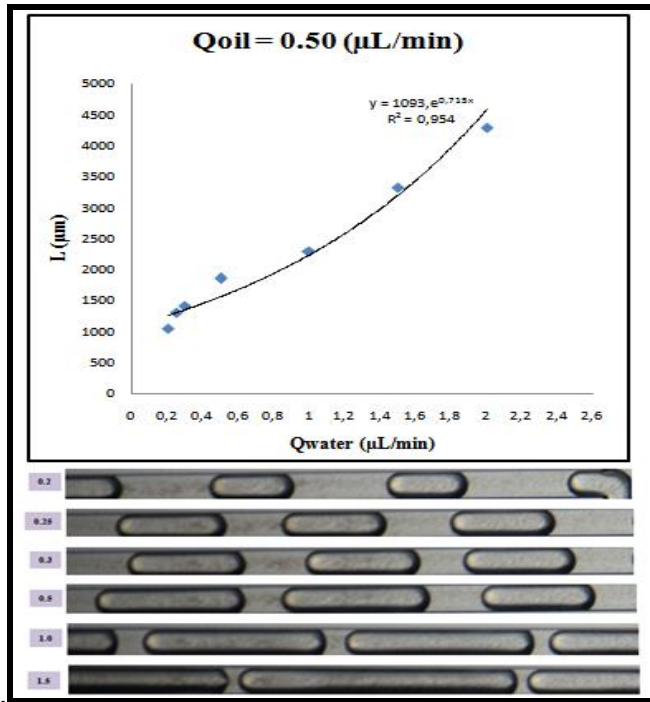


Figure 4.2: L verses  $Q_{\text{water}}$  for constant value of  $Q_{\text{oil}}$  ( $0.5\mu\text{L}/\text{min}$ ) with corresponding droplets lengths images,  $Q_{\text{water}} = 2.0-0.2 \mu\text{L}/\text{min}$ .

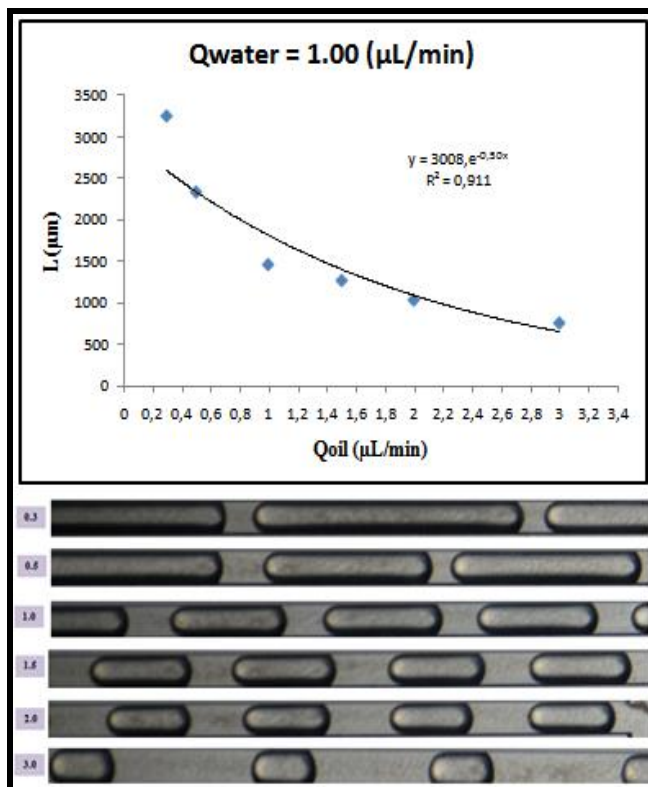
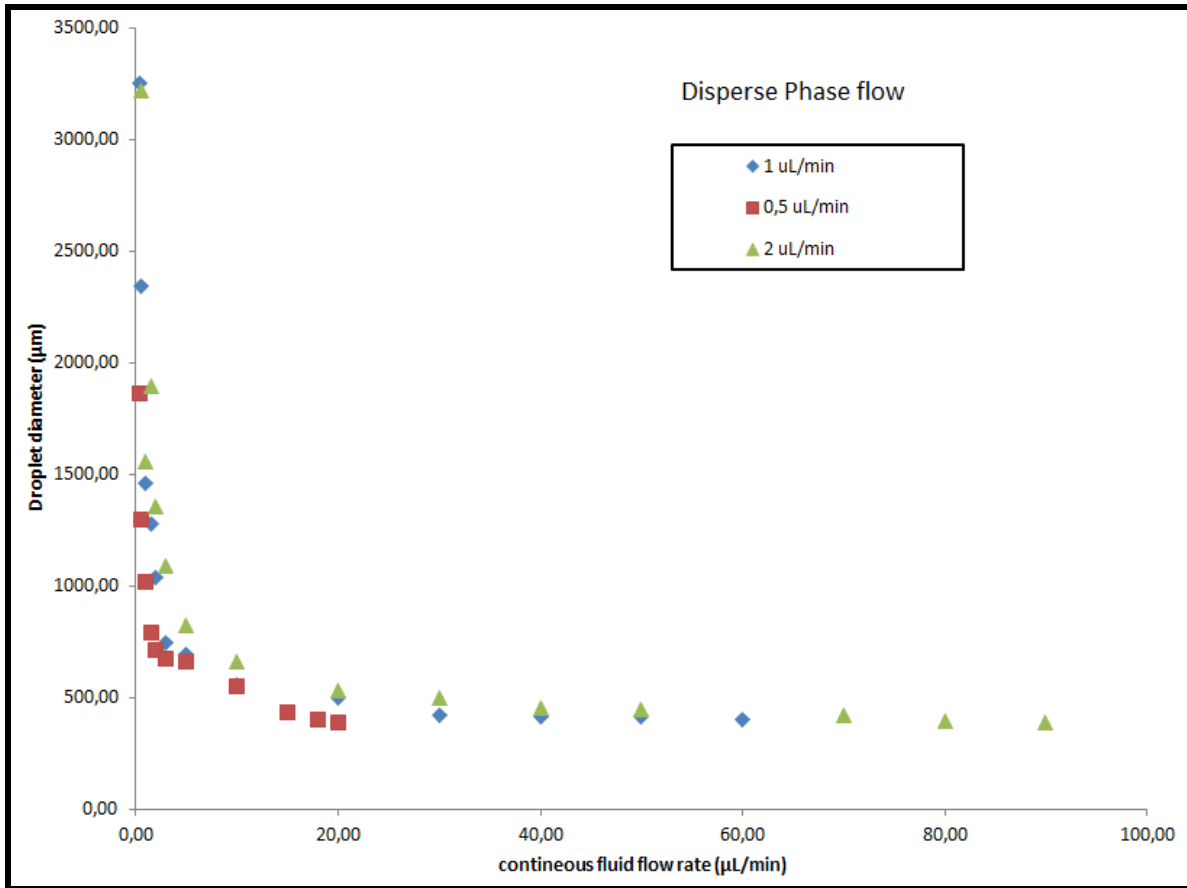


Figure 4.3: L verses  $Q_{\text{oil}}$  for constant value of  $Q_{\text{water}}$  ( $1.0 \mu\text{L}/\text{min}$ ) with corresponding droplets lengths images,  $Q_{\text{water}} = 3.0-0.3 \mu\text{L}/\text{min}$ .



**Figure 4.4: Effect of continuous flow rate ( $Q_c$ ) on droplet size in different constant value of dispersed phase ( $Q_d$ ). Smallest droplet size was found to be around  $400\mu\text{m}$  or  $0.4\text{mm}$ .**

The relative effect of the viscous force to interfacial tension force is given by the capillary number,  $Ca = u\mu/\sigma$ , where  $u$  is the characteristic velocity of injected fluids,  $\mu$  the dynamic viscosity (Pa.s) of continuous phase and interfacial surface tension is  $\sigma$  (N/m) between the dispersed and continuous fluid. In our system, it has been measured the maximum and minimum capillary number by the following way:

For first system, Fig 4.2 the maximum flow rate was  $Q_{\max} = 2.00 + 0.50 = 2.50 \mu\text{l/min}$  and minimum flow rate was  $Q_{\min} = 0.5 + 0.20 = 0.70 \mu\text{l/min}$ , resulting corresponding maximum and minimum velocity

$$V_{\max} = Q_{\max} / A = 2.50 \mu\text{l per min} / A = 2.50 \mu\text{l} / (400 \mu\text{m})^2 \text{min} = 1.04 \times 10^{-3} \text{m/s} \quad (4.1)$$

$$V_{\min} = Q_{\min} / A = 0.7 \mu\text{l} / (400 \mu\text{m})^2 \text{min} = 2.91 \times 10^{-4} \text{m/s} \quad (4.2)$$

Where  $A$  is cross sectional area of microchannel ( $400 \mu\text{m} = 4 \times 10^{-4} \text{m}$ );  $1 \mu\text{l} = 1 \times 10^{-9} \text{m}^3$ ;  $1 \text{min} = 60$  seconds. The dynamic viscosity ( $\mu$ ) of silicone oil (100 cSt) is  $0.096 \text{ Pa.s}$  at  $25^\circ\text{C}$ , Antonoff, s rule is used to calculate the interfacial surface tension ( $\sigma$ ) I.e simply, surface tension of water ( $63,7 \text{ mN/m}$ ) - surface tension of silicone oil ( $20,9 \text{ mN/m}$ ) =  $42,8 \text{ mN/m} = 42,8 \times 10^{-3} \text{ N/m}$ . Therefore, maximum and minimum capillary number were found  $Ca_{\max} = 2,3 \times 10^{-3}$  and  $Ca_{\min} = 6,5 \times 10^{-4}$

Similarly for second system, Figure 4.3

$$V_{\max} = Q_{\max} / A = 1.65 \times 10^{-3} \text{ m/s}$$

$$V_{\min} = Q_{\min} / A = 5.2 \times 10^{-4} \text{ m/s}$$

We found  $Ca_{\max} = 3.7 \times 10^{-3}$  and  $Ca_{\min} = 1.17 \times 10^{-3}$

According to the Tica et al. (2004), the range of value of Ca in squeezing regime is  $7.0 \times 10^{-4}$  to  $7.6 \times 10^{-2}$ . The calculated value of Ca found in both systems (Figure 4.2 and Figure 4.3) for this experiment lies within this range. So, it suggested that the droplet formation was in squeezing regime.

To see the effect of viscosity in continuous phase on droplet size, we measured the length of the droplets produced in a reference T-junction as a function of  $Q_{\text{water}}$ , at different values of  $Q_{\text{oil}}$  and viscosity ( $\mu$ ). In this experiment the carrier fluid was silicon oil with two different viscosities (10 and 100cSt) and dispersed phase was water. Results showed that there are two distinct regimes characterized by different scaling of L with  $Q_{\text{water}}$  for any fixed value of  $Q_{\text{oil}}$  and  $\mu$ . At low values of  $Q_{\text{water}}$  in the first regime, droplets lengths L were almost constant. This is called plateau regime. In the second regime, L grows approximately linearly with increasing  $Q_{\text{oil}}$  (Figure 4.5). The system crosses over from L is approximately constant to L proportional to  $Q_{\text{water}}$ . Droplet size also slightly decreases with increasing viscosity of the continuous phase. It seems that the effect of viscosity on drop size is not straight forward, but the influence of viscosities on droplet formation can be read from the capillary number.

In the experiment, both viscosity and  $Q_{\text{oil}}$  were varied ( $\mu=10$  and 100 cSt and  $Q_{\text{oil}}=2.5, 5$  and 10  $\mu\text{l}/\text{min}$ ). It was observed that the value of L in the plateau regime does not depend on either  $Q_{\text{oil}}$  or  $\mu$ . Because the flow of discontinuous fluid much slower than the flow of the carrier fluid around the droplet at low  $Q_{\text{water}}$  and therefore,  $Q_{\text{water}}$  would not affect the balance between the shear stress and the interfacial tension. At large  $Q_{\text{water}}$ , the shear stress exerted by the continuous fluids on the droplet would decrease simply because the difference of the speeds of the two fluids would decrease with increasing  $Q_{\text{water}}$ . Our observation showed that there is a slight change of the size of the droplets despite the fact that the shear stress ( $\tau \propto \mu u$ ) span within the order of magnitude as the data shown in the Figure 4.5. There are five different series of data plotted on this figure, each corresponding to a different combination of viscosity ( $\mu$ ) of the continuous phase and its rate of flow ( $Q_{\text{oil}}$ ). The range of the measured capillary number ( $Ca = \mu u / \sigma$ ), calculated for the same series of data for each viscosity was  $1.2 \times 10^{-2}$  to  $2.4 \times 10^{-3}$  (for 100cSt) and  $1.2 \times 10^{-3}$  to  $4.6 \times 10^{-4}$  (for 10cSt). Lower capillary numbers indicate the droplet formation in each case is in the squeezing regime as we know according to the Tica et al. (2004) where in the squeezing regime the range of Ca is  $7.0 \times 10^{-4}$  to  $7.6 \times 10^{-2}$ .

It has been revealed that there has not been very significant effect on droplet size and the capillary number whether low (10cSt) and high (100cSt) viscosities have been used as continuous phase. Regular sized droplets were produced using both viscosity and the capillary number shown droplets are formed in squeezing regime. The assertion is that viscosities in continuous phase have small effect on droplet size in squeezing regime; we observed shear stress is not a primary factor responsible for breaking of the droplet in a T-junction with the consistent small values of capillary numbers. This implies that the interfacial tension dominates shear stress in the squeezing regime. This experiment performed with low flow rate of both discontinuous and continuous fluid. Therefore, only the effect of viscosity in squeezing regime was observed where the other regimes causes by high flow rate (dripping or jetting) might be affected by viscosities.

After changing each flow rate, an appropriate amount of time was needed to take measurement in order to let the system relax for steady-state flowing in the inlet channel and a stable break-up process. This relaxation time depended largely on the flow rate of the fluid through the system. It has been observed at high rates (3-1  $\mu\text{L}/\text{min}$ ) where equilibration was fast compared to lower rate. In the lowest rate (suppose 0.2  $\mu\text{L}/\text{min}$ ), the system required several minutes (almost 30 mins) to become stable. In practice, we waited for a while after changing each flow rate until the systems started to produce uniform series of droplets and added additional time (5 minutes at least) to ensure equilibration before proceeding with the measurements. In the experiment droplets were formed without using any surfactant or colloidal particle. So, the emulsion was not very stable. They were quickly coalescence in the reservoir.

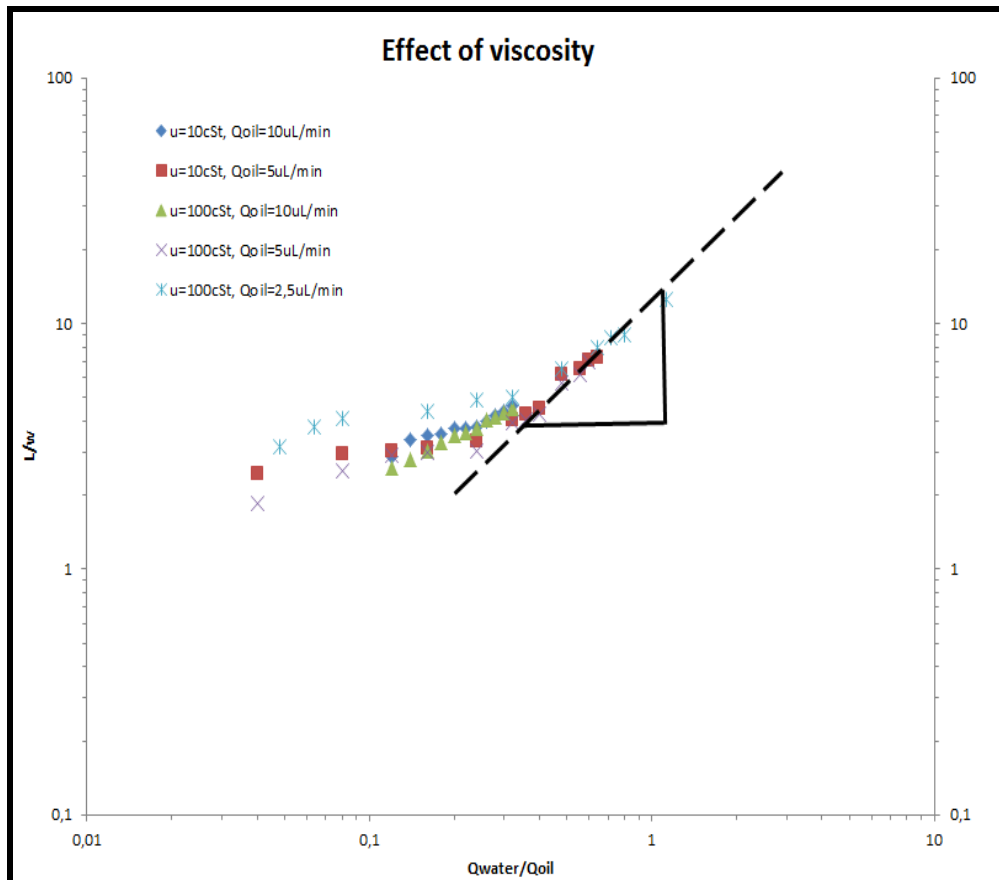


Figure 4.5: There are five different series of data plotted on this graph, each corresponding to a different combination of viscosity ( $\mu$ ) of the continuous phase and its rate of flow ( $Q_{oil}$ ). The legend is given in the figure.

## 4.2 Effect of clay and viscosity on droplet size in different regimes

Three different regimes of the two phase flows were found as a function of flow velocity and capillary number in this experiment. Droplets size measured at a fixed value of dispersed phase,  $Q_d$  (D.water with 1m% clay or without clay) by varying the flow rate of continuous phase. Silicon oils (10 and 100 cSt) were used here as continuous fluid. In the first system, the continuous phase viscosity was 10 cSt and discontinuous phase was de-ionized water with or without clay. We observed different regime by increasing total flow rate. The same thing

has been done in the second system for continuous phase viscosity 100 cSt. From the definition, we know the capillary number is  $Ca = \mu u / \sigma$ . The ratio  $\mu / \sigma$  indicate that the interface between the two phases move under the force of surface tension, resisted by the viscosity of the fluids. As long as the flow velocity remains much lower than the interfacial velocity, the surface tension dominates and the plugs snap off cleanly Figure 4.6(a). As the velocity of the driving flow increases, the interfacial velocity is not high enough for clean snap-off, and fluids proceed laminar for some distance before the snap-off occurs.

a)



b)



c)



**Figure 4.6: (a) Microphotograph of formation of plugs at low value of  $Ca$  ( $4.7 \times 10^{-3}$ ). The sharp breakup of droplet plugs due to the domination of the interfacial tension at low flow rates  $u$  (21mm) (b) microphotograp of flow that is in transition to laminar flow. By increasing the flow rates (41mm) and the  $Ca$  number ( $8.9 \times 10^{-3}$ ), the disperse phase flow a bit into the horizontal channel and forms a neck before the plugs are sheared off. (c) Microphotography of flow where long neck is formed and plugs sizes become smaller when the flow rates (58mm) and  $Ca$  ( $1.2 \times 10^{-2}$ ), increases further. This is due to the relative viscous force becomes more dominant and the interfacial tension force is not sufficient for sharp plugs breakups. For all picture,  $Q_c$  is silicon oil (10cS) and  $Q_d$ , De-ionized water with 1m%clay. length of the laminar segment is 2mm.**

In our experiment, sharp break up of plugs caused at the low values of continuous phase flow rate  $Q_c$ . It means that the plugs immediately separate from the aqueous stream at the junction where the aqueous stream met the stream of carrier fluid, silicone oil (Figure 4.6.a). This is due to the domination of interfacial tension over viscous force at low flow rate. The capillary number measured in this regime was  $4.53 \times 10^{-3}$  to  $8.3 \times 10^{-3}$  and  $4.46 \times 10^{-3}$  to  $6.06 \times 10^{-3}$  for 10 cSt with and without clay respectively. Similarly for 100 cSt  $Ca$  were  $4.6 \times 10^{-2}$  to  $7.4 \times 10^{-2}$  and  $4.73 \times 10^{-2}$  to  $7.5 \times 10^{-2}$  without clay and with clay respectively. This indicates a sharp break up of droplet formed in squeezing regime. To keep increasing the flow rate of continuous phase, it was found that dispersed phase flow a bit into the horizontal channel and forms a neck before the plugs are sheared off. In this regime our measured capillary number satisfied the theoretical value for dripping regime ( $1.9 \times 10^{-3} \leq Ca \leq 8.2 \times 10^{-2}$  according to Tica et



al., 2004) for both viscosities and in both conditions (with or without clay). Further increase of flow rate longer neck is formed and plugs sizes become smaller. This is due to the relative viscous force becomes more dominant and the interfacial tension force is not sufficient for sharp plugs breakups. The microphotography of droplet formed in different regimes shown in Figure 4.6.

**Table 4.1: Different regimes (squeezing and transition to dripping) in terms of capillary number (Ca)**

Viscosity of continuous phase	Dispersed phase	squeezing regime	Transition to Dripping regime
10 cSt	water with clay	$4.53 \times 10^{-3}$ to $8.3 \times 10^{-3}$	$Ca=8.9 \times 10^{-3}$ ; $u=4.1 \times 10^{-2}$
10 cSt	water	$4.46 \times 10^{-3}$ to $6.06 \times 10^{-3}$	$Ca=8.79 \times 10^{-3}$ ; $u=4.1 \times 10^{-2}$
100cSt	water with clay	$4.73 \times 10^{-2}$ to $6.34 \times 10^{-2}$	$Ca=7.5 \times 10^{-2}$ ; $u=3.83 \times 10^{-2}$
100cSt	water	$4.6 \times 10^{-2}$ to $6.43 \times 10^{-2}$	$Ca=7.4 \times 10^{-2}$ ; $u=3.83 \times 10^{-2}$

Table 4.1 represents different regime in terms of capillary number found in the experiment. Adding clay in dispersed phase slightly increased the droplet size and capillary value. Even in the same regime for different viscosity in continuous phase capillary number varied a lot, but not as much for clay in dispersed phase. We observed in Figure 4.7, clay has very little effect on droplet size in different regimes but due to the viscosity droplet size varied a lot. In our previous experiment performed only in squeezing regime with the same two viscosities (10 and 100 cSt). It has been found that viscosity has a little effect on droplet size in squeezing regime (Figure 4.5). So, these two results (Figure 4.7 and Figure 4.5) might be indicates that viscosity does not very effective on droplet with low flow rates in squeezing regime, but its effect the droplets in other regions (dripping and jetting) causes by high flow rate.

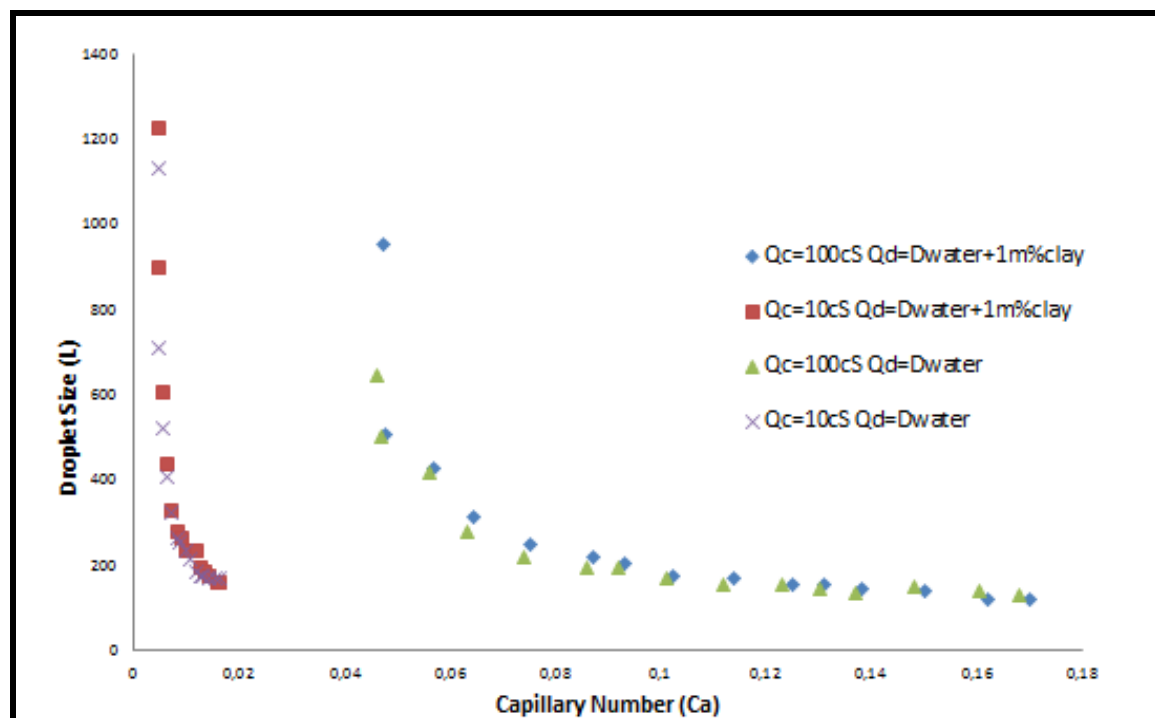


**Figure 4.7: Effect of clay and viscosity in continuous phase on droplet size.**

The time effect may be one of the reasons for not finding any effect or very small effect of clay on droplet size. The droplet size has been measured in microchannel. The channel length from the T-junction to the reservoir is approximately 20mm (measured manually by Paint). With a flow rate, for example 10  $\mu\text{L} / \text{min}$  in dispersed phase and 2.5  $\mu\text{L} / \text{min}$  in continuous phase, the droplet speed found by using equation (4.1)

$$V_{\max} = Q_{\max} / A = 12.50 \mu\text{l per min} / A = 12.50 \mu\text{l} / (400 \mu\text{m})^2 \text{min} = 5.28 \times 10^{-3} \text{m/s} \sim 5.2 \text{mm/s}.$$

Droplet travel time from the T junction to the reservoir is,

$$t = s / v = 20 \text{mm. sec} / 5.2 \text{mm} \sim 4 \text{sec} \quad (4.3)$$

When the droplets were generated at T-junction, the droplets lengths were measured within a second or little more than a second as the total travel time of the droplets in the channel is about 4 seconds. This is might be very short time to affect the droplets by clay. Unfortunately, no similar measurement was performed when droplets were in the reservoir and when they exit the chip because the droplets coalesce in the reservoir and formed very big size. So, it cannot be finalized that either clay needs much time to affect the droplets or not. As our experiment was performed only by 1% concentration of clay, there may a possibility of higher concentration of clay might affect the droplets lengths.



## 4.3 Pickering emulsion stabilized by Laponite RD in a microfluidic T-junction

### 4.3.1 Generation of emulsions with non-polar oil and Laponite RD in water

To investigate the possibility of preparing stable emulsions by Laponite RD, an experiment was set up by using non-polar oil, silicon oil (100cSt) as continuous phase and De-ionized water with different concentration of Laponite RD as dispersed phase in a microfluidic T-junction. Even with higher concentration (2%) of Laponite no stable droplets were found. Then NaCl as weak flocculating agent added in water with 2% Laponite. But it did not give any fruitful results Figure 4.8. Later, another experiment has been done by higher viscosities 500 cSt and 1000 cSt respectively. At higher viscosity a little amount of droplets appeared stable for a short duration of time.



**Figure 4.8: Very unstable droplets in the reservoir when the viscosity of the continuous phase (silicone oil) is 100cSt. Dispersed phase is 2% Laponite RD and 0.1 M NaCl in water.**

Figure 4.9 represents the droplets in the reservoir when the viscosity of the continuous phase (silicone oil) is 500cSt and dispersed phase is 2% Laponite RD and 0.1 M NaCl in water. Only few stable droplets were found at the beginning of the reservoir which were first flocculated and later coalesced at the middle part of the reservoir. Even higher viscosity (1000cSt) couldn't change the result much (see [video 4](#) attached in Appendix).

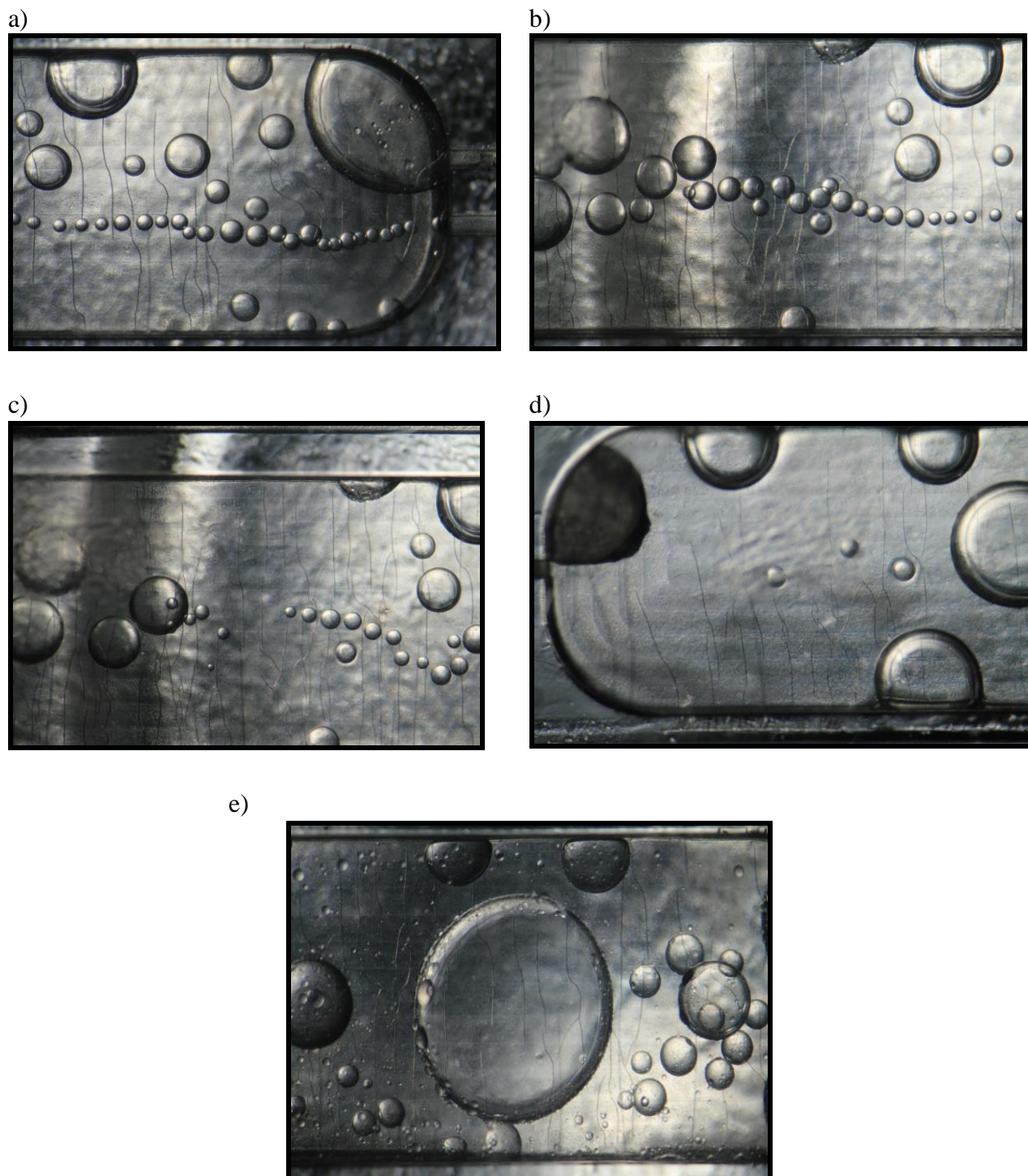


**Figure 4.9: Few stable droplets found in the system, viscosity of the continuous phase (silicone oil) is 500cSt and dispersed phase 2% Laponite RD with 0.1 M aqueous NaCl. Droplets are (a) at the beginning of the reservoir (b) & (c) at the middle part of the reservoir (d) at the end of the reservoir and (e) droplets after 30 minutes in the middle part of the reservoir.**



**Figure 4.10: Sampled collected in the small glass ampules. Left, stable water in oil emulsions by using castor oil as continuous phase. Right, unstable water in oil emulsions by using silicon oil as continuous phase. In both cases Laponite concentration is 2% and salt concentration is  $10^{-1}$ M. In unstable water in oil emulsions by using silicon oil as continuous phase, we found two clear, separate water (down) and oil (up) phase which are marked by arrow (red) signs. The appearances of the emulsions are after one week of preparation.**

### **4.3.2 Generation of emulsions with polar oil and Laponite RD in water**

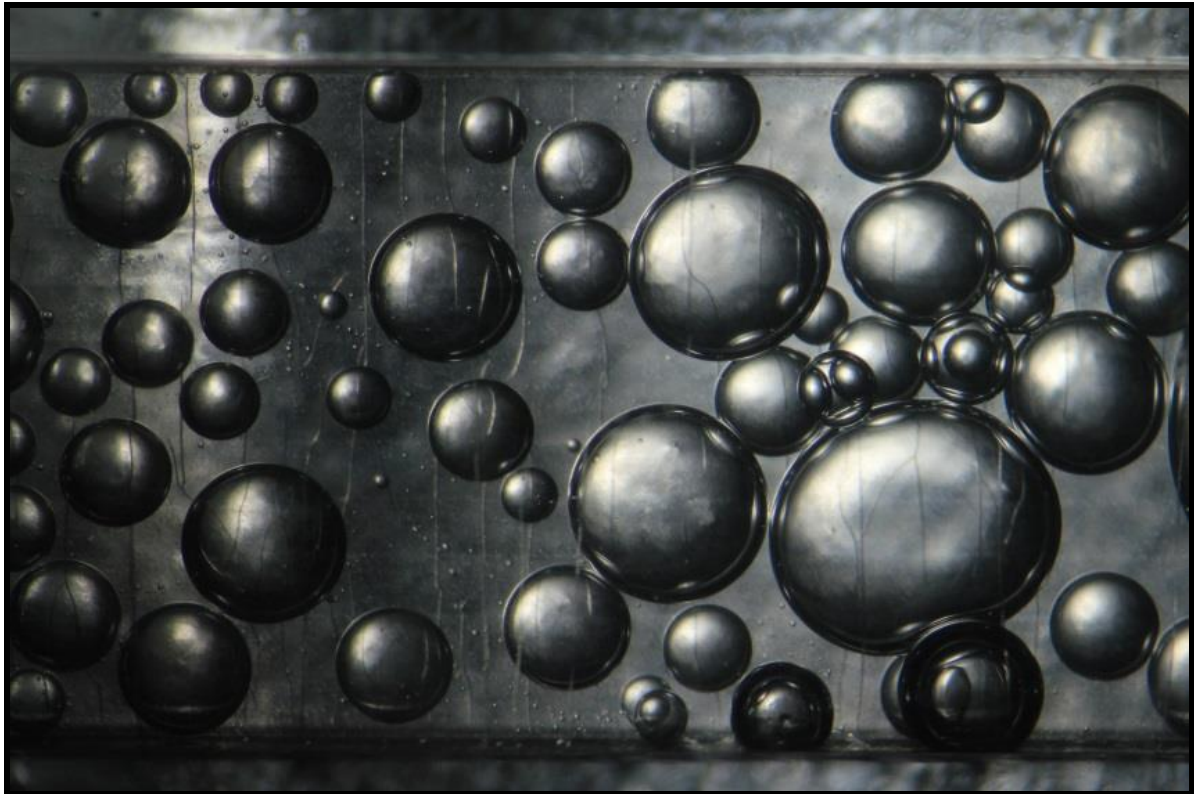
In this experiment castor oil (polar oil) has been used as continuous phase, whereas de-ionized water with different concentration of Laponite RD used as dispersed phase. The most stable emulsion appeared at the concentration of Laponite RD is 2% via salt (see [video 5](#) in the Appendix). Emulsions have been generated in a T-junction in two situations. At first, emulsions at constant salt concentration ( $10^{-1}$  M) for different clay concentrations. Second, emulsions at constant concentration of Laponite RD with decreasing concentration of salt.

#### **4.3.2.1 Emulsion generated at constant salt concentration ( $10^{-1}$ M) for different Laponite RD concentrations**

To observe the effect of clay concentration on stability of W/O emulsions, several emulsions with constant salt concentration ( $10^{-1}$  M) but differ in clay concentrations have been organized. It was found that emulsion formed in  $10^{-1}$ M salt is very unstable at low concentration (0.5%) of Laponite RD (fig 4.10). With same salt concentration ( $10^{-1}$ M), stable emulsion has been initiated from 1 % clay concentration and gradually becomes more stable at the concentration of 1.5% and 2% of clay. The reason for obtaining particularly unstable

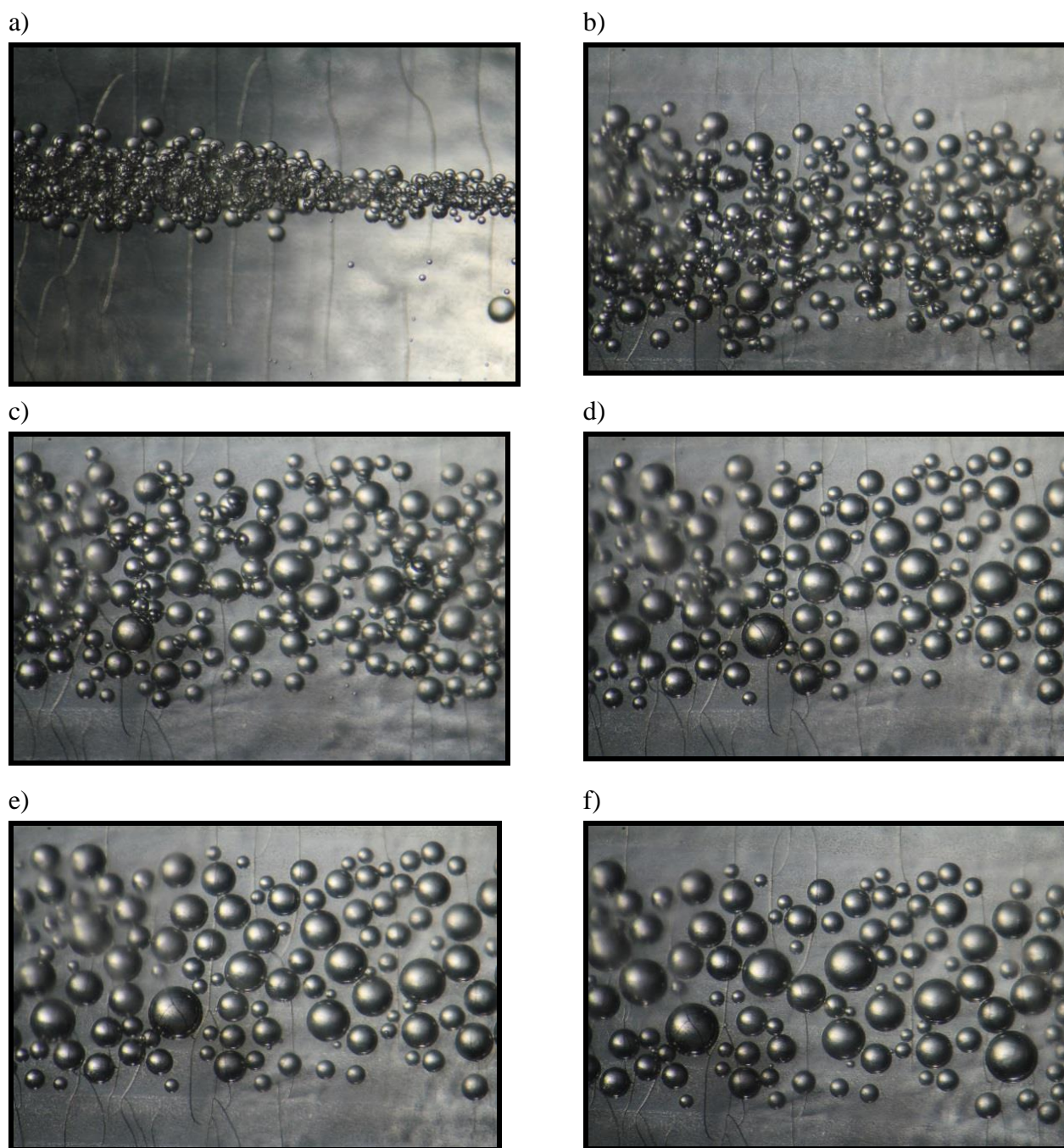


emulsion with low concentration of Laponite at high concentration of salt can be the lacking of sufficient dispersed clay particles for adsorption at freshly created W/O drops interfaces.



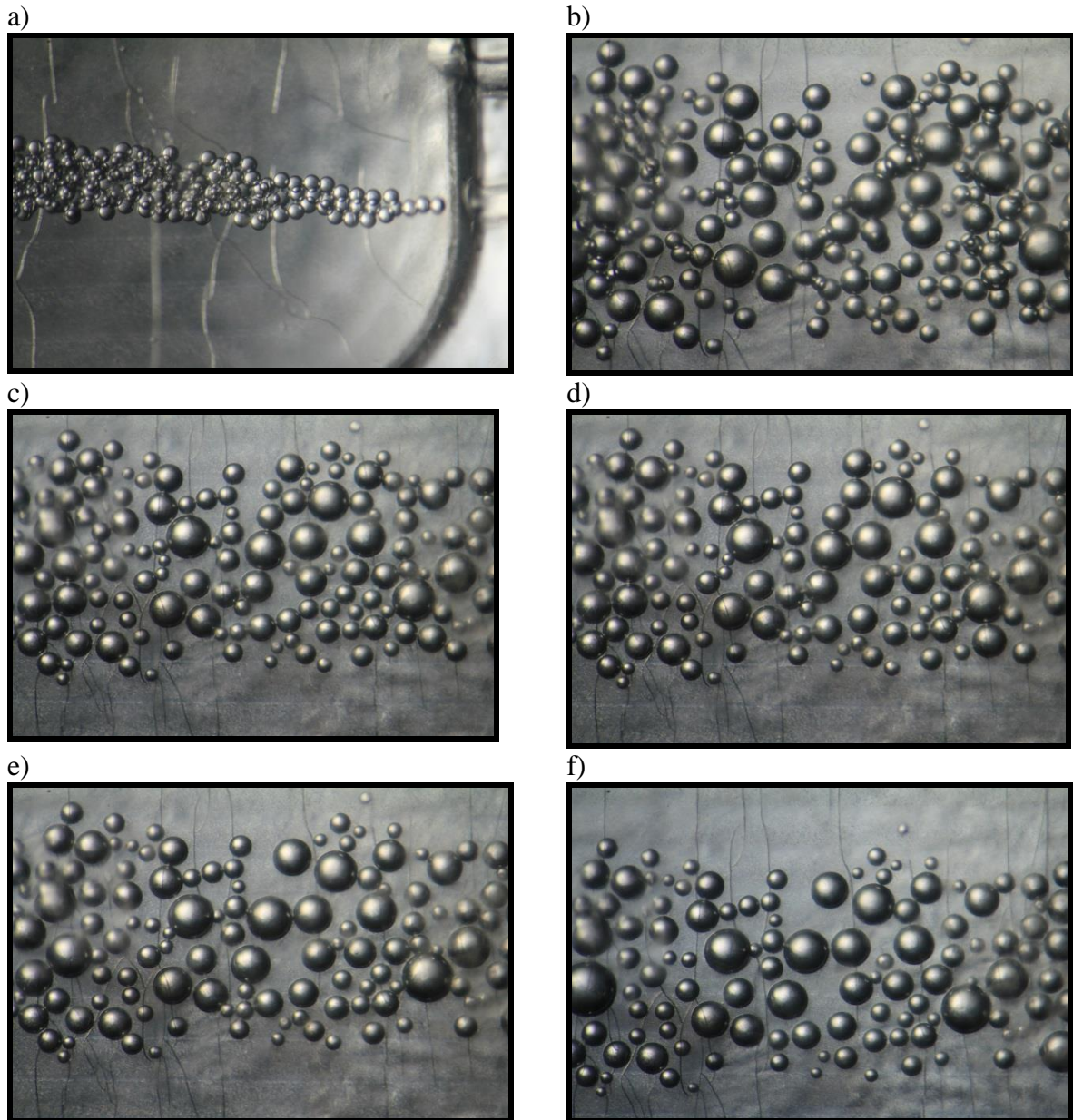
**Figure 4.11: Unstable emulsion formed in  $10^{-1}$ M salt at low 0.5% Laponite RD.**

Figure 4.11 and Figure 4.12 represent the stable emulsions at a constant salt concentration (0.1M) with higher clay concentrations (1.5 % and 2% LP-RD). The most stable W/O emulsions appear at these concentrations are significantly stable and only arise as conditions for which Laponite RD dispersions are flocculated via salt. It was very interesting to observe that the droplets don't break when they exit the reservoir. Another thing found that coalescence of the droplets increases slightly with higher clay content (Figure 4.13)



**Figure 4.12: Stable W/O emulsion with 1.5% Laponite at 0.1 M salt. Water droplets at different time (a) droplets at zero minutes (b) droplets at 15 minutes (c) at 20 minutes and (d) at 30 minutes (e) at 45 minutes and (f) at one hour. Images (b) to (f), were taken from the same part of the reservoir (near exit of reservoir) and image (a) taken from at the beginning of the reservoir.**





**Figure 4.13: Stable W/O emulsion with 2% Laponite concentration at 0.1 M salt. Water droplets at different time: (a) droplets at zero minutes, (b) droplets at 15 minutes, (c) at 30 minutes, (d) at 45 minutes, (e) 60 minutes and (f) after one day. Image (b) to (f), taken from the same part of the reservoir (near the exit) and image (a), taken from at the beginning of the reservoir.**

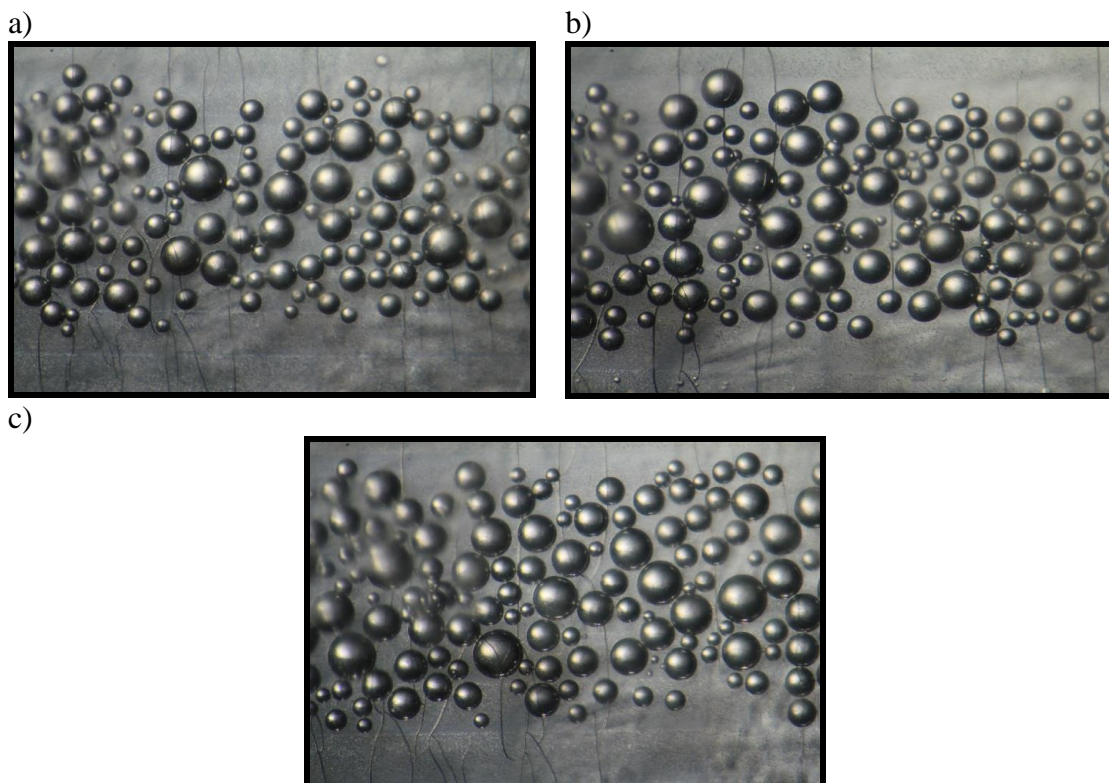


**Figure 4.14: Stable W/O emulsion with different Laponite RD concentration at constant salt 0.1% concentration. (a) Laponite RD 1% (b) Laponite RD 1.5% and (c) Laponite RD 2%. It was found that coalescence of the droplets increases slightly with higher clay content. In each of the image droplets are 30 minutes aged.**



**Figure 4.15: Sampled collected in the small glass ampoules. From left to right, emulsion with 2%, 1.5% and 0.5% Laponite RD concentration at constant 0.1 M salt. The stable emulsions found with higher clay concentrations. The appearances of the emulsions are after one week of preparation.**



**Table 4.2: The experimental results at constant salt concentration with varying clay concentrations.**

Continuous phase flow rate $\mu\text{L}/\text{min}$	Disperse phase flow rate $\mu\text{L}/\text{min}$	Continuous phase	LP concentration in water (%)	Salt concentration in water	Stability of emulsion
50	1	Castor oil	0.5	0.1	Unstable
			1		Stable
			1.5		Stable
			2		Most stable

#### 4.3.2.2 Emulsions generated at constant concentration of Laponite RD with decreasing salt concentration

We generated water in oil emulsions with 2% Laponite RD at different salt concentrations. The best stability of emulsion was found with 2% Laponite RD at 0.1M salt concentration. To see the effect of salt on emulsion stability, we gradually decreased the salt concentration in Laponite dispersion. At lower salt concentrations ( $10^{-3}$  M and  $10^{-2}$ M), only few stable droplets were found. Better number of stable droplets found without adding any salt in the Laponite dispersion (Figure 4.14 and Figure 4.15). In decrease in emulsion stability in lower salt concentration, in which the dispersions contain discrete particles, can be qualified to the effect of salt in showing the repulsions between charged particles. A video of W/O emulsion without adding salt attached in the Appendix ([video 6](#)).

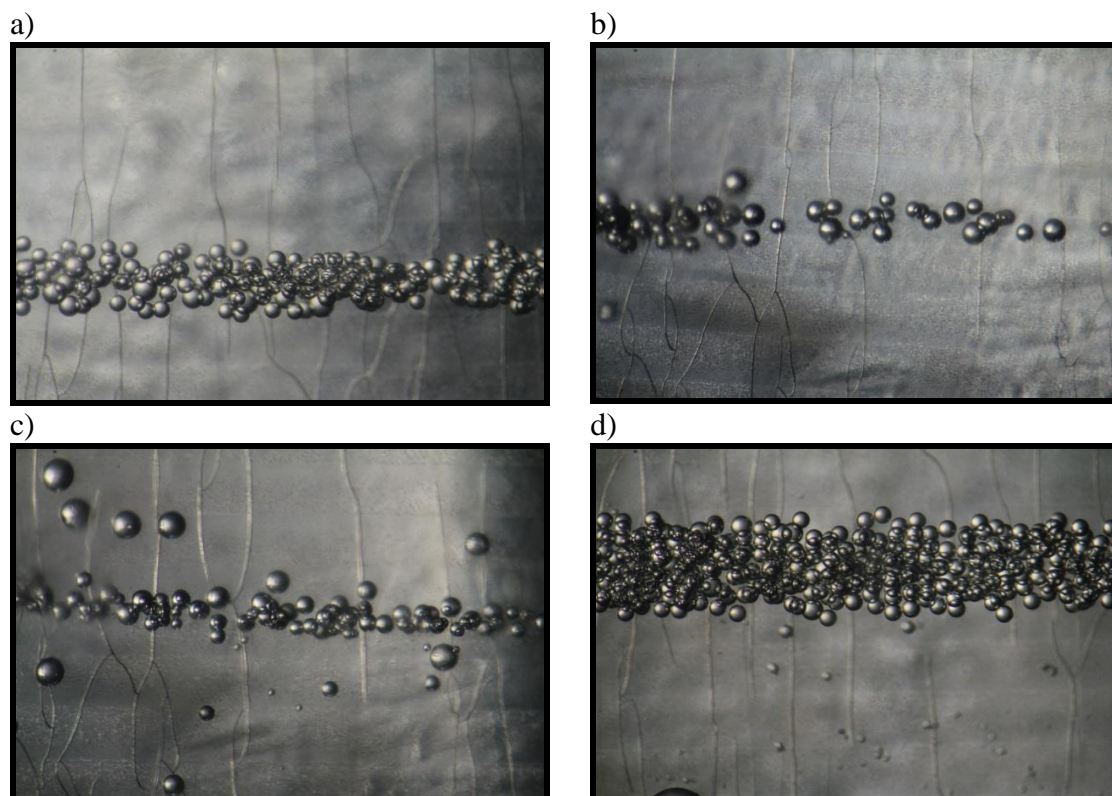


**Figure 4.16: Water in oil emulsions with 2% Laponite RD at different salt concentrations at zero minute. (a) Emulsion without any salt. (b) Emulsion with  $10^{-3}$ M salt. (c) Emulsion with  $10^{-2}$ M salt and (d) Emulsion with  $10^{-1}$ M salt.**



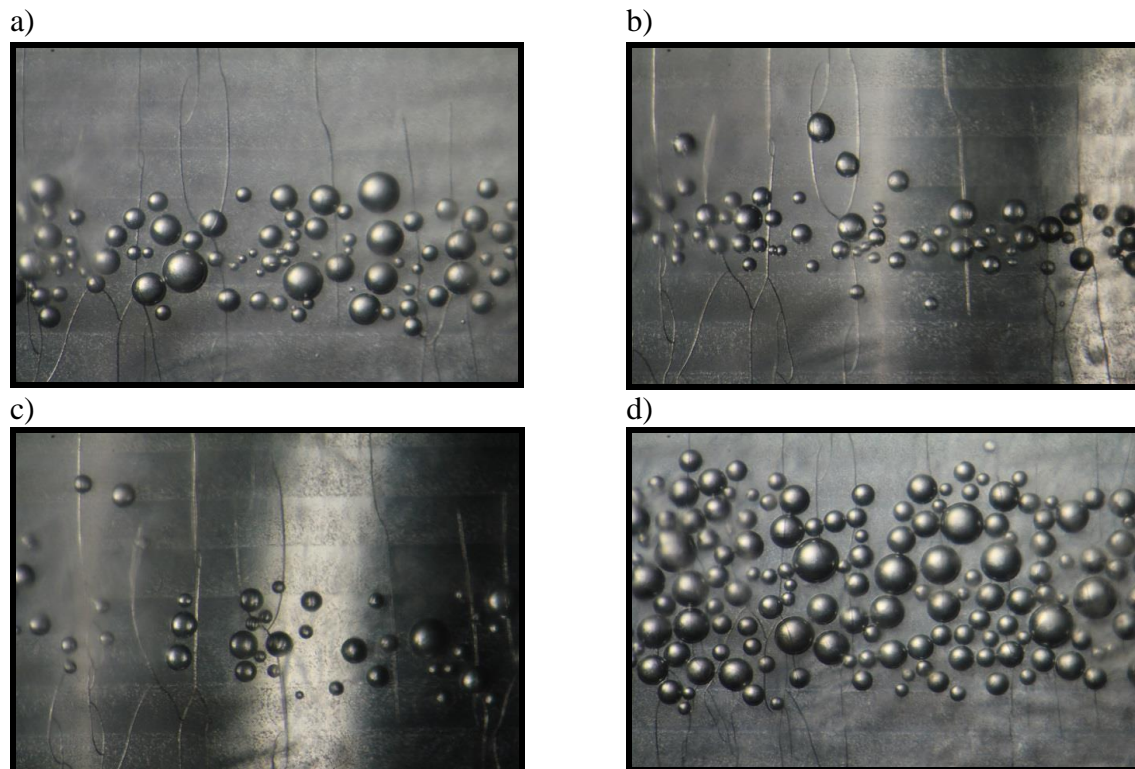


**Figure 4.17: Water in oil emulsions with 2% Laponite RD at different salt concentrations at 30 minutes. (a) Emulsion without any salt. (b) Emulsion with  $10^{-3}$ M salt. (c) Emulsion with  $10^{-2}$ M salt and (d) Emulsion with  $10^{-1}$ M salt**

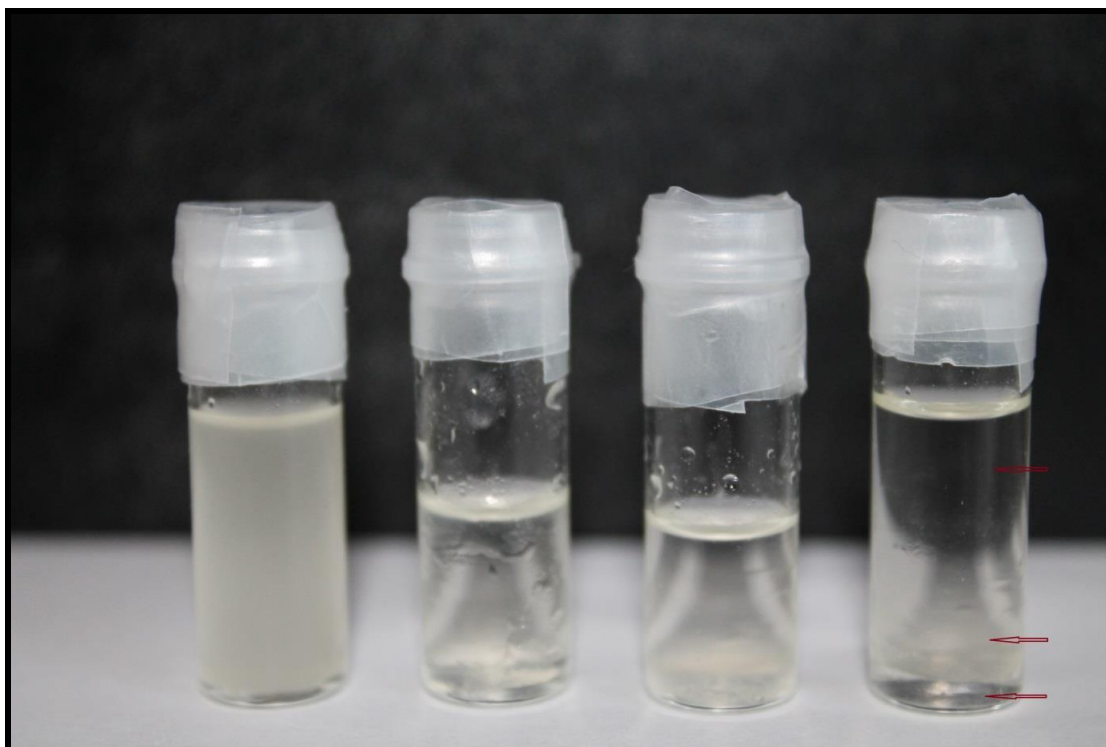


**Figure 4.18:** Sampled collected in the small glass ampules. From left to right, emulsion with  $10^{-1}\text{M}$ ,  $10^{-2}\text{M}$ ,  $10^{-3}\text{M}$  and  $0\text{M}$  salt concentration at a constant 2 % Laponite RD. The stable emulsions found with  $10^{-1}\text{M}$  concentrations. Emulsion found without adding any salt was better than lower salt ( $10^{-2}\text{M}$  &  $10^{-3}\text{M}$ ) concentrations where two clear phases, water (down) and oil (up) are visible. A small amount of emulsion stabilized between these two phases (see red arrows in last glass ampules from the left to right). The appearances of the emulsions are one week after preparation.

**Table 4.3:** The experimental results at constant LP with varying salt concentrations.

Continuous phase flow rate $\mu\text{L}/\text{min}$	Disperse phase flow rate $\mu\text{L}/\text{min}$	Continuous phase	LP concentration in water (%)	Salt concentration in water	Stability of emulsion
50	1	Castor oil	2.0	0.1	Most stable
				0.01	Less stable
				0.001	Less stable
				0	Stable

The typical way in which the sizes of the droplets change with time in the systems is represented in Figure 4.19. Size distributions of emulsion droplets have been obtained only for the most stable emulsion, 2% Laponite RD at 0.1M salt concentration. Two time intervals, 60 minutes and 24 hours were analyzed from this emulsion. First time interval (60minutes) indicated that there is an overall increase in the average drop diameter with some drops larger than  $1000\ \mu\text{m}$  or 1mm are present. The distribution remains largely unaltered in the second (24hours) time interval. The blending of two curves designates that they are coincides and droplets are stable. In practical the emulsion prepared from flocculated colloids at  $10^{-1}\text{M}$  NaCl is still very stable for up to last two weeks.

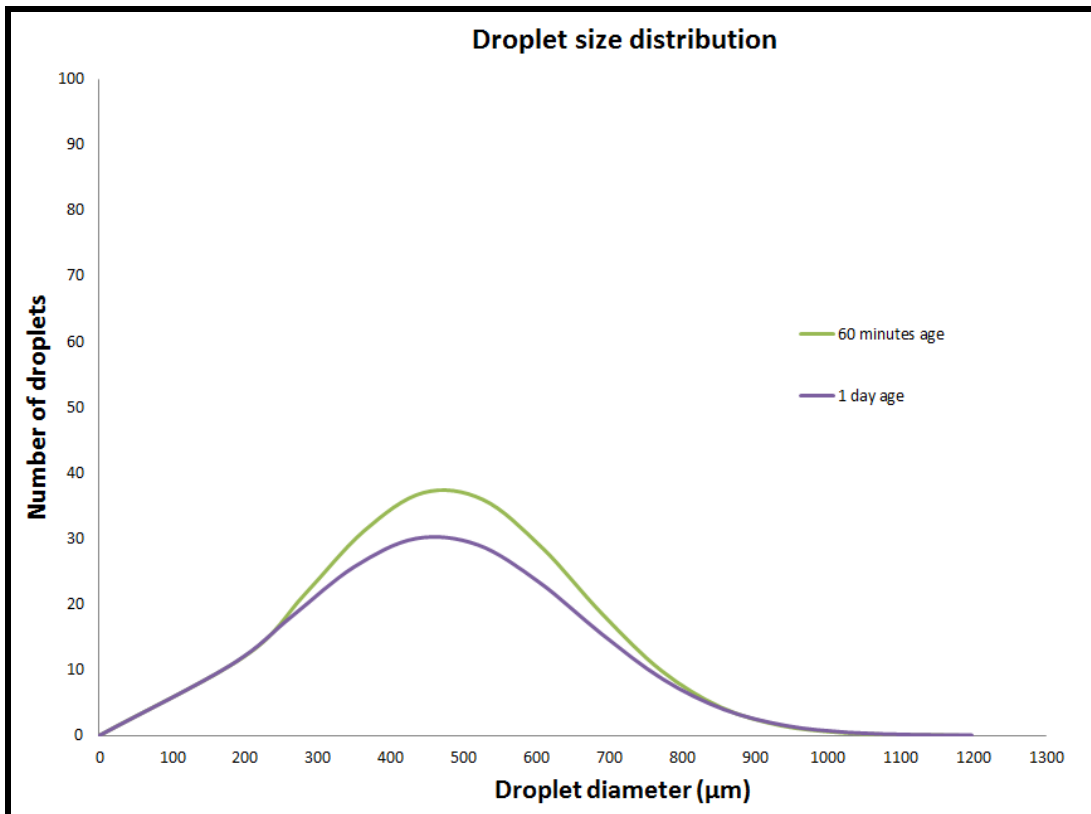


**Figure 4.19: Droplet diameter size distributions for water-in-castor oil emulsions stabilized by 2% Laponite RD in 0.1M NaCl. Times since emulsion formation are 60 minutes (upper green) and 24hours (lower blue). The blending of two curves designates that they are coincides and droplets are stable.**

Therefore, in the experiment most stable W/O emulsions of water, castor oil and Laponite RD clay particles are formed under conditions where the particles are flocculated via salt and at higher concentrations (1 % to 2 %) of clay. The addition of salt does not stimulate the isotropic liquid phase, but instead lowers the particle volume fraction at which the flocculation and glassy phase appears. The microfloculation of clay particles due to electrostatic attraction reinforced by van der Waals interactions between the positively charged edges (salt) and negatively charged faces of the plate-like particles resulting in a linked structure. There are two possible reasons which can be put forward in order to explain the effect of flocculation in emulsion stability, both related to the energy with which a particle is held at a water/oil interface. This energy of attachment depends on particle radius and on particle wettability. Firstly, the apparent size of the particles forming flocs is larger than that of individual particles, and if such flocs adsorb, their energy of attachment to emulsion drop interfaces is greater preventing disruption upon collisions between drops. Secondly, the addition of salt to systems containing charged, solid surfaces results in an increase in their hydrophobicity through the aqueous phase (Binks and Lumosdon, 2000). Changes in the droplet size distributions with time are rationalized in terms of either coalescence or Ostwald ripening, which is prompt initially but eventually stable.

Emulsions made with both non-polar oil (silicone oil) and polar oil (castor oil). It was found that the stability of emulsion was dependent on the type of oil. Nonpolar oils like silicon oil were not suitable for preparing W/O emulsions, whereas polar oil like castor oil made W/O emulsions preferentially. The reason may be the wettability of the particles at the water/oil interface from a consideration of the interfacial tension with oil and appropriate contact angles. The very hydrophilic nature of the clay particles favoring water, but water-in-oil

emulsions formed when clay particles are concentrated, hydrophobic by pre-adsorbing cationic salt onto their surfaces.

# Chapter 5

## 5 Conclusion and future studies

### 5.1 Conclusion

Two phase microfluidic flow experiments with or without smectite clay<sup>6</sup> have been performed in an oval microfluidic T-junction by using the cross-flow shear method<sup>7</sup>. Experimental studies also performed for the monodispersed Pickering emulsion<sup>8</sup> stabilized by smectite clay in a T-junction. The aim of the experiment was to understand better the fundamental of droplet formation mechanism in T- junctions and how the different parameters such as flow rates, viscosity or capillary numbers affect the droplets in a microchannel. In addition, understand better the background physics of stabilization of the W/O emulsion by Laponite RD with microfluidic T-junction geometry.

#### 5.1.1 Two phase microfluidic flow experiments

Monodispersed and regular sized with equal spacing droplets were produced in a microfluidic T-junction by controlling flow rates of dispersed and continuous phase. In the experiment, de-ionized water was used as discontinuous or dispersed phase and silicon oil was used as continuous phase. It was found that the individual continuous and discontinuous phase flow rate affects the droplet behavior. The droplet size is directly proportional to the flow rate of dispersed phase and inversely proportional to the flow rate of the continuous phase. In the same system, we observed the effect of viscosity on droplet size by using different viscosities of silicone oil (10 cSt and 100cSt) as continuous phase. It was found that the viscosity in continuous phase does not have any significant effect on droplet size in the squeezing regime. For a constant value of continuous phase regular sized droplets were produced with both of the viscosity. Droplet sizes are almost constant at the low flow rates of dispersed phase and the sizes start to increase linearly with higher values of the flow rates. This happens because at first the flow of the discontinuous fluid is much slower than the flow of the carrier fluid around the droplet at low  $Q_{\text{water}}$  (flow rate of dispersed phase) and therefore,  $Q_{\text{water}}$  would not affect the balance between the shear stress and the interfacial tension. At larger  $Q_{\text{water}}$ , the shear stress exerted by the continuous fluids on the droplet decreases simply due to the difference of the speeds of the two fluids that decreases with increasing  $Q_{\text{water}}$ . The low capillary (Ca) number places the droplet formation in the squeezing regime, indicating that droplets are sheared off right at the T-junction and that the breakup is dominated by the interfacial tension force.

We know from the definition of capillary number,<sup>9</sup> that the interface between the oil and water phases move under the force of surface tension, resisted by the viscosity of the fluids. As long as the flow velocity is much lower than the interfacial velocity, the surface tension dominates and the plugs snap off cleanly. As the velocity of the driving flow increases, the interfacial velocity is not high enough for clean snap-off, and fluids proceed laminar for some distance before the droplets snap-off occurs. Therefore, for a fixed flow rate in dispersed phase and different viscosity in continuous phase, flow rate of continuous phase varied and

---

<sup>6</sup>Laponite RD

<sup>7</sup>The continuous phase is introduced from the horizontal channel and the disperse phase flows through the perpendicular channel so that the droplets are sheared off by the cross-flowing shear force.

<sup>8</sup>Colloidal particles situated at the oil-water interface can stabilize emulsions of oil and water.

<sup>9</sup> Capillary number  $Ca = \mu u / \sigma$ . Where  $\mu$  is the dynamic viscosity (Pa.s);  $\sigma$  is the interfacial tension between the two fluids in contact (N/m);  $u$  is the characteristics velocity(m/s).

three different regimes of the two phase flow were found as a function of flow velocity and capillary number in our experiment. In the experiment de-ionized water without clay and with clay (1% Laponite RD) used as dispersed phase and continuous phase was silicon oil with viscosities 10 cSt and 100cSt respectively. Adding clay in dispersed phase slightly increased the droplet size and capillary value. Even in the same regime for different viscosity in continuous phase capillary number varied a lot, but not as much for clay in dispersed phase. In summary, it was found that viscosity does not affect the droplet production in the squeezing regime but might be affect the droplets in other regimes (dripping and jetting) caused by high flow rate. It was calculated that the travel time of the droplets from the beginning of the T-junction to the reservoir is 4 second. So, the droplets lengths were measured within 4 second. This is might be very short time to affect the droplets by clay. Unfortunately, no similar measurement was performed when droplets were in the reservoir and when they exit the chip because in the reservoir droplets coalesce into large sized drops. Therefore, we cannot be conclude anything about the time that clay need to affect the droplets. As our experiments were performed only by 1% concentration of clay, there might be a possibility that higher concentration of clay could affect the droplets lengths.

### 5.1.2 Stability of monodispersed Pickering emulsion by Laponite RD

The best stability of water-in-oil emulsions by Laponite RD was formed in the experiment under conditions where the particles are flocculated via salt and at higher concentrations (1 % to 2 %) of clay. Castor oil has been used as the continuous phase, whereas de-ionized water with different concentration of Laponite RD was used as dispersed phase in the experiment. Emulsions have been generated in a T-junction in two situations. First, emulsions at constant salt concentration ( $10^{-1}M$ ) for different clay concentrations. Second, emulsions at constant concentration of Laponite RD (2%) with decreasing concentration of salt. The addition of salt causes the flocculation and glassy phase appears in the Laponite dispersion due to electrostatic attraction reinforced by van der Waals interactions between the positively charged edges (salt) and negatively charged faces of the plate-like particles resulting in a linked structure. According to the earlier work in the literature Binks and Lumsdon, 2006, there are two possible reasons which can explain the effect of flocculation in emulsion stability, both related to the energy with which a particle is held at a water/oil interface. This energy of attachment depends on particle radius and on particle wet-ability. Firstly, the apparent size of the particles forming flocs is larger than that of individual particles, and if such flocs adsorb, their energy of attachment to emulsion drop interfaces is larger preventing desorption upon collisions between drops. Secondly, the addition of salt to systems containing charged, solid surfaces results in an increase in their hydrophobicity through the aqueous phase.

The changes in the drop size distributions with time are rationalized in terms of either coalescence<sup>10</sup> or Ostwald ripening<sup>11</sup> which is prompt initially but eventually stable. Size distributions of emulsion droplets have been obtained only for the most stable emulsion, 2% Laponite RD at 0.1M salt concentration. Two time intervals, 60 minutes and 24 hours were analyzed from this emulsion. There is an overall increase in the average drop diameter with some drops larger than 1000  $\mu m$  are present in first time interval (60minutes). The distribution remains largely unaltered in the second (24hours) time interval. The blending of two curves indicates that they are coincident and that droplets are stable. In practical terms,

---

<sup>10</sup> coalescence is the merging of two or more droplets to form a larger single droplet

<sup>11</sup> Ostwald ripening in emulsion is a process of gradual growth of the larger droplets at the expense of smaller ones due to mass transport of soluble dispersed phase through the continuous phase (Taylor, 1995).

the emulsion prepared from flocculated colloids at  $10^{-1}$ M NaCl is very stable for up to last two weeks (sampled collected in the small glass ampoules).

Emulsions were made with both non-polar oil (silicone oil) and polar oil (castor oil), and compared. It was found that the stability of emulsion was dependent on the type of oil. Nonpolar oils like silicon oil were not suitable for preparing stable W/O emulsions, whereas the polar oil such as castor oil made W/O emulsions preferential. The reason of this may be the wettability of the particles at the water/oil interface form a consideration of the interfacial tension with oil and appropriate contact angles. The very hydrophilic nature of the clay particles favors water, but water-in-oil emulsions formed when clay particles are concentrated, become hydrophobic by pre-adsorbing cationic salt onto their surfaces.

## 5.2 Future studies

The experiment done to observe the effect of flow rate and viscosity on droplet size was based on previous work done by Garstecki et al., 2006 and Tica et al., 2003. The experimental setup was more or less similar only with the exception that Laponite RD smectite clay has been used as emulsifier instead of a surfactant. The work described above couldn't establish evidence enough to point out any systematic correlation between clay and the length of the droplets formed in the microfluidic T - junction. It was found only a slight increase of droplet length by using 1% Laponite clay in dispersed phase where droplets lengths were measured within 4 seconds after they made in T-junction. We expect that either higher concentration of clay or more time is needed to affect the clay on droplet size effectively, which can be done in future studies. To increase the time, a chip with long channel length can be helpful.

The main interest of this thesis work was to prepare stable Pickering emulsions by using the Laponite RD with the T-junction geometry and study how the clay effect on the emulsion stability. Stable W/O emulsion using Laponite RD as emulsifier was successfully organized in a T-junction, but due to lack of sufficient time, it was not possible to characterize the stability efficiently. The main characterization was done only by visually. So, it will be highly appreciated if the characterization of stability may possibly be done more quantitatively and elaborately in the future. In future work, it may also be interesting study the reason of coarsening of emulsion drops due to either to coalescence or to Ostwald ripening which might help to find out the prevention of instability.





## 6 Appendix

Video link

Video 1: [Droplet at the beginning of the reservoir](#)

Video 2: [Droplet at the middle of the reservoir](#)

Video 3: [Exit of Droplets](#)

Video 4: [Water droplet in silicon oil \(1000cSt\)](#)

Video 5: [Water in oil emulsion with 2 % concentration without adding any salt+LP](#)

Video 6: [Water in oil stable droplets with 2 % LP via 0.1M salt](#)

## 7 Bibliography

I E Odom. Smectite clay minerals: Properties and uses. *Phil. Trans. R. Soc. Lond. A*, 311: 391-409, 1984.

Web of knowledge. <http://apps.webofknowledge.com/>. Searched for clay suspension in topics. Accessed May 2012.

C Oriakhi. Nano sandwiches. *Chem. Br.*, 34:59-62, 1998.

P Tabeling. *Introduction to microfluidics*. Oxford University Press, New York, 2005. p. 105-117.

F Bergaya, Theng B K G, and Lagaly G. *Handbook of clay science*. Elsevier, 2006. Amsterdam.

N P Ashby and B P Binks. Pickering emulsions stabilised by laponite clay particles. *Chem. Phys.*, 2(24):5640, 2000.

B P Binks. Particles as surfactants - similarities and differences. *Curr. Opin. Colloid In.*, 7 (1-2):21-51, 2002.

M De Menech, P Garstecki, F Jousse, and H A Stone. Transition from squeezing to dripping in a microfluidic T-shaped junction. *J. Fluid Mech.*, 595:141-161, 2008.

R Dreyfus, P Tabeling, and H Willaime. Ordered and disordered patterns in two-phase flows in microchannels. *Phys. Rev. Lett.*, 90:144505, 2003.

P Garstecki, H A Stone, and G M Whitesides. Mechanism for flow-rate controlled breakup in confined geometries - a route to monodisperse emulsions. *Phys. Rev. Lett.*, 94:164501, 2005.

P Garstecki, M J Fuerstman, H A Stone, and G M Whitesides. Formation of droplets and bubbles in a microfluidic T-junction - scaling and mechanism of break-up. *Lab on a Chip*, 6:437-446, 2006.

X B Li, F C Li, J C Yang, H Kinoshita, M Oishi, and M Oshima. Study on the mechanism of droplet formation in T-junction microchannel. *Chem. Eng. Sci.*, 69:340-351, 2012.

T Nissiako, T Torii, and T Higuchi. Droplet formation in a microchannel network. *Lab on a Chip*, 2:24-26, 2002.

X Niu, M Zhang, J Wu, W Wen, and P Sheng. Generation and manipulation of smart droplets. *Soft Matter*, 5:576-581, 2009.

H Song, D L Chen, and R F Ismagilov. Reactions in droplets in microfluidic channels. *Angew. Chem., Int. Ed.*, 45:7336-7356, 2006.

H A Stone, A D Stroock, and A Ajdari. Engineering flows in small devices: Microfluidics toward a lab-on-a-chip. *Annu. Rev. Fluid Mech.*, 36:381-411, 2004.

Nakajima M Sugiura, S, S Iwamoto, and S Seki. On water-in-oil emulsions stabilized by fine solids. *Langmuir*, 17:5562, 2001.

S Sugiura, M Nakajima, T Oda, M Satake, and M Seki. Effect of interfacial tension on the dynamic behavior of droplet formation during microchannel emulsification. *J. Colloid Interf. Sci.*, 269:178-185, 2004.

Y C Tan, J S Fisher, A I Lee, V Cristini, and A P Lee. Design of microfluidic channel geometries for the control of droplet volume, chemical concentration and sorting. *Lab on a Chip*, 4: 292-298, 2004.

T Thorsen, R W Roberts, F H Arnold, and Quake S R. Dynamic pattern formation in a vesicle-generating microfluidic device. *Phys. Rev. Lett.*, 86:4163-4166, 2001.

J D Tice, H Song, A D Lyon, and R F Ismagilov. Formation of droplets and mixing in multiphase microfluidics at low values of the Reynolds and the capillary numbers. *Langmuir*, 19:9127-9133, 2003.

J D Tice, A D Lyon, and R F Ismagilov. Effect of viscosity on droplet formation and mixing in microfluidic channels. *Anal. Chim. Acta*, 507:73-77, 2004.

S Torza, R G Cox, and S G Mason. Electrohydrodynamic deformation and burst of liquid drops. *Philos. T. Roy. Soc. A*, 269(1198):295-319, 1971.

P B Umbanhowar, V Prasad, and D A Weitz. Monodisperse emulsion generation via drop break off in a coflowing stream. *Langmuir*, 16(2):347-351, 2000.

S van der Graaf, C G P H Schroen, R G M van der Sman, and R M Boom. Influence of dynamic interfacial tension on droplet formation during membrane emulsification. *J. Colloid Interf. Sci.*, 277:456-463, 2004.

S van der Graaf, M L J Steegmans, R G M van der Sman, C G P H Schroen, and R M Boom. Droplet formation in a T-shaped microchannel junction: A model system for membrane emulsification. *Colloid Surface A*, 266:106-116, 2005.

V van Steijn, M T Kreutzer, and C R Kleijn.  $\mu$ -piv study of formation of segmented flow in microfluidic T-junctions. *Chem. Eng. Sci.*, 62:7505-7514, 2007.

B Velde. *Introduction to Clay Minerals*. Chapman and Hall, London, 1992.

J H Xu, S W Li, J Tan, Y J Wang, and G S Luo. Controllable preparation of monodisperse O/W and W/O emulsions in the same microfluidic device. *Langmuir*, 22:7943-7946, 2006a.

J H Xu, S W Li, J Tan, Y J Wang, and G S Luo. Preparation of highly monodisperse droplet in a T-junction microfluidic device. *AIChE Journal*, 52:3005-3010, 2006b.

J H Xu, G S Luo, and G G Chen. Shear force induced monodisperse droplet formation in a microfluidic device by controlling wetting properties. *Lab on a Chip*, 6:131-136, 2006c.

J H Xu, S W Li, J Tan, and G S Luo. Correlations of droplet formation in T-junction microfluidic devices: from squeezing to dripping. *Microfluidics and Nanofluidics*, 5:711-717, 2008.

N X Yan and J H Masliyah. Adsorption and desorption of clay particles at the oil-water interface. *J. Colloid Interf. Sci.*, 168(2):386-392, 1994.

N X Yan, M R Gray, and J H Masliyah. On water-in-oil emulsions stabilized by fine solids. *Colloid. Surface. A*, 193(1-3):97-107, 2001.

C X Zhao and A P J Middelberg. Two-phase microfluidic flows. *Chem. Eng. Sci.*, 66:1394-1411, 2011.

B Zheng and R F Ismagilov. Reactions in droplets in microfluidic channels. *Angew. Chem., Int. Ed.*, 44:2520-2523, 2005.

E K Zholkovskij, J H Masliyah, and J Czarnecki. An electrokinetic model of drop deformation in an electric field. *J. Fluid Mech.*, 472:1-27, 2002.

K. Golemanov, S. Tcholakova, P. A. Kralchevsky, K. P. Ananthapadmanabhan and A. Lips.: Latex-Particle-Stabilized Emulsions of Anti-Bancroft Type. *Langmuir* 2006, 22, 4968-4977.

Colloid chemistry Lecture 13: Emulsions - Academia.edu

S.Guggenheim, R.T.Martin. Definition of clay and clay mineral. *Clays and Clay Minerals*, Vol.43, No2, 255-256, 1995.

A. D. Dinsmore, Ming F. Hsu, M. G. Nikolaidis, Manuel Marquez, A. R. Bausch, D. A. Weitz. November 2002 Vol 298 *Science*.

Tadros, Th.F. and Vincent, B. (1983) in *Encyclopedia of Emulsion Technology* (ed.P. Becher), Marcel Dekker, New York.

Anne Silset. Emulsions (w/o and o/w) of Heavy Crude Oils. Characterization, Stabilization Destabilization and Produced Water Quality. Thesis for the degree of philosophiae doctor. Norwegian University of Science and Technology Faculty of Natural Science and Technology Department of Chemical Engineering.

Klaus Tauer. Microemulsions and miniemulsions MPI Colloids and Interfaces. Am. Mühlenberg, D-14476 Golm, Germany.

Ajay Mandal, Abhijit Samanta, Achinta Bera, and Keka Ojha. Characterization of Oil-Water Emulsion and Its Use in Enhanced Oil Recovery. *Ind. Eng. Chem. Res.* 2010, 49, 12756–1276.

Katerina Loizou, Wim Thielemans and Buddhika N. Hewakandamby. Effect of geometry on droplet generation in a microfluidic t-junction. *Fedsm2013-16161*.

P. Jankowski, D. Ogonczyk, A. Kosinski, W. Lisowski and P. Garstecki. Hydrophobic modification of polycarbonate for reproducible and stable formation of biocompatible microparticles. DOI: 10.1039/c0lc00360c.

V. Castelletto, I. A. Ansari, and I. W. Hamley. Influence of Added Clay Particles on the Structure and Rheology of a Hexagonal Phase Formed by an Amphiphilic Block Copolymer in Aqueous Solution. *Macromolecules* 2003, 36, 1694-1700.

Jie Xu, Aijing Ma, Tianqing Liu, Chunli Lu, Dayang Wang and Haolan Xu. Janus- like Pickering emulsions and their controllable Coalescence. DOI: 10.1039/c3cc46738d. [www.rsc.org/chemcomm](http://www.rsc.org/chemcomm)

F.L.O. Paula, G.J. da Silva, R. Aquino, J. Depeyrot, J.O. Fossum, K.D. Knudsen, G. Helgesen and F.A. Tourinho. Gravitational and Magnetic Separation in Self-Assembled Clay-Ferrofluid Nanocomposites. *Brazilian Journal of Physics*, vol. 39, no. 1A, April, 2009.

Barbara Ruzicka and Emanuela Zaccarelli. A fresh look at the Laponite phase diagram. Cite this: *Soft Matter*, 2011, 7, 1268.

P. Taylor Ostwald ripening in emulsions. *Advances in Colloid and Interface Science* 75, 1998. 107-163.

Vladimir Alvarado, Xiuyu Wang and Mehrnoosh Moradi. Stability Proxies for Water-in-Oil Emulsions and Implications in Aqueous-based Enhanced Oil Recovery. *Energies* 2011, 4, 1058-1086; doi:10.3390/en4071058.

X. Wang and Vladimir Alvarado. Kaolinite and Silica Dispersions in Low-Salinity Environments: Impact on a Water-in-Crude Oil Emulsion Stability. *Energies* 2011, 4, 1763-1778; doi:10.3390/en4101763.

Danuta M. Sztukowski, Harvey W. Yarranton. Oilfield solids and water-in-oil emulsion stability. *Journal of Colloid and Interface Science* 285 (2005) 821-833.